Dissertation zur Erlangung des Doktorgrades der Fakultät für Biologie der Ludwig-Maximilians Universität München

Genetic and functional characterization of *Caenorhabditis elegans srf-3*, a gene involved in regulating surface antigenicity

von

Jörg Höflich

aus

Wilhelmshaven

2004

1. Gutachter: Prof. Dr. Harry MacWilliams

2. Gutachter: Prof. Dr. Thomas Cremer

Sondervotum: Prof. Dr. Ralf Baumeister

Tag der Einreichung bei der Fakultät für Biologie: 22. März 2004

Tag der mündlichen Prüfung: 15. April 2005

Die vorliegende Arbeit wurde von Mai 2000 bis Februar 2004 im Labor von Prof. Dr. Ralf Baumeister an der Ludwig-Maximilians Universität angefertigt.

Ehrenwörtliche Versicherung

Diese Dissertation wurde selbstständig und ohne unerlaubte Hilfe angefertigt.

München, 17.03.2004

Acknowledgements

I like to thank my PI Prof. Dr. Baumeister for the research project, the chance of going to Boston, the fruitful research atmosphere he created in his lab and the opportunity to develop and test my own ideas.
I like to thank Prof. Dr. MacWilliams for reviewing my thesis and representing it in front of the Faculty of Biology. I also like to thank Prof. Dr. Cremer for reviewing my thesis.
I like to thank all former and present members of the Baumeister lab for the great time and their support. Especially I like to thank our "worm" post-docs Dr. Bernard Lakowski and Dr. Giuseppe Cassata for their help with worms, for beer and their willingness and time to discuss any strange idea or result. I like to thank Stefan Eimer for his inexhaustible pool of ideas. I like to thank Dr. Thorsten Hoppe for discussions, humour and support. Furthermore I like to thank Christine Goebel for her great technical assistance, her motivation and her ability to convert chaotic experimental designs into results. I also like to thank Bianca Sperl for maintaining the lab discipline and for doing the lab management and Roland Donhauser for my first worm pick and the initial help with worm handling. I like to thank Wolf-Dieter Springer for critical reviewing the latest football results.
I like to thank Torsten Martin for his help during our time as system administrators.

I also like to thank Andreas Boettcher, Ingo Hüser, Torsten Martin and Stefan Czogalla for their invaluable support during our exploration of the Munich nightlife.

I am grateful for the great and fruitful time I had in the Department of Molecular and Cell Biology at Boston University thanks to Prof. Dr. Carlos Hirschberg, Dr. Patricia Berninsone, Alfred Tamayo and Dr. Sam Politz; I enjoyed very much the discussions at our "worm" meetings. I like to thank Jonathan Hodgkin for providing strains prior to publication.

I like to thank my father Wulf Höflich and the Janssen family for morale and financial support.

Summary

The widespread emergence of pathogens resistant to the majority of available antibiotics makes it necessary to find new ways to combat the corresponding microorganisms. Adaptive immunity is specific to vertebrates but the mechanisms of innate immunity are ancient and highly conserved during evolution. Therefore it is reasonable to use model organisms to study the molecular mechanisms of host defence and the corresponding mechanisms of pathogenicity.

Microbacterium nematophilum adheres to the rectum of a *Caenorhabditis elegans* animal inducing a localized non-lethal response that causes swelling of the underlying hypodermal tissue. The aim of this thesis was to gain a first insight into the molecular mechanisms underlying the resistance of *srf-3* animals to the bacterial pathogens *Microbacterium nematophilum* and *Yersinia pestis/pseudotuberculosis*. *M. nematophilum* adheres to the cuticle of wild type animals but fails to adhere to the surface of *srf-3* worms. This is a novel type of resistance because pathogens like *P. aeruginosa* or *Salmonella typhimurium* do not adhere to the cuticle but kill *C. elegans* by colonization and accumulation in the intestine. Molecular cloning of *srf-3* showed that this gene codes for a type III transmembrane protein similar to the family of UDP-galactose transporters. Expression analysis revealed that SRF-3 is expressed in a set of active secretory cells consistent with a function of this gene in cuticle or surface modification. A functional characterization of SRF-3 revealed that this protein can function as a nucleotide sugar transporter. The protein showed multisubstrate specificity capable of translocating UDP-galactose and UDP-N-acetylglucosamine *in vitro* as judged by transport assays done with Golgi/ER enriched vesicles, as well as *in vivo*, as shown by the phenotypic correction of mutants defective in UDP-galactose or UDP-N-acetylglucosamine transport.

The data presented in this thesis emphasize the importance of glycosylation in regulating the surface antigenicity of *C. elegans*. This can help to understand the process of pathogen adherence, the first step in the establishment of an infection, as well as how parasitic nematodes modulate the surface in order to escape the host response.

Introduction

Contagious diseases always represented a major threat to mankind and had a significant impact in human history. A disastrous example is the influenza pandemic 1918-1919 (Spanish influenza) killing approximately 40 million people worldwide (Crosby, 1989) Another prominent example is plague which caused one of the major biological-environmental events in European history in the mid-14th century (Black Death) killing approximately 17 to 28 million people and thereby 30 to 40% of the European population (Gottfried, 1983) (Figure 1 shows an example of a plague infected individual). Whereas the European of the middle age facing the Black Death was overwhelmed by a sense of inevitable doom, the common person of the late 20th century does not come into contact with plague or other dangerous infectious diseases. But it was not until the late 19th century that due to the pioneering works of Louis Pasteur (1822-1895) and Robert Koch (1843-1910), transferable diseases are viewed as a microbiological problem. Today we know that various species of worms, protozoa, fungi or viruses can cause diseases. Therefore pathogens are mircoorganisms and smaller biological active entities that have the ability to infect higher organisms and cause disease.

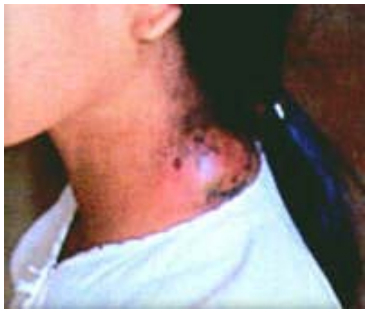

Figure 1: Picture of the swollen nymph glands in the neck of a bubonic plague patient (http://groups.msn.com/CellNEWS/plague.msnw)

The development of a vaccine against Smallpox by Edward Jenner in 1798, against Rabies by Louis Pasteur in 1885, and the discovery of penicillin (Fleming, 1929) represent the breakthroughs in the combat against infectious diseases and led to a worldwide retreat of this threat. In the 1960s it seemed that many infectious diseases had been nearly eliminated. However, an increasing number of antibiotic-resistant pathogens have been reported since then and in 1997 a *Staphylococcus aureus* strain, the major cause of hospital-acquired infections, resistant to all antibiotics currently available was isolated from a patient sample (Hiramatsu et al., 1997). Therefore, the development of new therapeutic and prophylactic approaches in the treatment of infectious diseases has become a major challenge for the future. Currently two strategies are being pursued. One approach is to develop modified versions of currently available antibiotics to inhibit the classic targets like cell wall synthesis, nucleotide/protein synthesis, DNA replication or the cytoplasmic membrane (Walsh, 2000). A second and new approach is to identify and fight bacterial factors that are essential to the infection process. The idea is that, if important virulence factors can be neutralized, the infection can be blocked at their earliest step which is the establishment of the corresponding

pathogens within the host (Ziebuhr, 2002). Molecular characterization of virulence factors showed that genes affecting virulence of pathogens can be classified in specific and non-specific factors. Specific factors like capsules, adhesins, toxins or invasions factors play an active role in the outbreak of the disease, e.g. breaking through the host defences, whereas non-specific factors like iron-complexing systems generate the biological prerequisite for the onset of disease (Finlay and Falkow, 1997). The fact that certain pathogens are capable of infecting a broad range of organisms points to the existence of universal virulence factors necessary for full pathogenicity in every host. On the other hand, the remarkable host specificity shown by some pathogens, e.g. the human specific gastric pathogen *Heliobacter pylori*, the causative agent in chronic active gastritis and peptic ulcer disease (Dubois, 1995), strongly suggests a bidirectional interaction between pathogen and host. Therefore, to understand diseases one has to study both sides of the bacteria-host interaction.

Complex multicellular organisms have developed sophisticated mechanisms to protect themselves against invading microorganisms. Whereas the vertebrate immune system can respond to infection with an innate or a potent adaptive defence, most other multicellular organisms solely rely on the phylogenetically conserved innate immunity. The marked conservation of the innate immune defence system makes it possible to study and understand the mechanisms of this immune response in invertebrate organisms (Hoffmann et al., 1999). For example, the involvement of the Toll pathway, one of the major defence signalling cascades in innate immunity, was first described in *Drosophila melanogaster* (Lemaitre et al., 1996).

Caenorhabditis elegans as a model in innate immunity

Originally, the soil nematode *C. elegans* (see Figure 2) was chosen by Sydney Brenner for studying fundamental aspects of developmental and neuronal biology (Brenner, 1973). It offers great potential for genetic analysis because of its three day life cycle, small size, combination of self and cross fertilization and the fact that it can be easily cultivated in the laboratory. Due to its transparency the anatomy of the animals can be analysed by light microscopy leading to the description of the entire cell lineage. The full genome sequence has been determined in 1998 and a broad set of tools for genetic and biochemical manipulations has been developed.

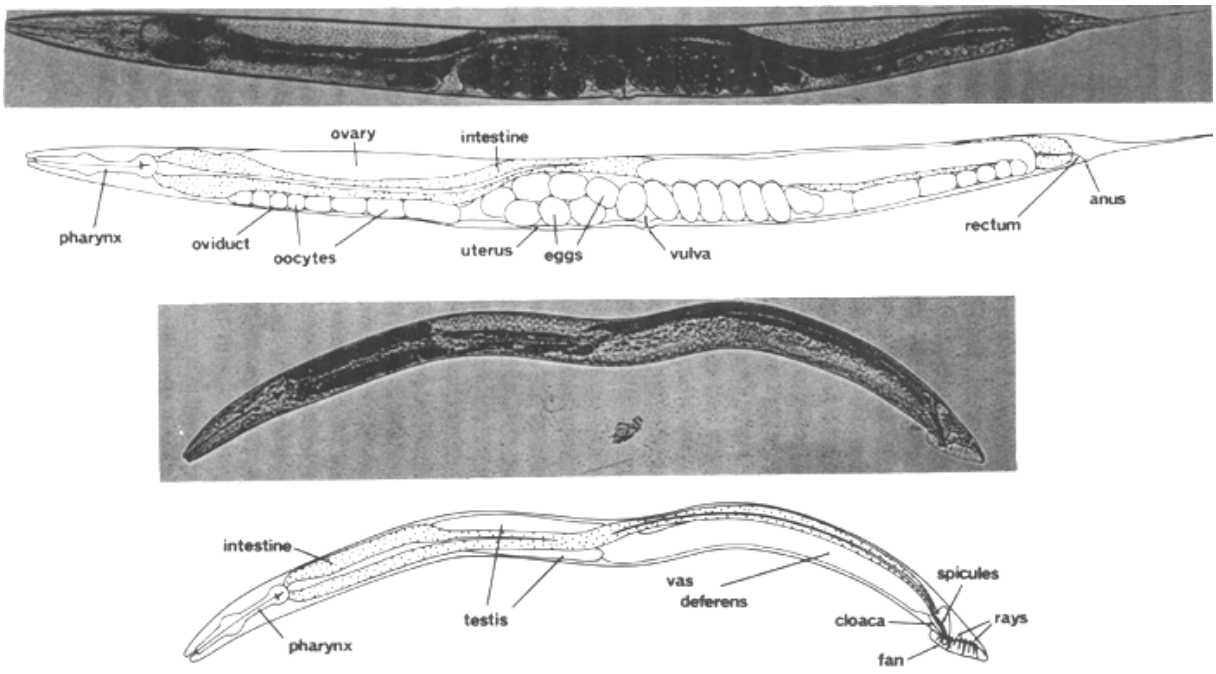

Figure 2: Photographs showing an adult *C. elegans* hermaphrodite (top) and a male (bottom) animal

In nature, *C. elegans* dwells in the soil and feeds on bacteria and is therefore in constant contact with an environment teeming with microbes. In order to survive, *C. elegans* is protected by physical barriers, the cuticle and the grinder. However, theses barriers offer only imperfect protection against microbial entry, as shown by the fact that a small proportion of GFP labelled bacteria can pass through the grinder and enter and colonize the intestine (Figure 3 and Tan et al., (1999)).

In the case of *Salmonella typhimurium* and *Pseudomonas aeruginosa* the bacteria accumulate in the intestine of the worm and kill the animal (see Figure 3c - 3f). The *P. aeruginosa-C. elegans* interaction was used to screen for bacterial clones with attenuated virulence (Mahajan-Miklos et al., 1999). Interestingly, the corresponding clones showed also reduced virulence in the mammalian model proving that the nematode can be used as a model for host-pathogen interactions. But until recently it was not clear whether *C. elegans* possesses an immune defence system. Although genome analyses revealed the existence of putative antimicrobial peptides, some of the components (e.g. Rel/NFκB) in the toll pathway seem to be absent in the worm genome

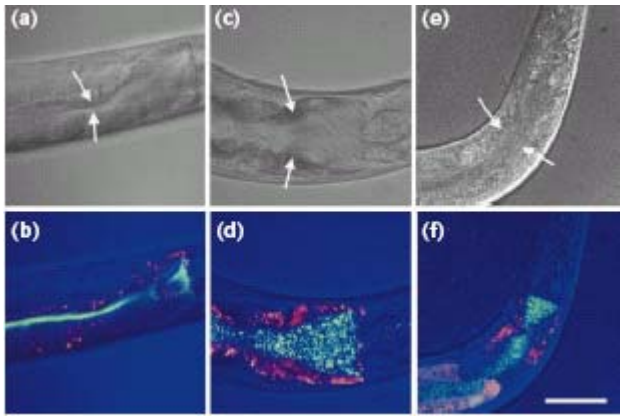

Figure 3: Confocal images showing bacterial colonization of the *C. elegans* intestine. (a,b): *E. coli* DH5a–GFP, (c,d): *S. typhimurium* SL1344-GFP, (e,f): *P. aeruginosa* PA14–GFP. Scale bar represents 50 µm. Intestinal margins are indicated with arrows. Figure was taken from Aballay et al., (2000)

and deletion of the existing genes did not alter the resistance of worms to various pathogens (Banyai and Patthy, 1998; Kato et al., 2002; Pujol et al., 2001). By screening for *C. elegans* mutants with enhanced susceptibility to infection by *P. aeruginosa* several *esp* genes (esp = enhanced susceptibility to pathogens) were identified (Kim et al., 2002). This enhanced susceptibility was not specific to the Gram-negative bacterium, *P. aeruginosa*, because the mutants were also hypersusceptible to the Gram-positive pathogen *Enterococcus faecalis.* Cloning of two of these mutants revealed that *esp-8* codes for MAP kinase kinase kinase and *esp-2* codes for a MAP kinase kinase. It has been shown that MAP kinases play an important role in the mammalian cellular immune response to lipopolysaccarides (LPS) and therefore it can be concluded that *C. elegans* possesses a conserved and ancient innate immune pathway (Dong et al., 2002). Microarray analysis of worms infected with *Serratia marcesens* revealed that animals can, if challenged with a pathogen, induce the expression of various genes e.g. lectins and lipases (Mallo et al., 2002). Lipases have been shown to be induced upon infection of *D. melanogaster* and lectin binding motifs are known to be involved in recognition of pathogens (De Gregorio et al., 2001; Fujita, 2002). Therefore *C. elegans* is obviously able to respond to infection with the induction of a set of defence genes. Table 1 shows an overview of bacteria capable of infecting *C. elegans*.

Species	Reference
	Gram-positive
Bacillus megaterium	(Andrew and Nicolas, 1976)
Bacillus thuringiensis	(Borgonie et al., 1995)
Enterococcus faecalis	(Garsin et al., 2001)
Microbacterium nematophilum	(Hodgkin et al., 2000)
Staphylococcus aureus	(Garsin et al., 2001)
Streptococcus pneumoniae	(Garsin et al., 2001)
	Gram-negative
Burkholderia pseudomallei	(O'Quinn et al., 2001)
B. thailandensis	(O'Quinn et al., 2001)
B. cepacia	(Tan and Ausubel, 2000); (O'Quinn et al., 2001)
Pseudomonas aeruginosa	(Tan et al., 1999)
P. fluorescens	(Tan et al., 1999); (Darby et al., 1999)
Salmonella typhimurium	(Aballay et al., 2000); (Labrousse et al., 2000)
Serratia marcescens	(Pujol et al., 2001); (Kurz and Ewbank, 2000)
Yersinia pestis	(Darby et al., 2002)
Yersinia pseudotuberculosis	(Darby et al., 2002)

Table 1: Known bacterial pathogens of *C. elegans*

A pathogen specific for *C. elegans* and closely related nematodes has been described recently (Table 1). Worms grown on bacterial lawns containing *Mircobacterium nematophilum* develop a variably swollen post-anal region named deformed anal region phenotype (Dar). The swelling is not due to cell proliferation as shown by the fact that the *C. elegans* conditional cell division mutant *stu-7* still exhibits a swollen post-anal region if infected with *M. nematophilum*. The animals become constipated due to the swelling and therefore feed less which results in a slower growth rate (see Figure 4). The *M. nematophilum* infection is novel and distinctly different in nature from the toxicity of some strains of *P. aeruginosa* for *C. elegans*. A large screen with previously characterized mutants showed that certain mutants with altered surface antigenicity, notably *srf-2*, *srf-3* and *srf-5*, are resistant to infection by *M. nematophilum*. Currently, it is not clear if the swelling is due to an activation of a host defence system or due to a subversion of a host cellular process by the bacteria. In order to understand the mechanism of infection and the induced swelling a screen for mutants showing normal growth rate and the absence of swelling was performed (Bacterially UnSwollen (Bus) phenotype; (Gravato-Nobre et al., 2001)). The recovered mutants could be grouped into 18 complementation groups and 4 mutants (*e2789*, *e2680*, *e2689* and *e2797*) failed to complement *srf-3(yj10)*.

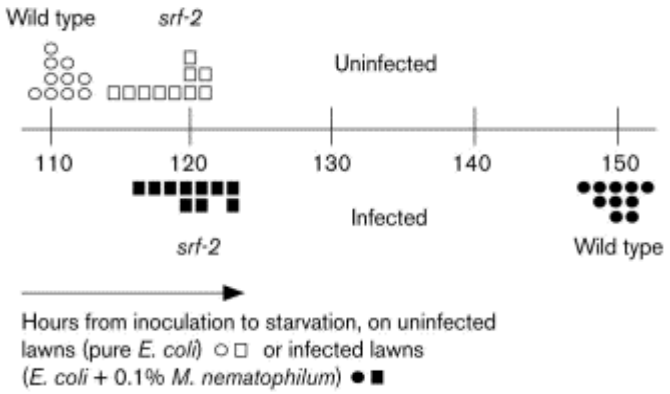

Figure 4: Comparison of feeding rates in the presence and in the absence of *M. nematophilum* CBX102. Arrow indicates the time scale representing the time at which descendants from one single hermaphrodite consumed available bacterial food (○□ *E. coli*; ●■ *E.coli* + 0.1% *M. nematophilum*). Growth rates for wild type and for *srf-2* mutants are shown. The figure was taken from Hodgkin et al., (2000).

The surface of nematodes: *C. elegans srf* mutants

Parasitic nematodes can survive for long periods in otherwise immunocompetent hosts (Maizels and Selkirk, 1988). First evidence how parasitic nematodes can defy the host immune system came from studies with *Trichnella spiralis*. Radiolabelling experiments of *T. spiralis* surface indicated that the cuticle of this nematode is a dynamic organ which showed dramatic changes at the molecular level during the moulting process and gradual modifications during growth within a stage (Philipp et al., 1980). Since then, stage-specific expression of surface-associated antigens has been described for several species of parasitic nematodes (Philipp and Rumjanek, 1984). The outermost layer of the nematode cuticle, the

surface coat that is only loosely attached to the epicuticle, is a remarkable dynamic structure implicated in antigen shedding. Antigen shedding is thought to be an important parasite defence mechanism against antibody-mediated immune effector mechanisms (Blaxter et al., 1992). The problem is that the study of most parasitic nematodes is always limited by the paucity of worm material because parasites are often very hard to grow under laboratory conditions due to their complicated life-cycles including several specific hosts. Therefore it was very desirable to find an appropriate model organism for parasitic nematodes. Besides its experimental advantages, the use of *C. elegans* as a model for parasitic nematodes is justified for the following reasons: First of all, the overall architecture of the cuticle in almost all nematodes is similar, it is composed of five layers: surface coat, epicuticle, cortical, median and basal layers (see Figure 5). All nematodes follow the same developmental programme: the zygote gives rise to the five somatic tissue founder cells followed by the germ line founder cell and postembryonic development proceeds through 5 stages separated by moults.

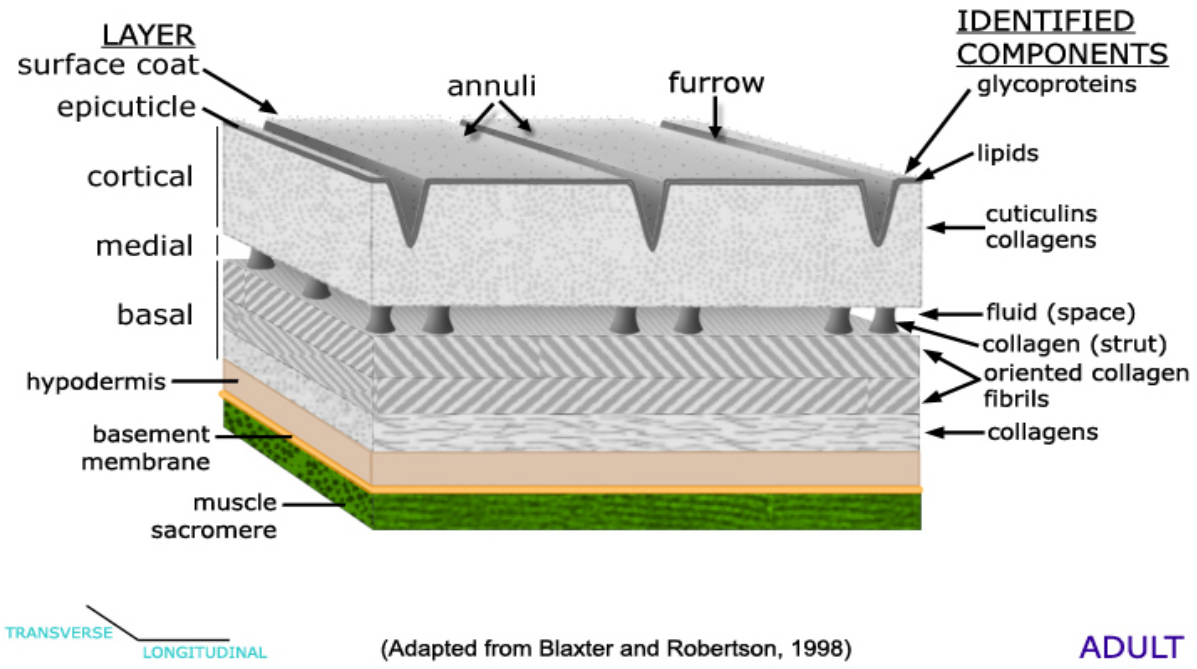

Figure 5: Schematic representation of an adult *C. elegans* cuticle. On the left side the 5 layers of the cuticle and the underlying structures (hypodermis, basement membrane and muscle sacromeres) are indicated. On the right side the components which can be found within a specific layer are listed. Figure is taken from http://www.wormatlas.org/handbook/cuticle/cuticle.htm (Blaxter and Robertson, 1998)

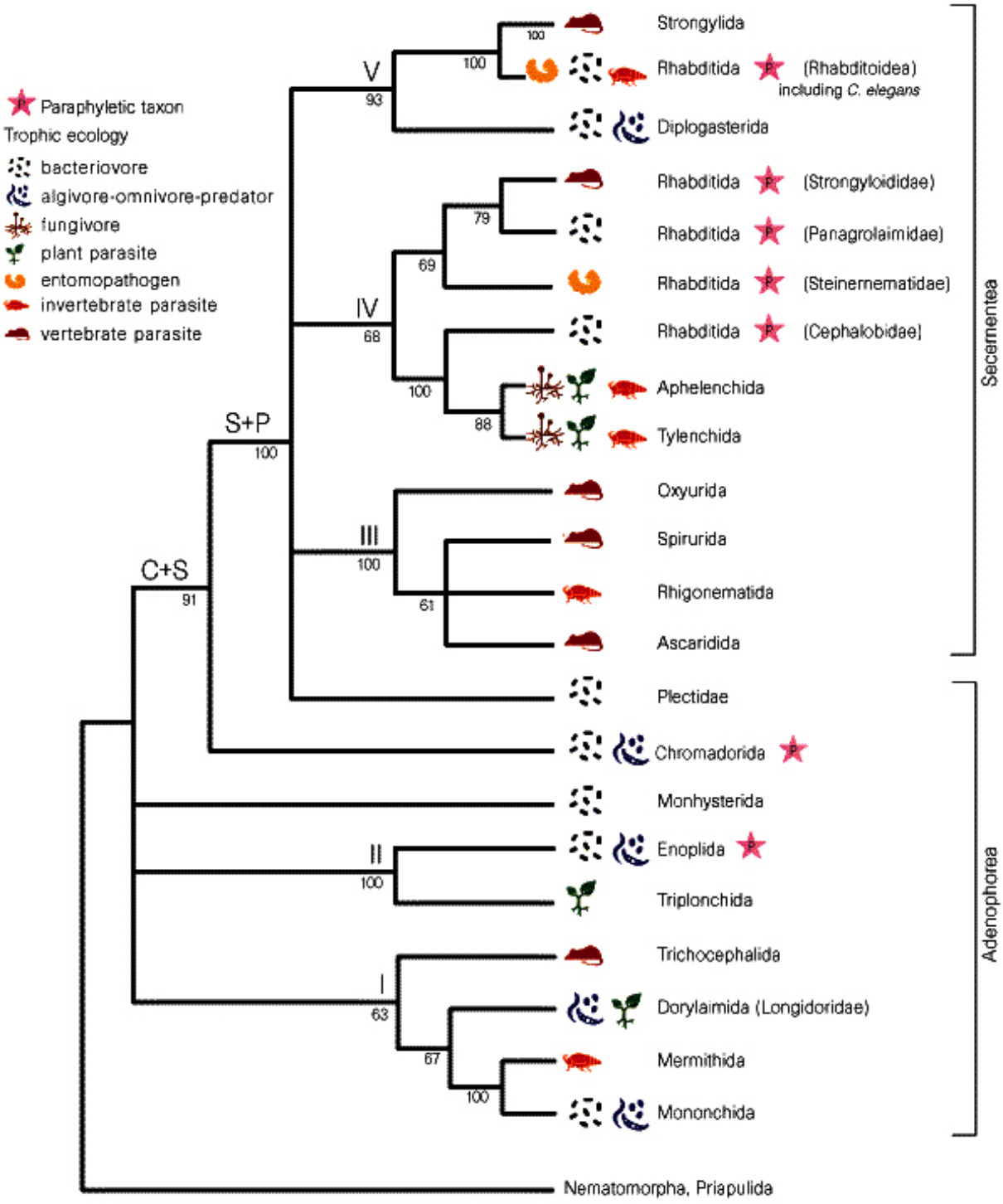

Figure 6: A phylogenetic hypothesis for the phylum Nematoda based on the SSU-sequence dataset. The tropic ecology of the taxa is represented by coloured icons (shown in the upper left corner). Branch lengths are drawn to be proportional to the number of changes inferred from the consensus. The major clades are indicated (I-V). C+S indicates the clade Chromadoria plus Secernentea; S+P indicates Secernentea plus Plectidea. Taken from Blaxter et al. (1998)

A phylogenetic analysis using the sequence of small subunit sequences (SSU) from 53 taxa suggested a deep intercalation of free-living and parasitic life modes in the phylum Nematoda (Figure 6). According to this phylogenetic relationship *C. elegans* is most closely related to the vertebrate parasitic Strongylida (Blaxter et al., 1998). This finding strongly supports the idea that the advances arising from the *C. elegans* work can be applied at least to some parasitic nematode species.

In order to examine if *C. elegans* expresses stage-specific surface antigens a polyclonal rabbit antiserum prepared against total cuticle proteins of adult wild type worms (Bristol N2) was adsorbed on intact larvae. The resulting antiserum was no longer able to bind to the surface of larvae but to the surface of adult worms (Politz et al., 1987). Therefore, it was concluded that *C. elegans* expresses stage-specific surface antigens. Interestingly, the cuticle of other wild type isolates, e.g. PA-1 or Bergerac BO, failed to label with the corresponding antibody suggesting an antigenic polymorphism. This antigenic polymorphism was mapped on Chromosome II suggesting that a single gene or gene cluster controls the expression of the adult class of surface antigens. The corresponding locus was named *srf-1* (surface antigenicity abnormal). To understand the mechanism underlying the Srf phenotype a genetic screen for mutants with altered surface antigenicity was performed (Politz et al., 1990). To do so the anti-adult antiserum used to identify *srf-1* was depleted of anti-surface antibodies by adsorbing it onto intact adult worms. Then worms were mutagenized with ethyl methansulphonate (EMS) and animals labelling with the adsorbed antiserum were maintained. This led to the identification of two new loci: *srf-2(yj262)* on Chromosome I and *srf-3(yj10)* on Chromosome IV. Radioiodination experiments revealed that several components of the wild type cuticle were undetectable or less readily labelled in extracts from *srf-2* and *srf-3* animals, most notably a non-collagenous, hydrophobic, non-glycosylated heterodimeric protein composed of 12 kDa and 6.5 kDa subunits (Blaxter, 1993). Therefore, it was proposed that the mutations caused a loss of components from the cuticle surface which led to the exposure of antigenic determinants usually hidden in the wild type cuticle.

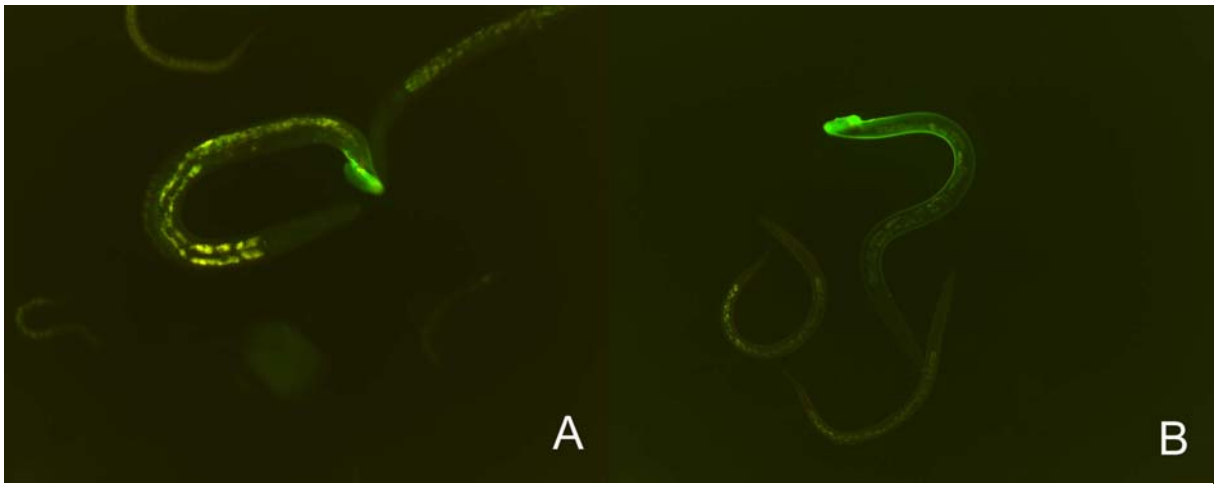

Figure 7: A N2 male (A) and a *srf-3(yj10)* (B) male stained with WGA-FITC. In N2 only the male tail shows fluorescence, whereas in *srf-3* animals the tail plus the posterior part of the animal is labelled. Scale bar represents 100 µM (Photographs taken by Jörg Höflich).

A second independent evidence that *C. elegans* expresses stage specific surface antigens came from a study with a monoclonal antibody (Hemmer et al., 1991). A mouse monoclonal antibody named M38 was found to bind specifically to the cuticle of wild type L1 larvae. A biochemical characterization revealed that the epitope recognized by M38 was pronase and O-glycanase sensitive suggesting that it is an O-linked glycoprotein. In order to find factors regulating the timing of antigen expression, an EMS screen for mutants showing altered M38 binding was performed. This led to the discovery of *srf-6(yj43),* a mutant where the L1 specific antigen is expressed at all larval stages. In protein extracts made from *srf-2(yj262)* and *srf-3(yj10)* animals the antigen was not detectable. Furthermore, a *srf-6(yj43); srf-3(yj10)* double mutant was antigen defective as the *srf-3(yj10)* mutant alone showing that the *srf-6* phenotype requires *srf-3* activity. A putative O-linked epitope as the antigen of M38 is consistent with the finding that the surface coats of nematodes are polyanionic and contain carbohydrate and mucin-like proteins (Himmelhoch and Zuckerman, 1983; Jansson et al., 1986; Page et al., 1992; Zuckerman et al., 1979). Cuticle surface binding of lectins has been reported for free-living and parasitic nematodes (Rudin, 1990; Zuckerman et al., 1979). *C. elegans* N2 animals stained with fluorescein isothiocyanate conjugated wheat germ agglutinin (FITC-WGA) show labelling at the hermaphrodite vulva and labelling at the male tail (see Figure 7). In a screen for mutants showing ectopic WGA binding various mutants were identified (see Figure 7 and Link et al., (1992)). Complementation analysis revealed that the 45 mutants found could be assigned to 6 complementation groups, notably the previously described genes *srf-2* and *srf-3* as well as the newly identified genes *srf-4*, *srf-5*, *srf-8* and *srf-9*. All genes show a highly penetrant ectopic lectin binding phenotype in both sexes, but males show a stronger posterior staining if compared to hermaphrodites. Besides the ectopic

lectin binding, *srf-2*, *srf-3* and *srf-5* animals show wild type gross morphology whereas *srf-4*, *srf-8* and *srf-9* mutants are uncoordinated, have distinct body morphology, a protruding vulva, a progressive egg laying defect and show male infertility. Based on the additional phenotypes observed in some mutants, *srf* animals have been divided into two classes: pleiotropic (*srf-4, srf-8* and *srf-9*) and non-pleiotropic (*srf-2, srf-3* and *srf-5*) *srf* mutants. A *srf-4 srf-8 srf-9* triple mutant was phenotypically indistinguishable from the corresponding single mutants suggesting that these mutants act in a linear pathway. Double mutants between the pleiotropic and the non-pleiotropic mutants have not been reported yet. Nevertheless, the differences in the phenotypes of the non-pleiotropic mutants compared to pleiotropic mutants suggest that both classes are involved in distinct biological and molecular processes. This idea is further supported by the fact that the mutants resistant to infection by *M. nematophilum* are exclusively the non-pleiotropic *srf* mutants (Hodgkin et al., 2000).

Aim of the thesis

Many mutants with altered surface antigenicity have been described since now but none of these mutants have yet been identified on the molecular level. Although it has been proposed that these mutants are involved in glycosylation or secretion, it is impossible to draw any conclusions without knowing the molecular identity of the *srf* genes. The resistance of the non-pleiotropic *srf* mutants to infection by *M. nematophilum* offers an assayable phenotypic marker to clone these mutants. In order to get first insights into the molecular and genetic network underlying the surface phenotype and the resistance to infection by *M. nematophilum*, I decided to clone and characterize *srf-3*.

Results

srf-3 animals are resistant to infection by *M. nematophilum* and to biofilm formation of *Yersinia pseudotuberculosis*

N2 worms grown on agar plates containing *M. nematophilum* CBX102 develop a post-anal swelling (see Figure 8A). The distortion of the anal region prevents the defecation muscles from working properly and therefore the infected animals become constipated. The constipated animals grow more slowly and therefore feed less (Figure 4). *srf-3* animals have also been reported to be resistant to infection by *M. nematophilum* (Hodgkin et al., 2000) and as can be seen in Figure 8B and Table 2, all *srf-3(yj10)* worms grown on a *Eschericha coli* OP 50 lawn containing 0.1% *M. nematophilum* do not exhibit a Dar phenotype. Additional *srf-3* alleles have been identified in a screen for Bus mutants (see Introduction), showing that this resistance is not allele specific. In order to characterize the novel alleles (gift of Jonathan Hodgkin, Oxford), the penetrance of the Dar phenotype of individual *srf-3* mutants was compared (Table 2). All alleles except *srf-3(e2797)* show a 100% resistance (no animals with a deformed anal region) to the infection by *M. nematophilum*. *srf-3(e2797)* animals are only partly resistant at 15 and 20°C but fully resistant at 25°C, indicating that *e2797* is a temperature-sensitive allele.

Under unfavourable environmental conditions, *C. elegans* can develop into an alternative third-stage larva specialized for dispersal and long-time survival (Riddle, 1988). Dauer larvae show a remarkable resistance to environmental stress, e.g. they survive one hour treatment in 1% sodium dodecyl sulphate (SDS), a property routinely used to enrich or purify dauers from

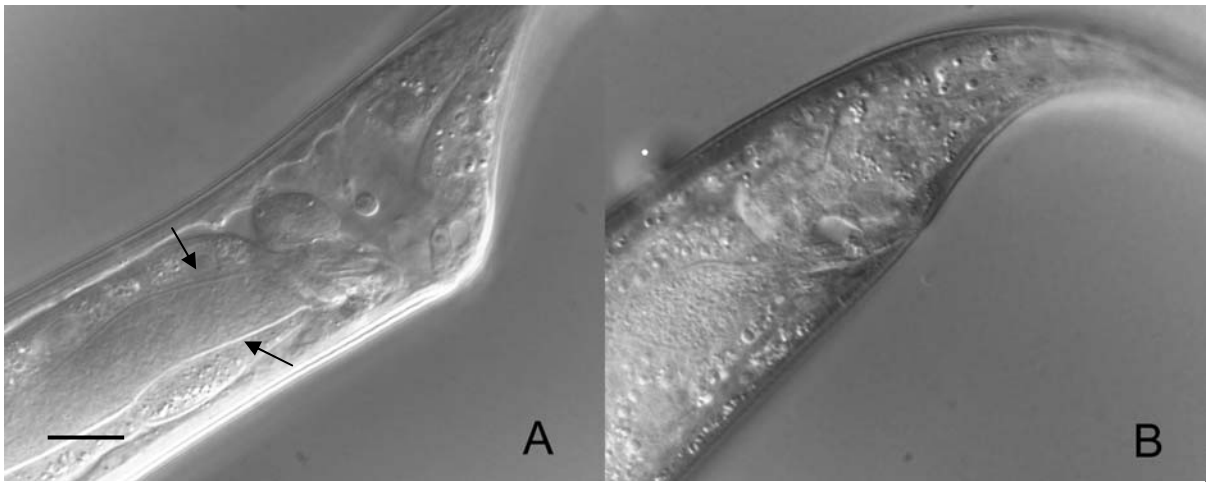

Figure 8*: srf-3* animals are resistant to infection by *M. nematophilum*. Normarski differential interference contrast (DIC) photographs of the tail region of a N2 animal (A). The Dar phenotype, characterized by a distinctive swollen tail, is clearly visible. The arrows indicate the distended intestinal lumen characteristic for constipation. (B) A *srf-3* animal grown on plates containing *M. nematophilum*. Tail region is indistinguishable from worms grown on standard *E. coli* OP 50 food source. Scale bar represents 20 μM.

Table 2: Penetrance of Dar phenotype in N2 and *srf-3* animals on plates containing *M. nematophilum*

T	wild type (N2)	*yj10*	*e2789*	*e2680*	*e2797*	*e2689*	*br6*
25°C	100% (n=322)	-	0% (n=238)	-	0% (n=279)	-	-
20°C	100% (n=403)	0% (n=543)	0% (n=464)	0% (n=395)	19% (n=243)	0% (n=460)	0% (n=135)
15°C	100% (n=183)	-	0% (n=253)	-	22% (n=385)	-	-

cultures. *srf-3* dauer larvae have been reported to be sensitive against SDS treatment of one hour, probably due to their altered cuticle (Politz et al., 1990). To test if the dauer larvae of the novel *srf-3* alleles exhibit a similar phenotype, they were crossed into a *daf-2(e1370)* mutant background. *daf-2(e1370)* is a temperature sensitive mutant involved in a insulin signalling pathway controlling dauer formation (Gottlieb and Ruvkun, 1994). At the restrictive temperature (25°C) all *daf-2(e1370)* L1/L2 animals enter the dauer pathway independent of the environmental conditions. The dauer larvae of all tested alleles, notably *e2789*, *e2689*, *e2680* and *e2797* showed SDS sensitivity identical to *srf-3(yj10)*. Therefore it can be concluded that all *srf-3* alleles show a similar behaviour, not only in terms of resistance, but also in terms of the SDS sensitivity of their dauer larvae. *srf-3* mutants have been originally isolated due to their altered surface antigenicity (see Introduction) and therefore it seems most likely that the resistance is due to altered surface properties of the cuticle, which may alter the adherence or recognition of the bacteria. To evaluate the specificity of the *srf-3* pathogen resistance, the resistance to other pathogens was tested.

C. elegans has recently described as a model to examine biofilm formation of *Yersinia pseudotuberculosis* and *Yersinia pestis*, the latter which is the causative agent of plague (Darby et al., 2002). A biofilm can be defined as a microbial derived sessile community characterized by cells that attach to a substratum or interface, embed in a matrix of extracellular polymeric substance, and exhibit an altered phenotype with respect to growth, gene expression and protein production (Shirtliff et al., 2002). After initial surface attachment, extracellular replicating bacteria very often develop biofilms which increases adherence and allows them to survive in a hostile environment. Biofilm forming bacteria play an important role in contaminating medical implants, for example *Streptococcus staphylococci*, *P. aeruginosa*, *S. aureus, S. epidermidis,* or in the case of lung infections of cystic fibrosis patients (*P. aeruginosa*) and a characterized by their remarkable antibiotic resistance as compared to their planktonically grown counterparts (Davey and O'Toole, 2000).

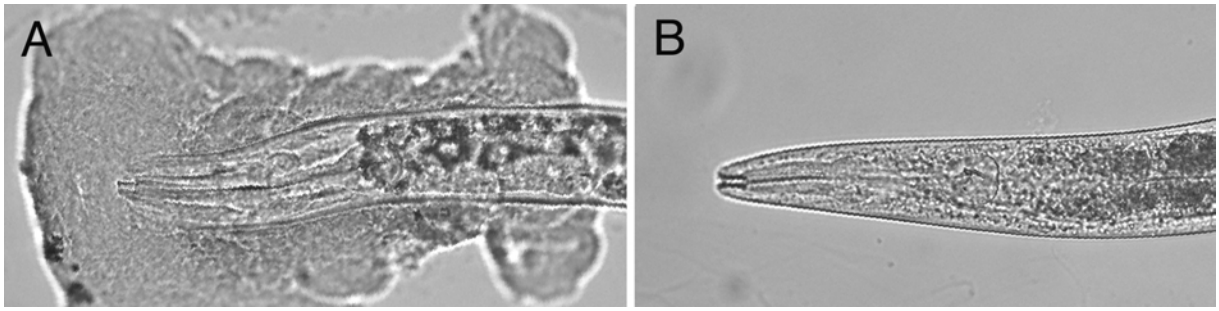

Figure 9: *srf-3* animals are resistant to biofilm formation of *Y, pseudotuberculosis*. Biofilm formation of *Y. pseudotuberculosis* on wild type (N2) and *srf-3* animals. DIC photographs of the head region of a N2 (A) and *srf-3* (B) animal grown on plates containing *Y. pseudotuberculosis*. (A) Biofilm at the head becomes visible within an hour and increases in size during continuing exposure. (B) No biofilm appears in a *srf-3* mutant (Bah phenotype). Photographs taken by Creg Darby (Birmingham, Alabama)

Table 3: *Y. pseudotuberculosis* biofilm formation on N2 animals and on *srf-3* animals*

T	wild type (N2)	*yj10*	*e2789*	*e2680*	*e2797*	*e2689*	*br6*
25°C	7.9% (n=764)	-	-	-	56.7% (n=716)	-	99.5% (n=664)
20°C	3.4% (n=(641)	100% (n=420)	100% (n=680)	100% (n=528)	1.4% (n=452)	100% (n=725)	99.4% (n=436)
15°C	0% (n=395)	-	-	-	1.8% (n=365)	-	98.9% (n=201)

* given is the percentage of the number of total L4's to the number of total worms (see also Material and Methods). The numbers in Table 3 show the average of three independent experiments.

Table 4: Fecundity* of N2 and different *srf-3* alleles on plates containing standard OP50 as food source and on plates containing *M. nematophilum*.

Strain	*Escherichia coli* OP50	*Escherichia coli* OP50 + 0.1% *M. nematophilum*
N2	310 ± 05 (n=15)	144 ± 09 (n=16)
srf-3(yj10)	285 ± 09 (n=20)	260 ± 07 (n=20)
srf-3(e2798)	248 ± 09 (n=18)	259 ± 06 (n=20)
srf-3(e2680)	262 ± 20 (n=17)	241 ± 19 (n=20)
srf-3(e2797)	272 ± 08 (n=18)	231 ± 13 (n=20)
srf-3(e2689)	253 ± 12 (n=18)	295 ± 08 (n=20)

*given is the number of progeny (mean ± SD) counted as L4 animals. n represents the number of hermaphrodites analysed.

Y. pestis is transmitted by the bites of infected fleas whose digestive tracts are blocked by a mass of bacteria. Blockage is dependent on the hemin storage (*hms*) locus which is required for biofilm formation (Darby et al., 2002; Hinnebusch et al., 1996). When *C. elegans* is exposed to *Y. pestis* or the closely related bacterium *Y. pseudotuberculosis*, a biofilm becomes visible on the worms' head (Figure 9A). The biofilm increases in size by continued exposure

and covers the head of the animal. This leads to a severe impairment of feeding which in the case of *C. elegans* larvae leads to delayed development or growth arrest. Interestingly, there is no sign of colonization of interior tissues of the exposed animals (Darby et al., 2002). Therefore it seemed reasonable to test mutants with altered surface antigenicity for resistance to biofilm formation of *Y. pseudotuberculosis*. *srf-3* animals had no biofilm and grew normally in the continuous presence of *Yersinia*, and are therefore Bah (Biofilm Absent on Head) (Figure 9B). Table 3 shows that all *srf-3* alleles are resistant to biofilm formation of *Y. pseudotuberculosis*. *srf-3(e2797)* animals are only resistant at 25°C confirming the finding of the *M. nematophilum* interaction that this allele is a temperature-sensitive allele. Furthermore, an additional *srf-3* allele, *br6*, could be identified in an N-ethyl-N-nitrosourea (ENU) induced mutagenesis for animals showing the Bah phenotype (Creg Darby, personal comm.). *srf-3(br6)* animals are also resistant to infection by *M. nematophilum*. Therefore *srf-3* resistance to infection by *M. nematophilum* is not limited to one species, as shown by the fact that this mutant seems to be unaffected in the presence of two distinct, unrelated bacterial species. To examine additional consequences of *srf-3* mutations, the brood size was determined. Measuring the amount of progeny produced by a single worm is a sensitive indicator for the viability of a certain strain. On standard *Escherichia coli* OP50 plates the number of progeny from the tested *srf-3* alleles was in the range of or slightly lower when compared to N2 worms (Table 4). On plates containing 0.1% *M. nematophilum* the

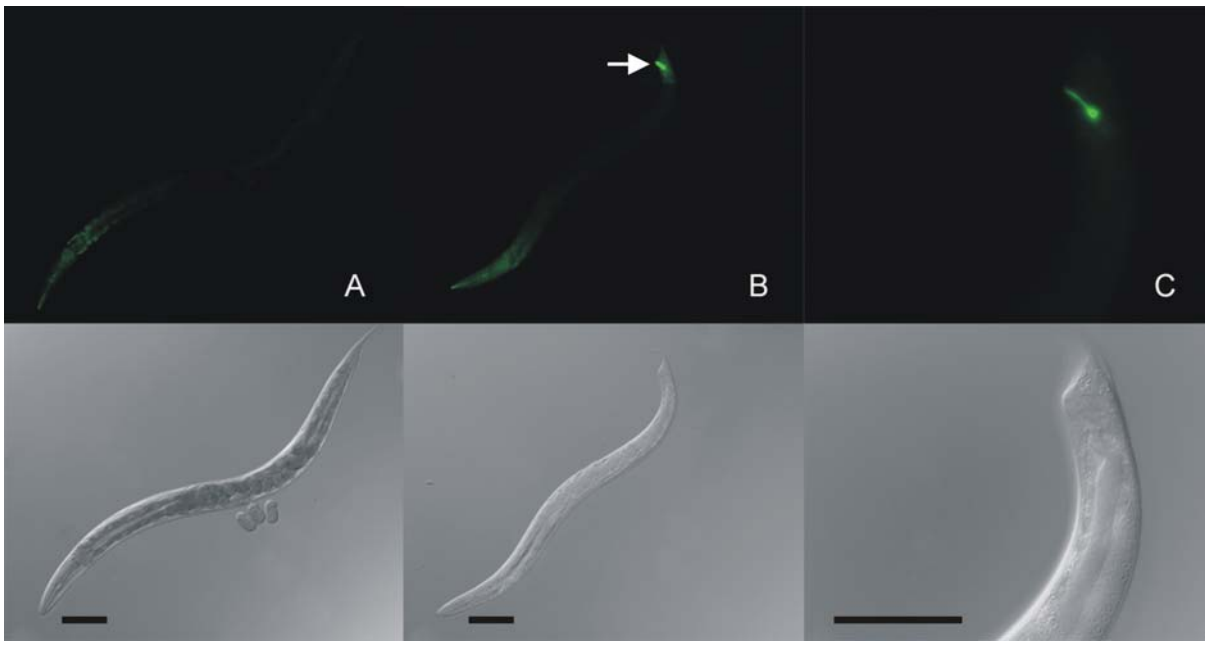

Figure 10: *M. nematophilum* cannot adhere to the surface of *srf-3* animals. Fluorescence and DIC photographs of *srf-3* (A) and N2 (B) animals grown on plates containing *M. nematophilum* and subsequently stained with Syto 13. Arrow in B indicates the bacteria adhering to the surface. The tail of the N2 animal in B at higher magnification (C). The black bar represents 100µM.

number of progeny of N2 worms was only 50% compared to the brood size of *srf-3* alleles demonstrating that *srf-3* mutants are barely affected by *M. nematophilum*. It has been proposed that the resistance of the non-pleiotropic *srf* mutants is due to a change in the surface properties of the cuticle, which may alter adherence or recognition by the bacteria (Hodgkin et al., 2000). However, it is also possible that the bacteria can adhere to the cuticle of *srf* animals but fail to induce the post-anal swelling. To answer this question worms were grown on plates containing *M. nematophilum* and stained with the dye Syto13, which stains nucleic acids of live cells, under conditions where bacteria are stained preferentially. In N2 animals the bacteria adhere to the walls of the rectum and to a small patch of cuticle behind the anus (Figure 10B and C). There is no visible staining at the surface of *srf-3* animals (Figure 10A) and therefore it can be concluded that *M. nematophilum* fails to infect *srf-3* mutants because the bacteria cannot adhere. The adherence of *Yersinia* is mediated by the biofilm polysaccharide and there is no evidence for signalling between *Yersinia* and *C. elegans* (L. Tan and C. Darby, personal comm.). Therefore, it can be concluded that resistance against two unrelated bacterial strains that use different pathogenic strategies can be conferred by mutations in a single factor, *srf-3*.

srf-3 codes for a protein similar to nucleotide sugar transporters (NSTs)

To better understand the mechanism underlying the resistance it was crucial to determine the molecular identity of *srf-3*. *srf-3* was initially mapped to the right of *unc-22* on Chromosome IV (Politz et al., 1990). Three factor crosses placed *srf-3* between *unc-31* and *lev-1*, close to *unc-31* (Libby, 1998). In order to clone *srf-3*, 15 cosmids were chosen which cover a 300kb region to the right of *unc-31* (Figure 11). Injection of cosmid pools as well as injection of single cosmids showed that one cosmid, M02B1, was sufficient to restore the infection of *M. nematophilum* in *srf-3* animals. M02B1 carries 39 kb of genomic DNA containing 5 predicted ORFs. To narrow down the region required for *srf-3* activity subclones of M02B1 were generated (Figure 12). Transgenic animals carrying an array generated with a clone constructed by deleting 17 kb in M02B1 via *Pac*I failed to rescue which indicated that the ORFs M02B1.4 and M02B1.3 are not coding for *srf-3*. In contrast, a subclone covering 13.8 kb of M02B1 (pBY1454) showed rescuing activity. This clone carried two predicted open reading frames, M02B1.1 and ZK896.9, both annotated as coding for proteins similar to mouse CMP-sialic acid transporters (http://www.wormbase.org). To identify the ORF providing *srf-3* activity two separate deletions within pBY1454 were generated.

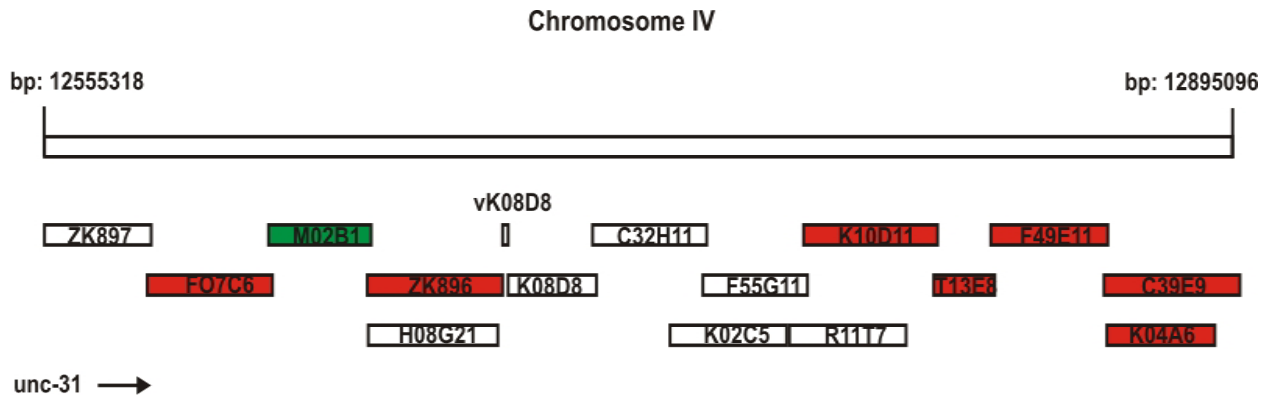

Figure 11: The cosmid M02B1 rescues the *srf-3* resistance to *M. nematophilum*. A schematic diagram of the physical map in the genomic region of *srf-3* covering approximately 300kb. The squares represent the cosmids in the region where *srf-3* was mapped. Red squares are cosmids which failed to rescue and the cosmid in green indicates the one which carries rescuing activity. Cosmid designation is written within the square. The position and the size of the cloned gene *unc-31* (ZK897.1) is indicated. A transgenic line derived from an injection of a pool of cosmids (K10D11, T13E8, F49E11, C39E9 and K04A6) failed to rescue the resistance of *srf-3* animals to *M. nematophilum*, as well as lines derived from the injections of the single cosmids F07C6 and ZK896. Lines derived from the injection of M02B1 rescued the resistance.

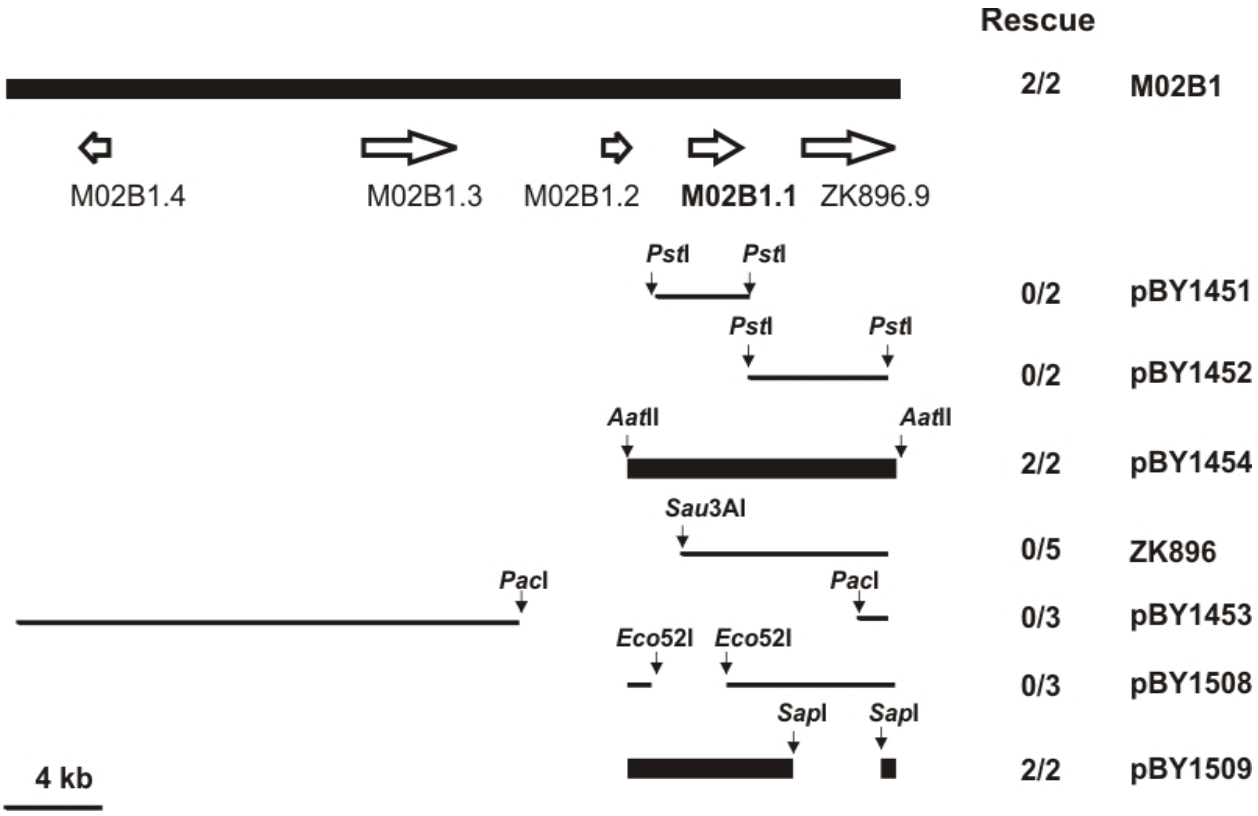

Figure 12: M02B1.1 provides *srf-3* activity. Bar on top represents M02B1. Bold bars represent rescuing subclones. The number of transgenic lines tested for rescue is shown at the right (rescue/tested). The name of the generated constructs is indicated at the right side. Position of the restriction sites which have been used to generate the corresponding subclone are indicated with an arrow. Position and size of the predicted ORFs are shown below the bar representing the cosmid. The rescuing ORF is written in bold.

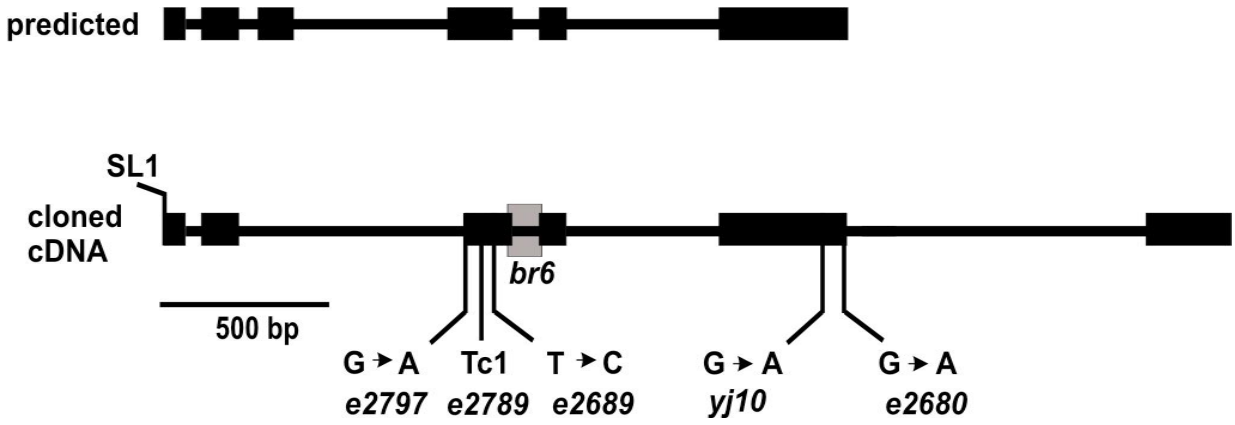

Figure 13: The genomic *srf-3* structure differs from the predicted exon-intron boundaries. The upper diagram represents the predicted exon-intron structure whereas the lower diagram represents the exon-intron structure according to the cloned cDNA. Exons are shown as black boxes, introns are shown as lines. Type and site of mutation in the different *srf-3* alleles are indicated by a bar. Position and size of the deletion in the allele *br6* is shown by a grey box.

A 3.2 kb deletion via *Eco*52I destroyed the M02B1.1 ORF (pBY1508) and a 4.2 kb *Sap*I deletion destroyed the ZK896.9 ORF (pBY1509). Animals of transgenic lines injected with an *Eco*52I deletion in pBY1454 did not show rescue whereas animals of transgenic lines generated with a *Sap*I deletion in pBY1454 showed rescue. Therefore it was concluded that M02B1.1 is the ORF providing *srf-3* activity.

M02B1.1 was annotated in the database as a gene encoded by 6 exons, however no expressed sequence tag (EST) was available (http://www.wormbase.org). To confirm the exon-intron structure of *srf-3* the cDNA was cloned. Initial attempts to amplify the cDNA from cDNA libraries or reverse transcribed RNA with primer annealing to the region of the predicted ATG and STOP codon failed. *Caenorhabditis briggsae* has diverged from *C. elegans* approximately 50 million years ago and is morphological almost indistinguishable from *C. elegans*. Areas of protein coding sequence seem to be conserved between both species whereas intergenic regions and introns are not. The genome of this nematode has been sequenced and can therefore be used to identify conserved regions between *C. briggsae* and *C. elegans* (Stein et al., 2003). To check if the exon-intron boundaries of *srf-3* are conserved the *C. elegans* genomic region was compared to the corresponding *C. briggsae* region. This suggested that the exon-intron structure of *srf-3* differs significantly from the genefinder prediction. Additional evidence came from the cloning results in which a *Pst*I derived fragment of M02B1 (pBY1451) failed to rescue. According to the *C. briggsae-C. eleg*ans alignment the 3' *Pst*I site removed a unpredicted exon which offered an explanation why this construct did not rescue the *srf-3* resistance to infection by *M. nematophilum*. RT-PCR from N2 RNA and subsequent sequencing revealed that the predicted exon 3 is missing and an

additional exon exists downstream of the predicted STOP codon thereby corroborating the exon-intron structure of the *C. briggsae-C. elegans* alignment (Figure 13). Most nematode messenger RNAs (mRNAs) have at their 5' end a common 22 nucleotide leader sequence, the trans-spliced leader or SL1 (Davis, 1996). The presence of this leader in the *srf-3* cDNA was verified by the fact that it was possible to amplify the cDNA using a SL1 specific oligonucleotide as a forward primer. Therefore it was concluded that the cloned cDNA includes the 5' end (Figure 13). The *srf-3* cloning results were confirmed by three additional, independent experiments: a) Injection of dsRNA prepared from the *srf-3* cDNA into *rrf-3(pk1426)* animals, which show increased sensitivity to RNA interference (RNAi), rendered the progeny resistant to infection by *M. nematophilum*. b) *srf-3* animals carrying an array which expresses the *srf-3* cDNA under the control of the *srf-3* genomic 5' and 3' regulatory elements (pBY1865, see appendix) were susceptible to infection by *M. nematophilum*. c) Sequencing of the *srf-3* locus in the different *srf-3* alleles revealed mutations within the ORF (Figure 13). The reference allele *yj10* had a G-A transition in exon 5 (position 707 of the cDNA) which leads to a nonsense codon in the protein. *e2689* carried a C-T transition in exon 3 (position 424 of the cDNA) leading to a nonsense mutation in the protein. *e2680* showed a G-A transition in exon 5 (position 734 of the cDNA) leading to a missense codon (conserved glycine to glutamate) at amino acid 245 of the protein. *e2789*, an allele found in a transposon induced screen (mutator strain *mut-7* (Ketting et al., 1999)), showed the presence of a transposable element (Tc1) sequence disrupting the ORF in exon 3. Allele *br6* carried a 110 bp deletion starting 16 bp upstream of the splice donor in exon 3 and extending 16 bp downstream of the splice acceptor in exon 4. The temperature sensitive allele *e2797*, showed a destroyed splice acceptor sequence in exon 3 due to a G-A transition. The mutations observed in *yj10*, *br6*, *e2789* and *e2689* would lead to a severe truncation of the encoded protein and are therefore most likely null alleles. One way to test genetically whether an allele is a partial or complete loss of function allele is to cross the corresponding mutant with a deletion covering the locus. If the gene product possesses residual activity a further reduction of the abundance of this product by reducing the copy number of the gene would result in a more severe phenotype whereas in a case of a null mutation no difference in the phenotype can be observed. *srf-3(e2789)* animals were mated with a strain carrying a deletion, *sDf22*, covering the *srf-3* locus. *srf-3(e2789)/sDf22* heterozygous animals had phenotypes no more severe than *srf-3(e2789)* homozygous animals. This showed that the *srf-3(e2789)* allele is a null allele and therefore, due to their identical phenotypical behaviour, *br6*, *e2689*, and *e2680* are also most likely null alleles.

srf-3 codes for a 328 aa type III transmembrane protein belonging to the members of the family of nucleotide sugar transporters (NSTs) (Figure 14). Secreted and membrane proteins and lipids are often glycosylated in the lumen of the endoplasmatic reticulum (ER) and/or Golgi apparatus. However, the substrates for these glycosylation reactions, the nucleotide sugars, are synthesized in the cytosol or, in the case of cytosinemonophosphate (CMP) sialic acid, in the nucleus. Therefore, there must be a transport mechanism capable of translocating these nucleotide substrates from their site of synthesis into the lumen of the organelles where glycosylation occurs. The existence of such transporters was first confirmed when the molecular defect in some glycosylation defective cell lines was discovered. CHO Lec8, CHO clone 13 (Stanley, 1985) and MDCK II-RCAr (Brandli et al., 1988) cells which have been isolated due to their resistance to plant lectins show a 70-90% deficiency of galactose in their glycans. This phenotype was shown to be due to a defect in uridindiphosphate (UDP)-galactose transport into Golgi vesicles (Hirschberg et al., 1998). Molecular cloning by phenotypic correction of the corresponding mutants led to the identification of cDNAs coding for nucleotide sugar transporters and, since then, various NSTs with different transport activities and from distinct species have been described (Berninsone and Hirschberg, 1998; Gerardy-Schahn et al., 2001). Nucleotide sugar transporters are type III transmembrane proteins containing 6-10 membrane spanning domains and they localize to the ER or the Golgi apparatus (Figure 14 and 15). The N- and C-terminus of a NST faces the cytosolic site and these proteins functions as antiporters exchanging the nucleotide sugar with the corresponding nucleotide monophosphate. The function of nucleotide sugar transporter is necessary for subsequent addition of the corresponding sugar to proteins and lipids *in vivo* and disruption of this function can lead to severe phenotypic consequences (see Discussion).

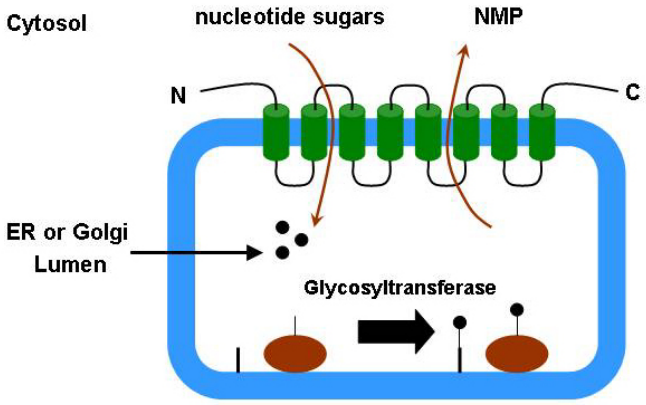

Figure 14: Schematic view of NST structure and function. Blue box represents the membrane of ER or Golgi. Green tubes indicate transmembrane domains. Red circles represent glycosyltransferases and black circles indicate nucleotide sugars.

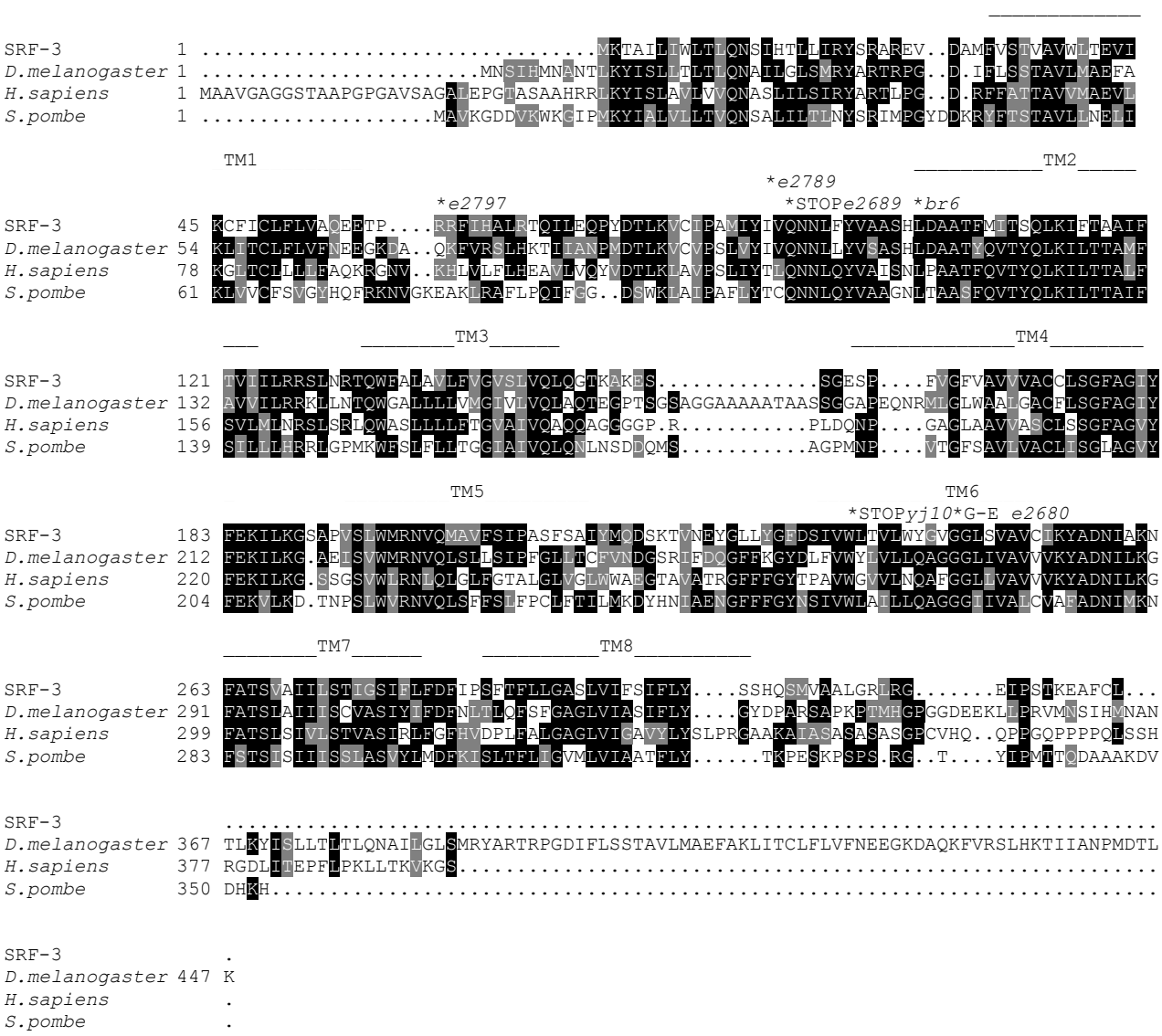

Figure 15: SRF-3 is similar to the family of nucleotide sugar transporters. Alignment of SRF-3 with functionally characterized UDP-galactose/UDP-N-acetylgalactosamine (GalNAc) transporter from *Drosophila melanogaster* (Accession number: BAB62747; (Segawa et al., 2002)), UDP-galactose transporter from *Homo sapiens* (Accession number: P78381; (Miura et al., 1996)) and UDP-galactose transporter *Schizosaccharomyces pombe* (Accession number: P87041; (Segawa et al., 2002)). Identical residues are shaded in black whereas similar residues are shaded with grey. Predicted transmembrane domains of SRF-3 are shown with lines. Missense and nonsense mutations or the end of the native protein are indicated with asterisks. The names of the corresponding alleles are written in italics.

srf-3 is expressed in a set of active secretory cells

In order to understand in which cells *srf-3* function is required, the expression of a *srf-3::gfp* construct was analysed. To do so the *srf-3* genomic region was cloned into *C. elegans* expression vectors generated by Andrew Fire (Fire et al., 1990 and ftp://www.ciwemb.edu/pub/FireLabInfo/FireLabVectors/). In the first place a construct was made where a SRF-3 green fluorescent protein (GFP) translational fusion is expressed under the control of the *srf-3* regulatory elements (Figure 16.1). GFP is a autofluorescent protein from the jellyfish *Aequoria victoria* which enables the direct observation of the spatial and temporal distribution of proteins in living animals (Chalfie et al., 1994; Prasher et al., 1992). The GFP signal is first visible in embryogenesis, in a lateral stripe of hypodermal cells, called lateral seam cells. Seam cells lie along the apical midline of the hypodermis, at the extreme left and right sides between nose and tail (see Figure 25 in the Discussion). Seam cell expression started in late embryos and continued until L4 stage, and later disappeared in adult animals after the L4/adult moult was completed (Figure 16.2 A-C). *srf-3* expression was also visible in the glandular cells g1 and g2, in the second bulb of the pharynx,. Expression in these gland cells started in L1 larvae and was maintained through adulthood (Figure 16.2 C and D). In adult animals expression became also visible in the spermatheca (Figure 16.2 C and E). The intracellular GFP localization showed a perinuclear staining reminiscent of an ER or Golgi resident protein (Figure 16.2 F). Expression in males resembles the observed pattern in hermaphrodites: glandular cells, seam cells and the vas deferens, a male structure which is functional similar to the spermatheca in hermaphrodites (data not shown). To test whether the observed expression pattern reflects the distribution of the native gene the corresponding array was crossed into a *srf-3* mutant background. *srf-3 (e2789) unc-30(e191)* animals carrying an array expressing *srf-3::gfp* were susceptible to infection by *M. nematophilum* and therefore it was concluded that the array is expressed in all tissues required for proper *srf-3* function. However, it is still possible that the reporter gene is present at low levels in other tissues than the described ones and therefore cannot be detected with GFP. To exclude this possibility, a C-terminal, translational fusion of SRF-3 and β-galactosidase protein encoded by the *E. coli lacZ* gene was constructed (Silhavy and Beckwith, 1985) (Figure 17.1). An extremely sensitive assay for the detection of β-galactosidase activity is the cleavage of the chromogenic substrate X-Gal (5-bromo-4-chloro-indolyl-β-D-galactoside) which leads to an accumulation of a blue precipitate.

16.1

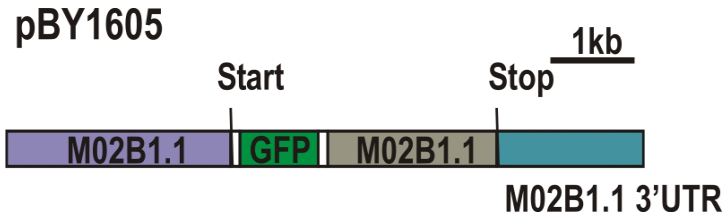

16.2

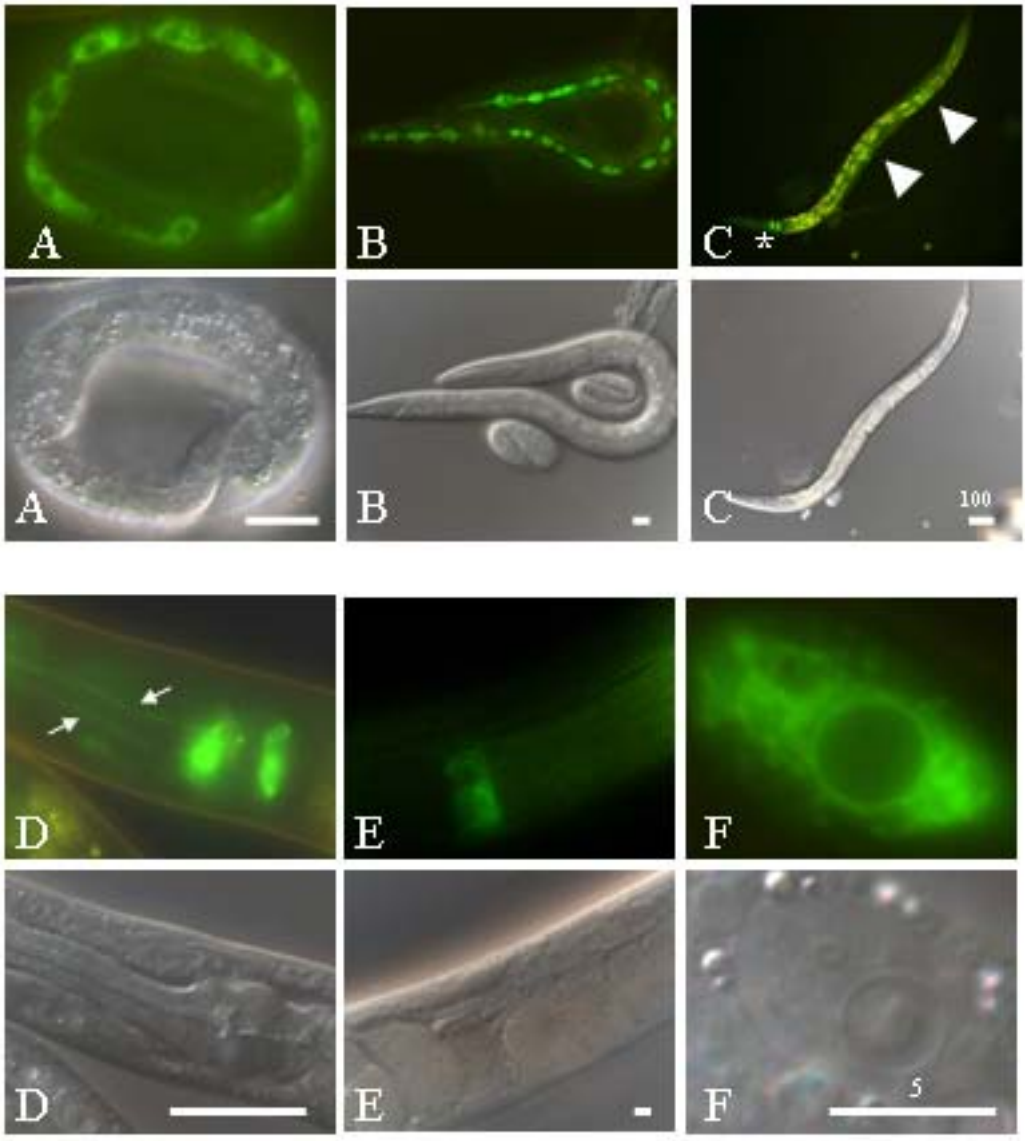

Figure 16: SRF-3::GFP is localized to the lateral seam cells, glandular cells g1 and g2 and spermatheca. 16.1: Structure of the expression construct pBY1605. GFP was fused to the N-terminus of SRF-3 (M02B1.1) and expressed under the control of *srf-3* 5' and 3' regulatory elements. Magenta coloured bar indicates *srf-3* promoter and the khaki coloured bar represents the *srf-3* genomic coding region. The white boxes show the position of the multiple cloning sites (MCS) region **16.2**: Localization of a SRF-3::GFP fusion. For each GFP the corresponding DIC is shown below. Unless otherwise indicated the scale bar represents 10µm. (A) Seam cell expression in late embryo prior to hatching. (B) Seam cell expression in L2 larvae. (C) SRF-3 expression in an adult hermaphrodite. Spermatheca expression is indicated by white arrows, expression in the glandular cell g1 by an asterisk. (D) g1 expression at higher magnification reveals strong fluorescence in the cell bodies and a very weak fluorescence of processes (white arrows). (E) Spermatheca expression at higher magnification. (F) Intracellular SRF-3::GFP localization shows a perinuclear staining. Photograph is taken from a seam cell of an L2 larva.

17.1

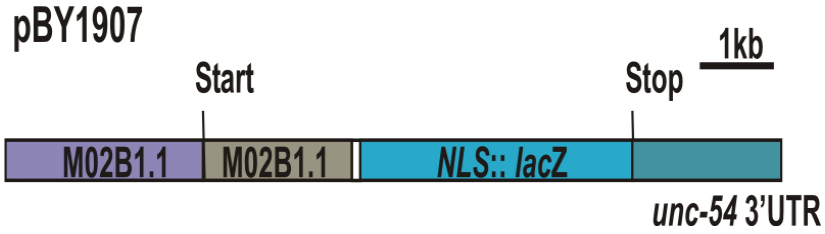

17.2

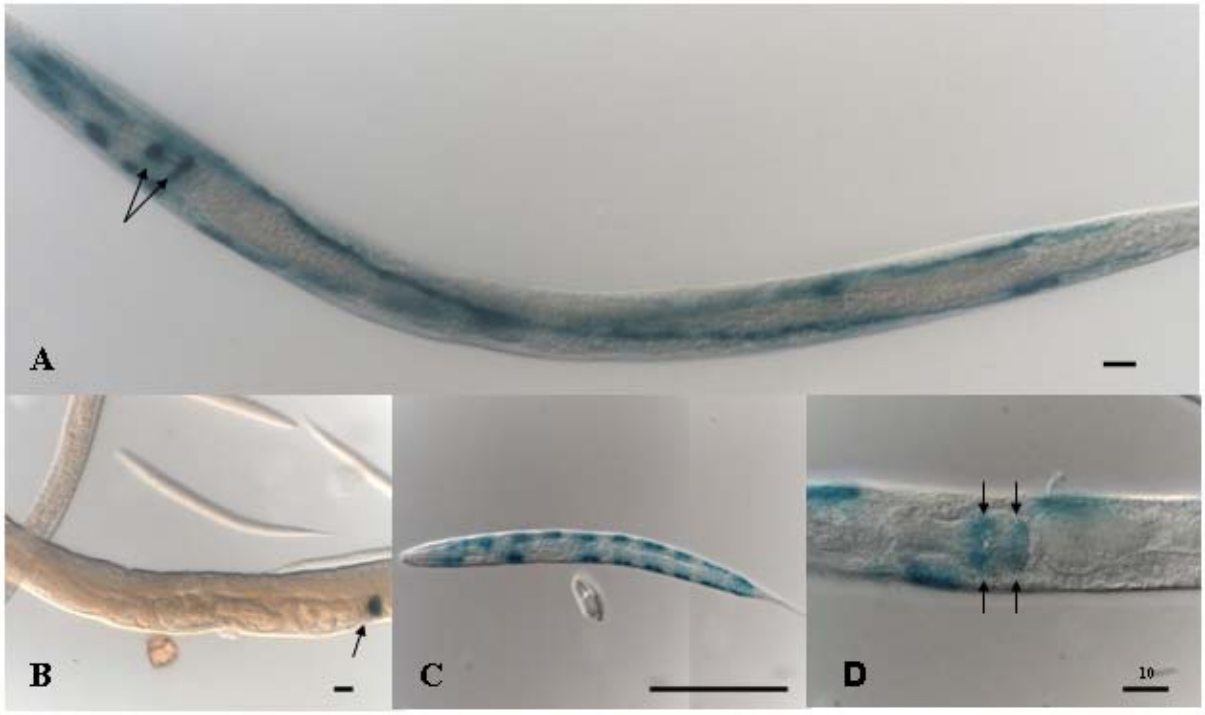

Figure 17: SRF-3::NLS::LACZ is localized to seam cells, glandular cells g1 and g2 and spermatheca. 17.1: Structure of the expression construct pBY1907. β-galactosidase was fused to the C-terminus of SRF-3 (M02B1.1). Magenta coloured bar indicates *srf-3* promoter and the khaki coloured bar represents the *srf-3* genomic coding region. The white box shows the position of the multiple cloning site (MCS) region. **17.2**: β-galactosidase staining of a L4 larvae (A). The blue lines are the lateral seam cells. Glandular cells are indicated with arrows. Spermatheca (arrow) expression in an adult hermaphrodite (B). Seam cell expression in an L2 larva showing both rows of lateral seam cells (C). Glandular cell expression at higher magnification (D). Visible are four cell bodies (arrows) in the posterior bulb. The anterior cells are dorsal and ventral g1 and the posterior ones are the dorsal and ventral g2. Unless otherwise indicated scale bar represents 100 µM.

Due to the enzymatic activity of the β-galactosidase the signal in the *lacZ* reporter system undergoes a strong amplification leading to a more sensitive assay as compared to GFP, where every molecule represents a single fluorophore. Animals transgenic animals for *srf-3::NLS::lacZ* showed β-galactosidase staining in the lateral seam cells (Figure 17.2 A,C), the glandular cells g1 and g2 (17.2 A,D) and the spermatheca (Figure 17.2 B). Therefore, the

expression pattern of the β-galactosidase fusion was indistinguishable from the GFP reporter fusion and it was concluded that the observed expression pattern represents the full expression detectable by reporter gene analysis. As shown in Figures 16.1 and 17.1, the used expression constructs differ with respect to their 3' untranslated region (UTR). The construct pBY1605 contains the *srf-3* 3'UTR whereas pBY1907 carries an *unc-54* 3'UTR implemented in the Fire vectors to ensure efficient processing of *C. elegans* transcripts in the analysis of reporter expression constructs. The expression of both construct was indistinguishable suggesting that the *srf-3* 3'UTR does not contain any important regulatory elements that cannot be substituted by unc-54.

The cuticle of *srf-3* animals is fragile to handling as indicated by the fact that mutant animals show a low survival rate after injections and *srf-3* dauer larvae are sensitive to SDS treatment (Politz et al., 1990). The observed *srf-3* expression led to the speculation that the described fragility of the cuticle can be attributed to a defect in the seam cells. To address this question an integrated array expressing *ajm-1::gfp*, which localizes localizing to the apical borders of the *C. elegans* epithelium (Mohler et al., 1998) was crossed into a *srf-3* mutant background. *ajm-1::gfp* expression in *srf-3* animals was indistinguishable from N2 animals (data not shown) suggesting that at least number and shape of seam cells in *srf-3* mutants are unaffected (see Figure 25 for the position of the apical junctions).

To test if *srf-3* expression is altered upon infection, transgenic animals carrying an array containing *srf-3::gfp* were infected with *M. nematophilum*. Pattern and intensity of *srf-3::gfp* was undistinguishable from uninfected worms suggesting that *srf-3* expression is not modulated by the infection.

SRF-3 transports UDP-galactose and UDP-N-acetylglucosamine

The analysis of the *srf-3* primary sequence suggested a high similarity to nucleotide sugar transporters (Figure 14). This finding infers a critical role of glycosylation in regulating surface antigenicity. Determination of the substrate specificity of SRF-3 can demonstrate that this protein is able to function as a nucleotide sugar transporter and may help to understand in which way carbohydrate structures or glycosylated proteins are utilized by the bacteria. The substrate specificity of a certain NST cannot be deduced from the sequence alone but has to be determined experimentally. For example, the murine CMP-sialic acid transporter shows 40% amino acid sequence identity to a human UDP-galactose transporter, yet both transporters are highly substrate specific (Hirschberg et al., 1998). SRF-3 is 61% similar to Drosophila UDP-Gal/UDP-GalNac and 60% similar to a murine CMP-sialic acid transporter, however a mass spectrometry analysis suggested that *C. elegans* does not have sialic acid (Bacic et al., 1990). To identify the substrates translocated by SRF-3, the VSV tagged protein was expressed in *S. cerevisiae*. To determine the substrate specificity ER/Golgi enriched vesicles were isolated maintaining their in vivo topography and assayed for their ability to transport radiolabelled nucleotide sugars (see Material and Methods). Before the transport assay was performed it was ensured by immunoblotting that the protein is expressed in yeast (Figure 18). The VSV antibody detected a signal with an apparent molecular weight of 29 kDa in membrane fractions of cells transformed with a construct expressing *vsv-srf-3* but not in cells transformed with the vector alone. The molecular weight is consistent with a 32 kDa protein predicted from the translation of the *srf-3* cDNA and therefore it was concluded that SRF-3 is expressed in *S. cerevisiae*. *S. cerevisiae* exhibit an intrinsic UDP-glucose transporter activity (Hirschberg et al., 1998), a characteristic which can be used to test the quality of the isolated vesicles. Vesicles prepared from yeast cells expressing *vsv-srf-3* and cells transformed with the vector alone transported UDP-glucose in a comparable manner and were therefore of similar quality (Figure 19A). UDP-galactose and UDP-N-acetylglucosamine were transported into ER/Golgi enriched vesicles prepared from yeast cells expressing *srf-3* but not from vesicles prepared from yeast cells transformed with the vector control.

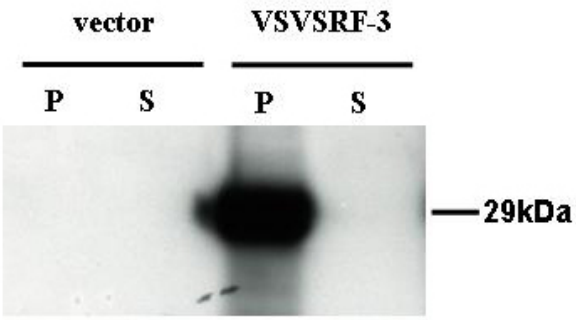

Figure 18: VSV-SRF-3 is expressed in *S. cerevisiae*. Immunoblotting of protein extracts made from *S. cerevisiae* cells transformed with vector alone or cells expressing *srf-3* cDNA fused with a single VSV-G tag (VSV-SRF-3) coding sequence. P represents the membrane fraction and S represents the cytosolic fraction.

A

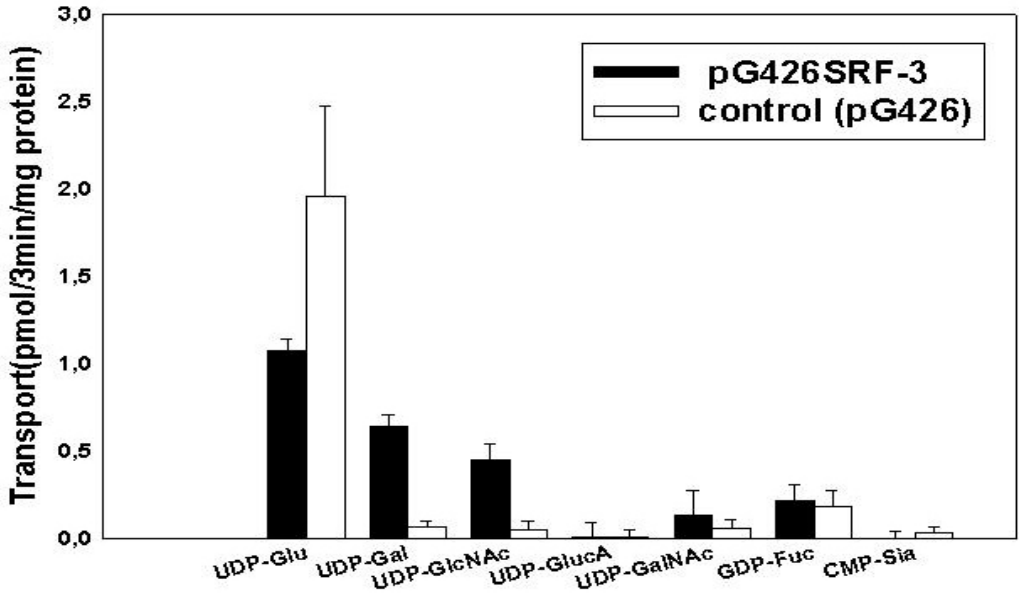

B

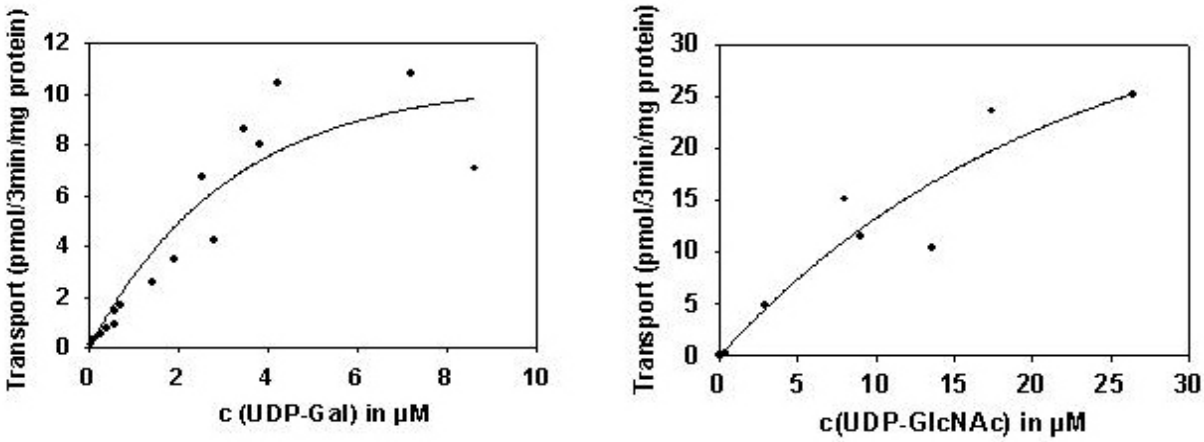

Figure 19: SRF-3 is able to transport UDP-galactose and UDP-N-acteylglucosamine into *S. cerevisiae* ER/Golgi-enriched vesicles. 19 A) Transport activity is displayed as amount of nucleotide sugars inside the vesicles at 30°C minus the corresponding amount at 0°C. Results shown are an average of six independent assays from two independent vesicle preparations. Black bars represent *S. cerevisiae* transformed with pG426 and white bars represent cells transformed with pG426-*vsv-srf-3*. **B)** Saturation curve for the transport of UDP-Gal and UDP-GlcNAc. Transport of substrate is plotted against the concentration of the corresponding nucleotide sugar. Abbreviations are: UDP-Glu (UDP-glucose), UDP-Gal (UDP-galactose), UDP-GlcNAc (UDP-N-acetylglucosamine), UDP-GlcA (UDP-glucuronic acid), UDP-GalNAc (UDP-N-acetylgalactosamine), GDP-Fuc (GDP-fucose), CMP-Sia (CMP-sialic acid).

No transport of UDP-glucuronic acid, UDP-N-acetylgalactosamine, GDP-fucose or CMP-sialic acid was detected in either *srf-3* or vector control vesicles. The analysis of the transport characteristics revealed that the substrates were transported with an apparent K_m of 5.9 µM for UDP-Gal and 20µM for UDP-GlcNAc (Figure 19B). SQV-7, a previously described *C. elegans* nucleotide sugar transporter with multisubstrate specificity has a K_m of 4 µM for UDP-GlucA, 8.7 µM for UDP-GalNAc and 4.6 µM for UDP-Gal and, therefore, the measured K_m values are in close agreement with previously described nucleotide sugar transporters (Berninsone et al., 2001). Hence, *in vitro*, SRF-3 is able to transport UDP-Gal and UDP-GlcNAc in a saturable and temperature dependant manner.

Another approach to determine the substrate specificity is to express the cDNA of interest in a mutant defective in a specific transporter and then assay phenotypic correction. To confirm the results from the *S. cerevisiae* experiments SRF-3 was expressed in mutants defective for UDP-Gal and UDP-GlcNAc transport. A *Kluyveromyces lactis* mutant with a defect in a Golgi resident UDP-GlcNAc transporter has been described (Abeijon et al., 1996a). This mutant shows a lack of N-acetylglucosamine in its outer mannan chains (Smith et al., 1975) leading to a differential binding of *Griffonia simplicifolia* II (GSII) lectin which recognizes terminal α– and β-linked N-acetylglucosamine. By transforming *K. lactis* with a cDNA library made from MDCK cells and subsequent labelling with FITC-conjugated GSII lectin a mammalian UDP-GlcNAc transporter was isolated (Guillen et al., 1998). This showed that the *K. lactis* system can be used for expression and identification of heterologous NSTs. *K. lactis* KL3 cells transformed with a construct expressing *srf-3-vsv* showed a increased GSII binding as compared to cells transformed with the vector alone (Figure 20A). Therefore, it can be concluded that SRF-3 is able to transport UDP-GlcNAc into the Golgi of *K. lactis* cells. The *S. cerevisiae* data also suggest UDP-Gal as a substrate for SRF-3 (Figure 19). The Madin-Darby canine kidney (MDCK) cell line RCAr was isolated due to the resistance to the toxin ricin (Meiss et al., 1982). RCAr cells grow at ricin concentrations 10 times higher compared to wild type MDCK cells. Ricin consists of two subunits, the α subunit, an N-glycosidase which is required for inhibition of protein synthesis and the β subunit, a lectin domain required for uptake of ricin into the cell (Sandvig and Van Deurs, 2002). Uptake of ricin requires binding to terminal galactosyl residues and resistance of RCAr cells is in agreement with an undergalactosylation of glycoproteins and glycolipids (Brandli et al., 1988). It was shown that this defect is linked to a Golgi localized UDP-Gal transporter and this system has been used to find substrates of previously unknown nucleotide sugar transporters (Berninsone et al., 2001; Ishida et al., 1996). MDCK RCAr cells transfected with

the vector alone grew at all concentrations tested whereas cells transfected with constructs expressing N- or C-terminal tagged SRF-3 were only viable up to a concentration of 0.25 ng/ml (Figure 20B). Hence, SRF-3 can restore the ricin sensitivity in RCAr mutants and is therefore able to transport UDP-Gal into the Golgi lumen of MDCK cells. Taken together these results demonstrate that SRF-3 is able to transport UDP-Gal and UDP-GlcNAc into the lumen of the ER and/or Golgi *in vitro* and *in vivo*.

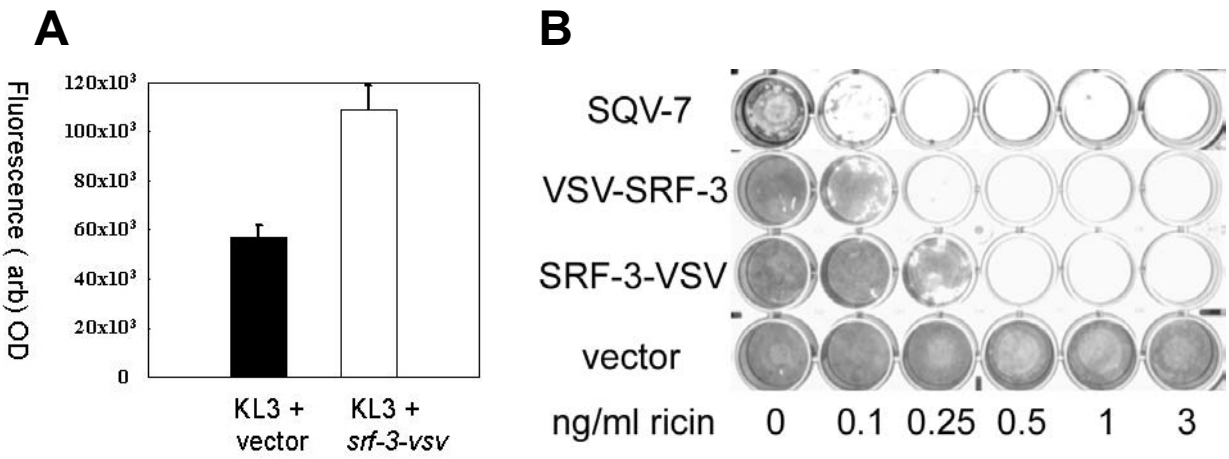

Figure 20: SRF-3 corrects the phenotypes of mutants defective in UDP-GlcNAc and UDP-Gal transport. A) *K. lactis* mutant KL3 which is defective for UDP-GlcNAc transport was transformed with *srf-3-vsv* (white bar) and shows restored *Griffonia simplicifolia* II (GSII) lectin labelling. The vector control (black bar) is KL3 mutant transformed with *K. lactis* expression vector pE4. **B)** MDCK cells transfected with N and C-terminal VSV-tagged SRF-3 were grown in the presence of different ricin concentrations and subsequently stained with Methylen blue. The SQV-7 UDP-Gal translocator activity has been described previously and served as a positive control. The vector control represents MDCK RCAr cells transfected with pCDNA3.1 vector alone. Three independently isolated clones were tested in each case.

Genetic interactions of *srf-3*

In order to find mutants genetically interacting with *srf-3*, previously described mutants with similar phenotypic properties and mutants of genes known to be involved in glycosylation were tested for resistance to *M. nematophilum*. Furthermore it was examined if double mutants between *srf-3* and other *srf* mutants or mutants affected in glycosylation would result in animals with more severe phenotypes.

bre (Bacillus-toxin resistant) mutants have been isolated in a screen for animals resistant to killing by the *Bacillus thuringiensis* δ-endotoxin Cry5B and one *bre* mutant, *bre-5(ye17)*, was shown to code for a putative β-1,3-galactosyltransferase (Griffitts et al., 2001; Marroquin et al., 2000). However, neither *bre-5(ye17)* nor any of the other *bre* mutants (Appendix, Table 5) showed resistance to infection by *M. nematophilum*.

Mutants with a lumpy, amorphous ray morphology (Ray morphology or Ram phenotype) have been shown to exhibit increased WGA-FITC binding (Ko and Chow, 2000). All of the tested *ram* mutants (all *ram* mutants listed in Table 5 in the Appendix have been tested) exhibit a strong Dar response on plates containing *M. nematophilum* and were therefore not resistant.

Various deletion mutants of glycosyltransferases have been generated, notably *gly-1(ev686)*, *gly-2(qa703)*, *gly-12*, *gly-13*, *gly-14*, *gly-16(qa701)* and *gly-18(qa704)* (see Table 5 and Warren et al., (2001); Warren et al., (2002); Chen et al., (2002); Chen et al., (2003)). Despite of *gly-13*, which is embryonic lethal, none of the *gly* mutants exhibit a visible phenotype and none of the mutants was resistant to infection by *M. nematophilum*. Moreover, animals of double mutants between *srf-3* and *gly-2*, *gly12*, *gly-14*, *gly-16* and *gly-18* did not show any obvious phenotypes as judged by visual inspection.

srf mutants can be grouped into pleiotropic and non-pleiotropic mutants (see Introduction). A triple mutant between the pleiotropic mutants, *srf-4*, *srf-8* and *srf-9* was indistinguishable from the corresponding single mutants suggesting that these genes act in a linear pathway (Link et al., 1992). To further understand the genetic relationship between the *srf* mutants, a *srf-3; srf-4*, a *srf-2; srf-3*, a *srf-3; srf-5* and a *srf-2; srf-5* double mutant was generated (see Table 5). Double mutants between the non-pleiotropic *srf* mutants were viable, showed similar lectin binding and did not show any other obvious phenotypes. However, a *srf-3; srf-4* double mutant was zygotic embryonic lethal demonstrating that the combined disruption of the biological processes to which *srf-3* and *srf-4* contribute, are essential for proper *C. elegans* development.

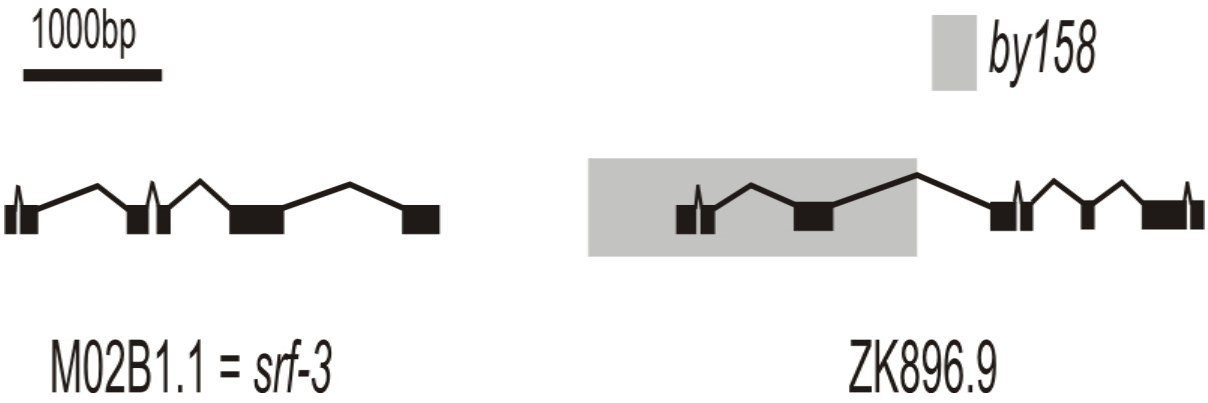

Figure 21: Genomic region of *srf-3*. A schematic representation of approximately 8 kb of genomic region of *srf-3*. ZK896.9 a nucleotide sugar transporter similar to SRF-3 is 1.7 kb downstream of the M02B1.1 ORF. The grey box indicates size and position of the deletion in the *by158* allele. Exons are represented by black boxes.

Analysis of the genomic region of the *srf-3* locus revealed the existence of an additional putative NST, ZK896.9, adjacent to *srf-3*. Cloning and sequencing of the ZK896.9 cDNA showed that the cDNA is spliced in *trans* to a SL1 and SL2 leader sequence and therefore contained the true 5' end. The observed SL2 suggests that both transporters, *srf-3* and ZK896.9, are organized within an operon. In *C. elegans* an operon is a cluster of closely spaced genes, transcribed from a regulatory region at the 5' end of the cluster, and whose monocistronic mRNAs are generated from an polycistronic precursor mRNA accompanied by *trans*-splicing to SL2 or a mixture of the two SLs (Blumenthal and Steward, 1997). Furthermore, the cloning of the cDNA confirmed that the exon-intron structure was correctly predicted by genefinder. ZK896.9 shows 38% identity and 52% similarity on protein level to SRF-3. It was tested whether ZK896.9 has a complementary expression pattern to *srf-3* and might therefore provide SRF-3 function in other tissues. To address this question, an expression construct in which GFP is fused to the C-terminus of ZK896.9 and which contained 2.8 kb of 5' sequence was generated (pBY1564, see Appendix). Transgenic animals carrying an array expressing ZK896.9::GFP showed a GFP signal in a pair of yet unidentified sensory neurons (Figure 22). Therefore ZK896.9 shows an expression pattern distinct from *srf-3*. To get a first insight into ZK896.9 function, RNAi was performed. Neither feeding bacteria containing dsRNA transcribed from the ZK896.9 cDNA nor injection of dsRNA made from the same cDNA, in N2 or *rrf-3(pk1426)* animals, resulted in worms with visible phenotypes. To test if simultaneous disruption of *srf-3* and ZK896.9 function would lead to animals with more severe phenotypes, *srf-3* animals were subjected to ZK896.9 RNAi (feeding). However no additional phenotypes were observed in the corresponding animals.

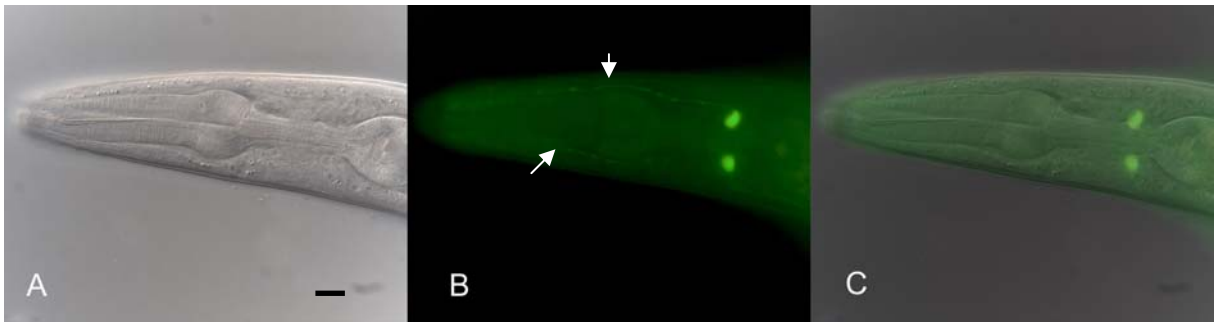

Figure 22: GFP expression pattern of ZK896.9. A) DIC photograph of an adult hermaphrodite. **B)** GFP signal in the same worm. Visible is a pair of yet unidentified sensory neurons (processes are indicated with arrows. **C)** Overlay of A and B. Bar represents 10 μM.

Due to the fragile cuticle resulting in low survival rates, injection of ZK896.9 dsRNA into *srf-3* worms was not feasible. In order to further understand ZK896.9 function a deletion mutant of this gene was generated (see Material and Methods). *by158* deleted 2.4 kb of ZK896.9 genomic region removing 700 bp of sequence upstream of the ATG plus the first three exons and is therefore most likely a null allele (Figure 21). Animals homozygous for *by158* did not show any obvious, visible phenotypes and were not resistant to *M. nematophilum* suggesting that the function of this gene is not essential for *C. elegans* development. Injection of *srf-3* dsRNA into *by158* animals also didn't result in animals with more sever phenotypes, hence *srf-3* and ZK896.9 seem to have distinct and unrelated functions in the worm.

Discussion

The aim of the thesis was to understand the molecular mechanisms underlying the resistance of *srf-3* animals to the bacterial pathogens *Microbacterium nematophilum* and *Yersinia pestis/pseudotuberculosis*. *M. nematophilum* adheres to the cuticle of wild type animals but fails to adhere to the surface of *srf-3* worms. This is a novel type of resistance because pathogens like *P. aeruginosa* or *Salmonella typhimurium* do not adhere to the cuticle but kill *C. elegans* by colonization and accumulation in the intestine. *srf-3* was identified by molecular cloning which showed that this gene codes for a transmembrane protein belonging to the family of nucleotide sugar transporters. Expression analysis revealed that SRF-3 is expressed in a set of active secretory cells consistent with a function of this gene in cuticle or surface modification. Heterologous expression of the *srf-3* cDNA showed that SRF-3 is able to transport UDP-galactose and UDP-N-acetylglucosamine. The results presented in this thesis strongly suggest that the inability of *Y. pseudotuberculosis* and *M. nematophilum* to adhere to the cuticle is due to an altered glycoconjugate composition of the *srf-3* surface.

srf-3, glycosylation and bacterial adherence

In order to be able to cause an infection a certain pathogen has to colonize its host. Colonization of hosts by microorganisms starts with a non-specific aggregation on certain cell types, e.g. the gut epithelium, followed by a specific adhesion to distinct host cell receptors and thereby defines the tropism of an infectious agent. Adhesion is achieved by microbial adherence factors called adhesins (Hacker, 2002). Adhesins, which are produced by all forms of pathogens e.g. viruses, fungi, bacteria and eukaryotic parasites are surface-exposed proteins with a special structure that enables them to interact with certain host receptors. Adhesin-receptor interactions very often trigger signal transduction events on bacterial and on the host side which are critical for colonization and infection (Hauck, 2002). Adhesive structures used by bacteria are proteins like fimbrial and non-fimbrial adhesins or polysaccharides (lipopolysaccharides (LPS), exopolysaccharides (EPS)) or lipoteichoic acids (LTA). Host structures utilized for adhesion by extracellular replicating microorganisms are very often components of the extracellular matrix (ECM) like integrins, cadherins and molecules of the immunoglobulin superfamily (IgCAMs) (Hauck, 2002). All of these components are glycoproteins and consistent with this finding most of the known binding sites of adhesins are glycoconjugates (Karlsson, 1998; Ofek et al., 2003). For example, *Yersinia pestis* and *Bordetella pertussis* have filamentous haemagglutinin (FHA) related proteins which have

been shown to be able to recognize and bind heparan sulphate proteoglycans (Menozzi et al., 2002).

Mutations in *srf-3* were isolated because the corresponding animals showed an altered surface antigenicity and pathogen resistance and therefore it is not surprising that the adherence of bacteria to the surface of this mutant is affected. The fact that the *C. elegans* cuticle is covered by a carbohydrate rich surface coat strongly suggests that an altered glycosylation pattern in *srf-3* mutants is the cause for the failure of *M. nematophilum* to adhere to the worm's surface. But what kind of receptors does *M. nematophilum* recognize and how? *M. nematophilum* has been discovered recently and no sequence information and no tools for genetic manipulations are available which might help to address these questions. There are some information about adhesion of *Y. pestis* and *Y. pseudotuberculosis* which both fail to form a biofilm on *srf-3* animals. By testing attenuated *Y. pseudotuberculosis* strains found in a transposon induced screen in a murine yersiniosis model Wren and coworkers identified six strains also showing altered biofilm formation in *C. elegans* (Joshua et al., 2003). Two of these mutants showed defects in genes required for LPS biosynthesis. LPS is an important component in the outer bacterial membrane and has powerful biological effects in mammals, including fever, septic shock and a variety of deleterious effects. Furthermore, it plays a crucial role in initial surface attachment of *P. aeruginosa* and *E. coli* (Davey and O'Toole, 2000) and an important role in effective colonization of host tissues in *Yersinia* species (Skurnik, 2003). However, the exact role of LPS in adherence remains largely unexplained and the *C. elegans – Yersinia/M. nematophilum* interaction might provide a valuable tool to further examine and understand the host and the bacterial processes involved in adherence on a biotic surface.

srf-3 is a nucleotide sugar transporter

To gain an insight into the molecular mechanisms underlying the altered surface antigenicity and the altered pathogen resistance, the molecular identity of *srf-3* was determined in this thesis. *srf-3* codes for a NST. All alleles carried mutations in the locus leading to a truncated or aberrant protein. *e2797*, the temperature sensitive allele, is a splice mutant. In *C. elegans* ts mutants are frequently observed to carry mutations in splice sites (Choy and Thomas, 1999; Röhrig, 2000). *e2680* carries a G-A transition leading to a glycine to glutamic acid exchange in the predicted transmembrane domain 6 (see Figure 15). The sequence at this position in wild type SRF-3 is V**GGL**SVA (residues in bold are conserved, Figure 23) with the first glycine being exchanged in *e2680.* A similar mutation was found in CHO cells of the complementation group Lec8 (Oelmann et al., 2001) where a glycine to aspartic acid

exchange at the position 281 occurred (sequence D84454 in Figure 23). This position is highly conserved within mammalian NSTs specific for UDP-Gal and CMP-Sia transport, as well as in SRF-3 (Figure 23). Consistent with the results from *srf-3(e2680)* as being a complete loss of function allele, a similar mutation in the hamster gene rendered the UDP-Gal transporter non-functional. What are the consequences of this mutation? There is evidence that this position is crucial for the formation of an active transporter.

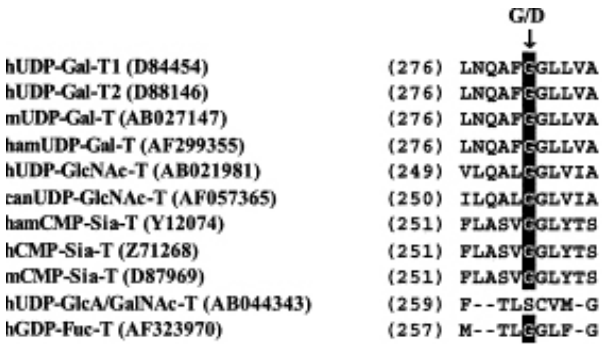

Figure 23: Sequence alignment of a highly conserved region in mammalian NSTs. Point mutation (*lec8*) identified in a hamster UDP-Gal transporter is given in the top lane. Numbers in parentheses indicate the amino acid with which the domains start. Taken from (Gerardy-Schahn et al., 2001)

Expression of a cDNA coding for the mutated hamster transporter in CHO K1 cells showed that the mutant protein is correctly localized arguing against a defective targeting of the molecule (Oelmann et al., 2001). Mutating the same position in a murine CMP-Sia transporter led to non functional protein showing that the corresponding amino acid residue is not involved in substrate recognition because CMP-Sia and UDP-Gal differ structurally with respect to their nucleotide and sugar part. Further evidence is coming from experiments with chimeras generated by exchanging segments of a human UDP-Gal and a human CMP-Sia transporter (Aoki et al., 2003; Aoki et al., 1999). Analysis of the substrate specificity and transport activity of these chimeras indicated that the C-terminal domain of NSTs is involved in generating an active transport site and might participate in the motile process required to translocate nucleotide sugars across the membrane. So one explanation why *e2680* is genetically a null allele is that the transporter is correctly targeted and maybe recognizes its substrates, but fails to translocate them across the membrane. However, additional binding and kinetic studies with mutant transporters have to be performed to definitely answer this question.

Transport of nucleotide sugars into the Golgi lumen is necessary for subsequent addition of sugars to proteins, lipids and glycosaminoglycans (GAGs). The pathophysiological relevance of NSTs is demonstrated in the case of congenital disorder of glycosylation type IIc (CDG IIc) which leads to immunodeficiency and severe mental and psychomotor defects. On the molecular level the disease is characterized by a generalized lack of fucosylated glycoconjugates, including immunological important selectin ligands and it was shown that this defect is due to a defect in a guanosinediphosphate (GDP)-fucose transporter (Lübke et

al., 2001; Lübke et al., 1999). An additional example is the human UDP-Gal/GalNAc Golgi transporter: Overexpression of the corresponding transporter is directly related to the metastatic capacity of colon cancer (Kumamoto et al., 2001).

Another example for phenotypic consequences of a defect in a transporter comes from the protozoal parasite *Leishmania donovani* which causes visceral leishmaniasis. The surface of this organism is covered by a mannose rich lipophosphoglycan (LPG). LPG is the critical receptor for *L. donovani* for recognition and entry into the macrophage and is generally required for the parasite's growth and survival in its host. This is shown by the fact that *L. donovani* mutants defective in LPG biosynthesis grow well *in vitro* but fail to grow in their vector, the sand fly, and fail to infect macrophages (Descoteaux and Turco, 1999). One avirulent mutant, *LPG2*, was shown to code for a GDP-mannose transporter (Descoteaux et al., 1995). This mutant synthesizes only truncated LPGs lacking the characteristic repeating saccharide units.

The aforementioned examples show that an alteration of NST activity can lead to severe changes in the subsequent addition of sugars to proteins and lipids *in vivo* and therefore to severe phenotypic consequences due to an altered glycosylation pattern.

Since now only one other *C. elegans* NST has been described in detail. Mutations in any of the eight squashed vulva genes (*sqv*) resulted in animals showing defects in vulva invagination and maternal effect lethality. The molecular identity suggested that these genes may act in a glycosylation pathway and one of the genes, *sqv-7*, encoded a protein similar to NSTs. As described above, defects in NSTs can lead to severe phenotypes and in accordance with this finding the null phenotype of *sqv-7* is embryonic lethal (Hwang and Horvitz, 2002). In contrast, the disruption of *srf-3* function results in animals which are viable and morphological indistinguishable from wild type animals. Analysis of the *C. elegans* genome led to the identification of 16 NST like proteins (Gerardy-Schahn and Eckhardt, 2000) with only three now being described in more detail. SQV-7 is a transporter with multisubstrate specificity capable of translocating UDP-Gal, UDP-GlcA and UDP-GalNAc (Berninsone et al., 2001), C50F4.14 was shown to transport GDP-Fuc (Lühn et al., 2001) and SRF-3 transports UDP-Gal and UDP-GlcNAc (this thesis). Therefore, it is possible that the transport activities provided by SRF-3 can at least in part be fulfilled by other yet unidentified transporters. However, a mass spectroscopy analysis of glycan composition revealed that the abundance of complex glycans containing galactose were severely reduced in *C. elegans srf-3* as compared to wild type animals (John Cipollo, Boston University, pers comm.) indicating that a loss of *srf-3* function leads to consequences on the molecular level *in vivo*.

The biochemical data show that SRF-3 is capable of transporting UDP-Gal and UDP-GlcNAc, a combination of substrate specificities not previously described. A phylogenetic analysis led to the arrangement of 87 NST like sequences into three clades with SRF-3 being grouped into family 1 (Martinez-Duncker et al., 2003). However, due to the low bootstrap values SRF-3 was not assigned to subfamily C, the UDP-Gal/GalNAc transporters (Figure 24). The biochemical results suggest now that SRF-3 indeed is a member of the subfamily of UDP-Gal transporters. It has been proposed that the transporters of subfamily C, due to their substrate specificity (UDP-Gal/UDP-GalNAc), utilize the position of the hydroxyl group (OH) group at C4 in the sugar ring to recognize their substrate. In Gal and GalNAc this OH group is in the axial position whereas in sugars like Glc, GlcNAc, GlcA and Xylose the OH group is in the equatorial position. SRF-3 transports UDP-Gal and UDP-GlcNAc which suggests that the position of the OH at C4 is not involved in substrate recognition of these transporters.

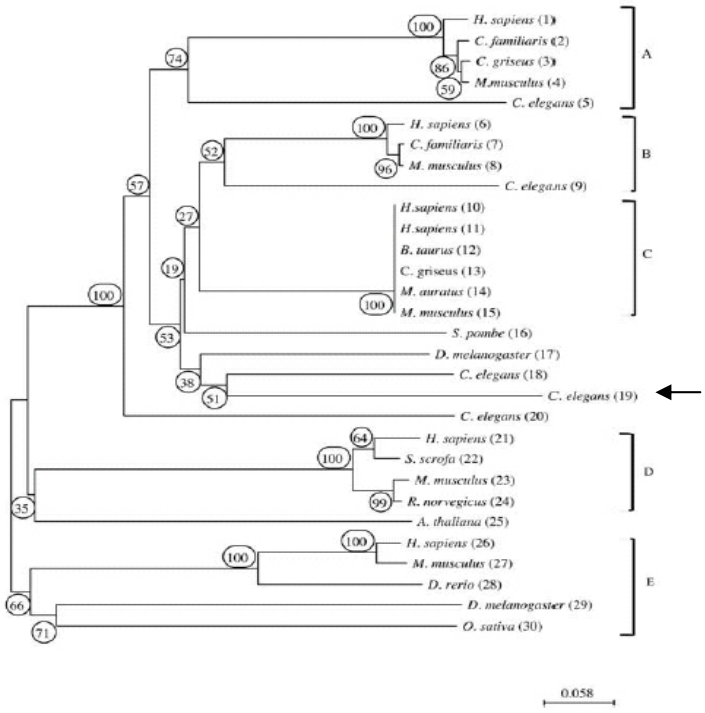

Figure 24: Neighbour joining phylogenetic tree of NST family 1. Subfamily A are CMP-Sia, subfamily B are UDP-GlcNAc and subfamily C are UDP-Gal/GalNAc transporters. Subfamily D and E have not been functionally characterized. Arrow indicates SRF-3. Bootstrap values next to divergence points have been circled. The scale bar represents the number of substitutions per site for a unit branch length. Figure was taken from (Martinez-Duncker et al., 2003).

Where is SRF-3 localized within the cell? The SRF-3::GFP signal indicates an ER or Golgi localization of the transporter which is consistent with the proposed function in glycosylation. There is no direct proof but some evidence that SRF-3 is localized in the Golgi membrane. The *K. lactis* UDP-GlcNAc and the MDCK UDP-Gal transporter have been shown to function in the Golgi (Abeijon et al., 1996b; Brandli et al., 1988) and therefore SRF-3 has to localize to this compartment in these heterologous systems in order to be able to correct the corresponding phenotypes. Furthermore, the SRF-3 protein lacks the consensus sequence for an C- terminal ER retention signal KKXX (Figure 15) and isolation of Golgi enriched vesicles

led to enrichment of VSV-SRF-3 as judged by immunoblotting whereas the isolation of ER enriched vesicles did not (Jörg Höflich, unpublished observation).

srf-3 expression pattern and phenotype

Analysis of the expression pattern by transgenic reporter lines revealed that *srf-3* is expressed in the lateral seam cells, the glandular cells g1 and g2, and the spermatheca. This expression pattern is consistent with the proposed function of *srf-3* in cuticle and/or surface modification. Each moult is preceded by a lethargus, a period during which pumping and locomotion are suppressed. There is evidence that the seam cells play the most active part in cuticle synthesis (see Figure 25 for the organization of the hypodermis). Between 2 and 4 hours before lethargus, the cytoplasm of the seam cells and to a much lesser extent the hypodermal syncytium (hyp7) becomes a granular appearance which is due to densely packed Golgi bodies (Singh and Sulston, 1978). In situ hybridization of a collagen probe showed primarily hybridization to the hypodermal seam, and much less hybridization to the rest of the hypodermis (Edwards and Wood, 1983). Another evidence came from studies with an adult specific collagen, *col-19* (Thein et al., 2003). Examination of the cuticle of various mutants affecting body morphology carrying a COL-19::GFP reporter showed that most of the defects in collagen mutants e.g. *dpy-5* occurred in the cuticle overlying the seam cells due to the failure of these cells to contract properly.

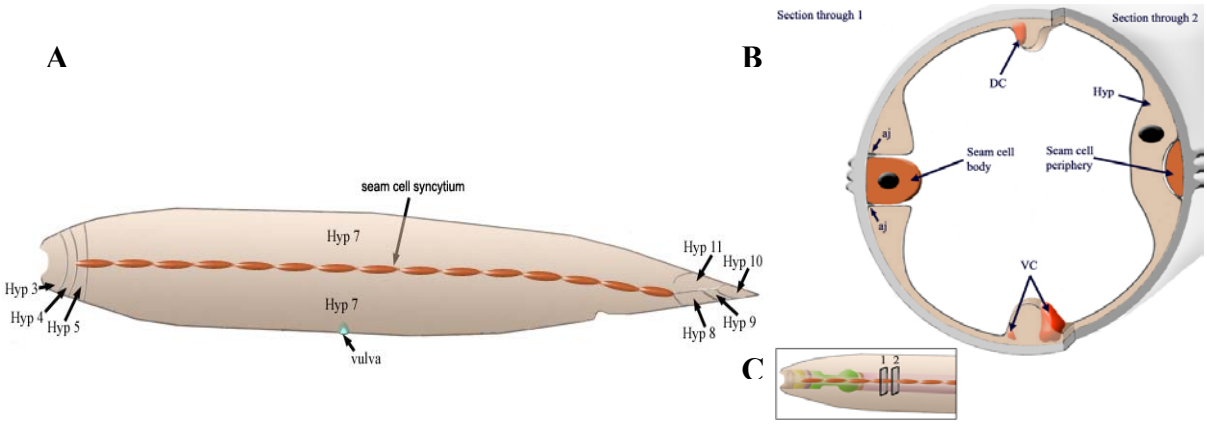

Figure 25: Schematic representation of the organization of the adult hermaphrodite hypodermis cells. (A) View of the hypodermis which is composed of two distinct types, the circumferentially contracting lateral seam cells (syncytium composed of 15 nuclei on each side) and the laterally contracting ventral-dorsal hypodermis (syncytium which contains 92 nuclei). (B) Cross section showing hypodermal and lateral seam cells. (C) The positions of the cross sections within the worm are shown. The seam cells are linked to the hypodermis by very small adherens junctions along the full length at their apical borders, and by small gap junctions on their lateral membranes. Original figures were obtained from http://www.wormatlas.org/handbook/hypodermis/hypsupportseam.htm.

Glandular cell staining is also cuticle/surface related. First of all the gland cells are active during moulting; shortly before ecdysis refractile granules accumulate in the g1 cells and move along the processes (see Figure 17.2 D) which open just behind the buccal cavity and the anterior bulb (Singh and Sulston, 1978). Secondly, studies with the parasitic nematode *Toxocara canis* have shown that antibodies which have been raised against carbohydrate epitopes of secreted (*Toxocara* excretory-secretory (TES)) antigens localize to the surface as well as to the esophageal glands (Page et al., 1992). In the same study, *T. canis* surface antigens have also been found to be secreted via the excretory system, an "H" shaped cell with lateral columns (Chitwood and Chitwood, 1950). *C. elegans* possesses a similar cell involved in part in kidney function, excreting saline fluid via the duct and pore in order to maintain the animal's salt balance (osmoregulation) and probably to remove metabolites (Buechner et al., 1999). The lack of *srf-3* expression within the excretory system suggests that, at least in *C. elegans*, the excretory apparatus is not involved in regulating surface antigenicity. This is supported by the finding that all excretory abnormal (exc) mutants, who show a degenerated or pathological changed excretory cell, are all non-Srf as judged by WGA-FITC labelling. *srf-3* is also expressed in the spermatheca and at 20°C there is no obvious fertility phenotype (Table 4, page 18). This suggests that the spermatheca is functioning normally with respect to sperm preservation and function, because otherwise sperm loss or dysfunction would result in much lower self-fertility. However, at 25°C animals of various *srf-3* alleles show a low penetrant sterility phenotype (Jörg Höflich, unpublished observation) indicating that *srf-3* might have a function in modifying or in storing sperm properly. The observed embryonic lethality of a *srf-3; srf-4* double mutant also indicates that *srf-3* has a function in the development of the embryo, however, in the moment this function remains unexplained.

Srf-3 expression may also be interpreted from a cell biological point of view: Glycosylation is the most extensive posttranslational modification and has a central function for sorting and quality control of proteins within the secretory pathway. Seam cells, glandular cells and spermatheca are a set of active secretory cells and SRF-3 provides the donor substrates for the subsequent glycosylation reactions and therefore affecting not only glycosylation per se but also protein trafficking.

What is the biological function of *srf-3*?

At the first glance it seems that *srf-3* function is dispensable. By visual inspection *srf-3* worms are undistinguishable from wild type worms and the mutant animals seem to benefit from the

resistance to some pathogens which they may encounter in their environment. There is no defect in the seam cells, as judged by the *ajm-1::gfp* staining. Even on an ultrastructural level, as judged by standard transmission electron microscopy (TEM) of thin sectioned and fixed with OsO_4 *srf-3* animals, no differences were detected (Castano and Politz, pers. comm.). However, there is evidence that *srf-3* function has an important function for cuticle formation/modification. *srf-3* animals are fragile to handling e.g. during microinjection, show increased susceptibility to drug treatment and the *srf-3* dauer larvae are SDS sensitive (Link et al., 1992; Schinkmann and Li, 1992). Radioiodination experiments revealed the absence of various compounds from the cuticle in *srf* mutants (see also Introduction). It was proposed that the Srf phenotype in *srf-2* and *srf-3* animals is a result of an unmasking of antigenic determinants which are normally hidden in the wild type cuticle (Politz et al., 1990). Given the molecular identity of *srf-3* it seems likely that the observed loss of components is due to underglycosylation and/or aberrant secretion of molecules usually embedded in the cuticle. How can this loss of components and the fragility of the cuticle and on the other side the lack of visible structural defects be interpreted? The lack of structural defects observed in the ultrastructural analysis can be explained by the experimental limitation due to the fixation procedure used in standard electron microscopy, a fixation procedure which does not or only poorly preserve the surface coat (Blaxter et al., 1992). Therefore, it is possible that the observed phenotypes are due to the lack or the alteration of the worm's surface coat. This would imply that this layer of the exoskeleton has an important function in its composition/maintenance, as judged by the defects (fragility, permeability) of the cuticle. Consistent with this idea is the finding that the surface coat is a carbohydrate rich structure (40% content in *T. canis*) with extensive O-glycosylation (Khoo et al., 1991) and it seems reasonable that a defect in an NST affects especially this structure. With SRF-3 transporting UDP-Gal and UDP-GlcNAc many glycosylated structures can be affected and at the moment it is unclear in which way the surface is altered. A global altered glycosylation pattern would be consistent with the fact that *M. nematophilum* and *Y. pseudotuberculosis* fail to adhere to *srf-3* animals; two bacterial species which are not closely related and therefore are suggested to use different mechanisms and utilize different host structures for their interaction with worms.

The surface of *C. elegans* wild type worms binds few if any lectins (see Introduction). Attachment of spores of some nematode trapping fungi is restricted to the sensory openings and the vulva (Barron, 1977; Jansson, 1994). Therefore, the limited lectin binding of the

worm's surface might reflect a passive defence mechanism which renders the worm biochemically less visible for his environment and therefore might help to avoid adhesive traps and spores of fungi and bacteria. *srf-3* mutants show an ectopic lectin binding phenotype and it is interesting to note that *srf-3* animals were found to be more susceptible to trapping by *Duddingtonia flagrans*, a nematode predatory fungi (Mendoza De Gives et al., 1999). This finding supports the idea of a protective function of surface glycosylation with respect to natural enemies. Further supporting results are coming from studies with parasitic nematodes which show that the nematode cuticle is a highly dynamic organ which has an important function to allow the worms survival in the host (see Introduction). Surface antigens are actively released from the animals and various parasitic nematode species have been shown to shed surface bound antibodies *in vitro* (Philipp and Rumjanek, 1984). Mice immunized with affinity purified *T. spiralis* antigens induced level of protection comparable to primary infection (Gamble, 1985). The model is that the loosely attached surface coat may slough off attached molecules (antibodies or cells in parasitic or spores and bacteria in free-living nematodes) and therefore serves as a dispensable sink for enzymatic effector mechanisms (Blaxter et al., 1992).

A lot of information is available on the structure and identity of surface antigens, however, nothing is known about the factors regulating the expression of these antigens. Cloning of the first *C. elegans srf* mutant, now offers the opportunity to examine the genetic and molecular mechanisms regulating surface antigenicity. For example, one question which can be addressed now is: What are the factors which regulate the distribution and timing of *srf-3* expression? An initial attempt to find genes interacting with *srf-3* by testing previously described genes, e.g. genes encoding putative glycosyltransferases, did not lead to the identification of factors modulating *srf-3*. However, the combined disruption of the processes in which *srf-3* and *srf-4* are involved in, are essential for proper worm development. At the moment this result remains unexplained but maybe the molecular identification of *srf-4* will shed light on this notion.

Material and Methods

Chemicals and Reagents

If not stated otherwise, chemicals and reagents (analytical grade) were purchased from Merck, Sigma, Roth, Fluka and Biorad. Reagents for molecular biology, restriction enzymes and other enzymes were purchased from MBI Fermentas, New England Biolabs (NEB), Qiagen, Promega, Molecular labs, La Roche and Boehringer Ingelheim. Media for cultivation of bacteria, yeast and worms were obtained from Difco and Gibco BRL. Radiolabelled chemicals were purchased from Amersham Pharmacia, Perkin Elmer and American Radiolabeled Chemicals.

C. elegans methods and strains

All *Caenorhabditis elegans* strains were grown as described (Wood, 1988). Transgenic animals were constructed as described (Mello et al., 1991). General methods as freezing worms, cleaning contaminated strains and obtaining synchronized populations were done as described (Stiernagel, 1999). Injection of dsRNA was done as described (Fire et al., 1998).

Syto13 staining

To detect bacteria tightly attached to the surface of the animal, worms were stained with Syto 13 (Hodgkin et al., 2000). Worms were grown on plates containing *M. nematophilum* for 3-4 days and washed three times with M9 and resuspended in TBS and incubated for 1 hour to remove bacteria loosely attached to the worms. Afterwards worms were incubated with 10µM Syto13 in TBS for 30-60 minutes and washed three times with TBS.

Staining *C. elegans* for β-galactosidase activity

β-galactosidase staining was done essentially as described (Mounsey et al., 1999). Worms were washed off from 1 or 2 five centimetre NGM plates with M9 buffer, which had just been cleared from bacteria. Worms were transferred into a 15 ml Falcon tube, washed two times with M9 buffer and transferred into 1.5 ml Eppendorf tubes. After centrifugation at 700 g the supernatant was removed and the worm pellet was frozen in liquid nitrogen and dried 30 minutes in a vacuum concentrator. 250 µl of cold acetone were added and the sample was frozen for 3 minutes at -20°C. After removing of excess acetone with a pipette, the sample

was dried for 30 minutes in a vacuum concentrator. 200 µl of freshly mixed staining solution were added and samples were incubated at 37°C. Appearance of the blue colour was monitored under a stereomicroscope. Reaction was stopped by washing three times with M9 buffer.

Staining *C. elegans* with lectins

Worms were grown on a standard OP50 food source and washed off the plate with M9. After three subsequent washes with PBS, worms were incubated for one hour in PBS and then transferred to an Eppendorf reaction tube. Then worms were incubated with 50 µl WGA-FITC in 1 ml PBS for one hour and subsequently washed three times with 1 ml PBS. Afterwards the samples were mounted for microscopy.

Infection of *C. elegans* with *M. nematophilum*

A mixture of *E. coli* OP 50 and 0.1 % *M. nematophilum* was grown on NGM plates for 48 h at 20°C. To infect worms, animals were transferred from plates containing standard OP 50 food source to plates with *M .nematophilum* and allowed to grow for 2 -3 days at 20 or 25°C. To determine the penetrance of the Dar phenotype the amount of infected worms was compared to the amount of uninfected worms.

Yersinia biofilm formation

The *Yersinia* biofilm formation assay was done by Creg Darby (University of Alabama) and performed as follows. *Yersinia pseudotuberculosis* was grown overnight on NGM plates. Five adult worms were picked to the *Yersinia pseudotuberculosis* lawns and were allowed to lay eggs for 2-4 hours. After removing the adults the plates were incubated at 20°C for two days and the number of L4 animals was compared to the number of total worms. Since the biofilm blocks feeding, the resulting percentage serves as an indirect measure of biofilm attachment.

Crosses

Simple crosses were done as follows: L4/young adult hermaphrodites were mated with males at a ratio of 1:3 on 3.5 cm NGM agar plates. Worms were transferred to a fresh plate every day for four consecutive days. The success of the cross was monitored by the amount of males in the F1 generation. The double mutant of interest was isolated in the F2 generation. *srf-3 unc-30 (e191)* double mutants were generated by recombination. *srf-3* males were

mated with *dpy-20 (e1282) unc-30 (e191)* hermaphrodites and in the F2 generation non-dpy unc recombinants were picked. F3 Unc animals only segregating Unc's were maintained and subsequently tested for the presence of the Srf phenotype by growing on plates containing *M. nematophilum*.

srf double mutants

All *srf* double mutants were created by marker exchange. *srf-3(e2789); srf-4(ct109)* was created as follows: *srf-4(ct109)* hermaphrodites were mated with *dpy-20 (e1282) unc-30 (e191)*/+ males. F2 Dpy Uncs were picked segregating *srf-4* animals. In the F3 generation then *srf-4* animals were maintained. *dpy-20(e1282) unc-30(e191); srf-4(ct109)* hermaphrodites were mated with *srf-3(e2789)* males and wild type worms were picked in the F1. In the F2 *srf-4* animals segregating Dpy Uncs and dead eggs were maintained. The resulting strain is homozygous for *srf-4* and heterozygous for *srf-3* with two mutations in genes flanking *srf-3*; *dpy-20* and *unc-30*.

A *srf-(yj262); srf-3(e2789)* double mutant was generated as follows: *srf-3(e2789)* males were mated with *dpy-5(e61) daf-16(m26) unc-75(e950)* hermaphrodites and in the F2 generation animals resistant to *M. nematophilum* segregating Dpy Uncs were picked. In the F3 Dpy Uncs animals were picked resulting in the strain *dpy-5(e61) daf-16(m26) unc-75(e950); srf-3(e2789).* In parallel, *srf-2* males were mated with *unc-30(e191)* hermaphrodites and Unc animals resistant to *M. nematophilum* were isolated. Next *srf-2(yj262); unc-30(e191)* males were mated with *dpy-5(e61) daf-16(m26) unc-75(e950); srf-3(e2789)* hermaphrodites. Animals homozygous for *srf-2(yj262)* and *srf-3(e2789)* were isolated by picking non Dpy non Uncs in the F2 generation which do not segregate any Dpy or Unc progeny in the F3. The success of the cross was verified by a complementation test using the resistance to *M. nematophilum* as a phenotypic marker.

The principle for generating a *srf-3(e2789); srf-5(ct115)* and a *srf-2(yj262); srf-5(ct115)* mutant was equivalent. The strain used to mark *srf-5* on Chromosome X was *lon-2(e678) unc-84(e1410)*.

Deletion library

To identify a deletion in the ORF ZK896.9, approximately 3 x 10^6 L4 animals were incubated with 50 mM methansulfonic acid ethylester (EMS) for 4 hours. Mutagenized worms were kept over night on standard plates and the next day eggs were prepared by hypochlorite treatment. L1 larvae were allowed to hatch overnight in M9 buffer and adjusted to the number

of 160 larvae/100 µl S-Medium. In parallel *E. coli* HB101 was grown in 1 liter LB overnight at 37°C, harvested by centrifugation and resuspended in S-Medium up to an OD_{600} of 2. HB101 was mixed with L1 larvae at a ration 1:1 and the mix was aliquoted in twenty-four 96 well plates with 40 larvae per well. After 4-5 days 12.5 µl of each well were pooled and the DNA was prepared by Phenol/Chloroform extraction and subsequent ethanol precipitation. The DNA was resuspended in Tris/HCl pH 8.0 and was used as a template for PCR.

Worm lysis for Single Worm Polymerase Chain Reaction (PCR)

Single worms were picked into PCR tubes containing 10 µl of Worm lysis buffer and frozen at -80°C for at least 30 minutes. Afterwards the samples were heated up to 95°C for 2 minutes and the Proteinasedigest was performed at 65 °C for one hour. One microliter of Wormlysis was used as a template for PCR.

Single Worm PCR

For the isolation of the ZK896.9 deletion mutant or single worm PCR, two rounds of PCR were performed using nested primer. The first PCR was done using outer primer pair (RB1483/RB1555), 1 µl template, 1U Taq Polymerase (MBI Fermentas) for each reaction, annealing temperature of 53°C, 90 seconds elongation time and 35 cycles. The conditions for the second PCR were identical to the first PCR except for the primer used (inner primer pair; RB1484/RB1557), 0.5 µl first PCR and the annealing temperature (56°C).

Preparation of RNA from *C. elegans*

To obtain total RNA of a population of mixed staged animals, 4 to 5 plates with unstarved worms were washed off with M9 buffer. After two washing steps with M9 buffer the worms were frozen in liquid nitrogen and stored at -80°C until the RNA was prepared. The frozen worms were transferred into a sterile mortar and homogenized with a sterile pestle. 600 µl of lysisbuffer were added to the homogenized worms and the resulting extract was transferred to a cold 1.5 ml Eppendorf tube. The extract was drawn five to seven times into a 2 ml syringe carrying a needle with 0.9 mm diameter. To remove the worm debris the extract was centrifuged at 16000 g for ten minutes. The supernatant was transferred to a new cold 1.5 ml Eppendorf tube and mixed with an equal volume of 70% ethanol. The RNA was purified with the RNeasy Mini Kit from Qiagen according to the manufacturer's instructions. The RNA obtained from this preparation protocol can be used for Northern blot analysis and RT-PCR.

Cell culture methods

Transfection

Madin-Darby canine kidney (MDCK) cells were stably transfected by lipofection (Felgner et al., 1987) using Lipofectin Reagent (Invitrogene). Cells were grown at 37°C in minimal essential medium (MEM, GIBCO BRL) supplemented with 10% fetale bovine serum (FBS) and 100 U Penicillin/Streptomycin (GIBCO, BRL). For transfection cells were grown in 24 well plates and transfection was performed when cells reached a confluency of 30-50%. 20 µl Lipofectin reagent were diluted into 100 µl Opti-MEM serum free medium (GIBCO-BRL) and incubated for 45 minutes at room temperature. 2 µg DNA of the plasmid to transfect were mixed with 100 µl Opti-MEM medium, added to the lipofectin-MEM and incubated for 15 minutes at room temperature. In parallel cells were washed once with Opti-MEM and overlaid with 1.8 ml of serum free medium. The Lipofectin-DNA mix was added and the culture was incubated for 6 hours at 37 °C. For recovery the medium was removed and the cells were grown for 72 hours in complete medium containing FBS and antibiotics. Cells were trypsinized and plated at low density in 92 x 16 mm Petri dishes containing MEM medium with 0.5 mg/ml geneticin (G418; GIBCO BRL). Plates were continuously monitored for surviving cells and resistant colonies were cloned.

Determination of ricin resistance

Ricin resistance was determined by growing pBY1821 and pBY1825 transfected cells at 30°C in 24 well plates containing MEM with various concentration of ricin (RCA II, EY Laboratories, San Mateo, CA). After seven days cells were washed three times with PBS and survival was determined by staining viable cells with methylen blue.

Yeast methods

Yeast was grown and treated as described (Gietz and Woods, 2002; Sherman, 1991). Yeast transformation was done by the PEG/LiAc method described in Gietz and Woods, (2002).

Preparation of a yeast protein extract

To prepare protein extracts for immunoblotting *S. cerevisiae* PRY225 cells were transformed with pBY1822 and grown in SD-URA media to an OD_{600} of three and harvested by

centrifugation. The cell pellet was washed with 1 ml deionised water and suspended in 200 µl membrane buffer. The cells were disrupted by adding an equal volume of glass beads (200-300 µm diameter) and subsequent vortexing (3 cycles of one minute vortexing and one minute cooling on ice). The supernatant was transferred into a new Eppendorf tube and centrifuged at 100.000 x g. The pellet (membrane fraction) was kept and the supernatant was transferred into a new Eppendorf tube. To concentrate the cytosolic fraction the supernatant was precipitated with 10% trichloracetic acid (TCA) centrifuged at 100.000 x g and the pellet was dissolved in 100 µl membrane buffer. The membrane fraction was mixed with an equal volume of 2x Laemmli buffer and incubated for 5 minutes at 65°C prior to loading on a polyacrylamide gel. The cytosolic fraction was mixed with an equal volume of 2x protein sample buffer and incubated for 5 minutes at 95°C prior to loading on a polyacrylamide gel.

Preparation of Golgi-enriched vesicles from *S. cerevisiae*

S. cerevisiae PRY225 cells were transformed with pBY1822 or pG426 were grown in SD-URA media to an OD_{600} of 3 and harvested by centrifugation. The cell pellet was resuspended in 10 mM NaN_3 up to a final volume of 50ml and a equal volume of 2x spheroblast buffer containing Zymolase 100T (20 mg per 50 g of cells) was added. Cells were converted into spheroblast by shaking the culture for 1 h at 37°C. The cell pellet was suspended in a small volume of a membrane buffer and drawn rapidly several times into a narrow-bore serological pipette which breaks the cells but maintains the vesicle integrity. After a low speed centrifugation step to remove cell debris Golgi enriched vesicles were collected by a high speed centrifugation (100.000 x g) and resuspended in 1 ml Membrane Buffer.

Transport assay

The theoretical basis for the translocation assay was described before (Perez and Hirschberg, 1987). The assay is only applicable to microsomal membranes which are sealed and have the same membrane topography as *in vivo*. The assay was performed in 1 ml transport buffer with 500 µg Golgi enriched vesicles, 30°C and in parallel at 0°C for three minutes and a concentration of 1 µM for the nucleotide sugar to be measured. To measure the transport activity the substrate was mixed with the 1 µCi of the corresponding tritiumlabelled nucleotide sugar. To determine the radioactivity, liquid scintillation spectrometry was used. After the incubation, the reaction was stopped by dilution with 3 ml stop solution, the vesicles were reisolated by ultracentrifugation (supernatant = concentration of nucleotide sugar in the incubation medium(S_m)), washed 3 times with ice cold stop solution and suspended in 500 µl

H_2O. The radioactivity in the corresponding pellet consisted of radiolabelled solutes which were transported across the membrane, radiolabel which was adsorbed and radiolabel which was transferred to macromolecules. The vesicles were broken by vortexing and the macromolecules were precipitated with 8% perchloric acid. After centrifugation at 16.000 x g radiolabelled solutes that were transported are in the supernatant (supernatant = amount of acid-soluble nucleotide sugars (S_t)). In order to be able to calculate the amount of transported nucleotide sugar the volume outside the vesicles had to be determined. For this purpose, vesicles were incubated in a separate reaction with the membrane non-penetrator [^{3}H]-acetate. The amount of solutes outside the vesicle (S_o) was obtained by multiplying the volume outside the vesicle V_o with the concentration of nucleotide sugar in the incubation medium (S_m). The amount of radioactive sugar inside the vesicles S_i was calculated by subtracting the amount of radioactive sugar outside the vesicles from the amount of acid-soluble nucleotide sugars (S_i=S_t-S_o). Transport activity was defined as amount of nucleotide sugars inside the vesicles at 30°C minus the corresponding amount at 0°C.

Cell surface labelling of *K. lactis*

K. lactis cells transformed with pE4-*srf-3-VSV* or vector alone were grown at 30°C in SD-URA media and then washed three times with 0.9% NaCl, 0.5mM $CaCl_2$. Approximately 5 OD_{600} of cells was resuspended in 100µl of 0.5 mg/ml GSII-FITC in 0.9% NaCl, 4 mM $CaCl_2$ and incubated for 1h at 30°C with shaking. Samples were washed three times and resuspended in 0.9% NaCl, 0.5mM $CaCl_2$. Fluorescence was measured at 535 nm with a Tecan microplate reader.

General molecular biology

General molecular biology methods, protein biochemistry and microbiology methods were done as described (Ausubel, 1987; Sambrook et al., 1989). Sequencing was performed by GATC (Konstanz). Oligonucleotides for sequencing or PCR were purchased at a desalted grade from Metabion GmbH (Martinsried) or MWG Biotech AG (Ebersberg) and HPLC purified from Thermo Electron Corporation (Ulm). The extraction of DNA out of agarosegels was done with the Qiagen Gel Extraction Kit according to the manufacturer's instruction. Precast Tris/Glycine gels from Biorad were used for polyacrylamide gel electrophoresis.

Isolation of plasmid and cosmid DNA from *E. coli*

For the isolation of plasmid DNA from *E. coli* a modified protocol from Birnboim and Doly, (1979) was used. The DNA was purified with columns provided by Qiagen according to the instructions of the manufacturer. Small DNA amounts were prepared from 5 ml cultures whereas larger amounts were purified from 100 ml cultures.

For the isolation of cosmids the culture was directly streaked out from the stock delivered by the Sanger Center (http://www.sanger.ac.uk/Projects/C_elegans/) and incubated at 30°C overnight on agar plates containing the appropriate antibiotic. Small (1-2 mm diameter), single bacteria clones were picked with a tip of a pipette using a stereomicroscope. 10 ml cultures were grown in LB selective medium until OD_{600} of approximately 1 (12-24h). 10 µl of the extracted DNA was loaded on 0.4 % agarose gel. DNA migrating with or above the 20 kb fragment of *Eco*RI/*Hin*dIII digested lambda DNA and without additional lower bands which indicate deletions was considered to be a full length cosmid. To obtain larger amounts of the cosmid DNA of interest, cultures were grown in 500 ml LB selective medium and the DNA was purified using Qiagen Midi Prep columns.

Polymerase Chain Reaction (PCR)

Reactions were performed in a volume of 25 µl or 50 µl with 100 ng Plasmid DNA as a template and one-fold concentrated reaction buffer with 0.2 mM of each desoxynucleotide and oligonucleotides at a concentration of 10 pmol/µl. For each reaction between 0.25 and 0.5 U Taq Polymerase or 3 U *Pfu* Polymerase was used. If the DNA was amplified with Taq Polymerase $MgCl_2$ was supplemented to a final concentration of 1 mM. The reaction was performed in a MJ PTC-200 cycler. The following parameters were considered for the adjustment of the reaction profile: Quantity and quality of the template DNA, length and G/C content of the oligonucleotides, type of polymerase used and length of the expected PCR fragment.

Literature

Aballay, A., Yorgey, P. and Ausubel, F.M. (2000) *Salmonella typhimurium* proliferates and establishes a persistent infection in the intestine of *Caenorhabditis elegans*. *Curr Biol*, **10**, 1539-1542.

Abeijon, C., Mandon, E.C., Robbins, P.W. and Hirschberg, C.B. (1996a) A mutant yeast deficient in Golgi transport of uridine diphosphate N-acetylglucosamine. *J.Biol.Chem.*, **271**, 8851-8854.

Abeijon, C., Robbins, P.W. and Hirschberg, C.B. (1996b) Molecular cloning of the Golgi apparatus uridine diphosphate-N-acetylglucosamine transporter from *Kluyveromyces lactis*. *Proc.Natl.Acad.Sci.U.S.A*, **93**, 5963-5968.

Andrew, P.A. and Nicolas, W.L. (1976) Effect of bacteria on dispersal of *Caenorhabditis elegans* (Rhabditidae). *Nematologica*, **22**, 451-461.

Aoki, K., Ishida, N. and Kawakita, M. (2003) Substrate recognition by nucleotide sugar transporters: further characterization of substrate recognition regions by analyses of UDP-galactose/CMP-sialic acid transporter chimeras and biochemical analysis of the substrate specificity of parental and chimeric transporters. *J Biol Chem*, **278**, 22887-22893.

Aoki, K., Sun-Wada, G.H., Segawa, H., Yoshioka, S., Ishida, N. and Kawakita, M. (1999) Expression and activity of chimeric molecules between human UDP-galactose transporter and CMP-sialic acid transporter. *J Biochem (Tokyo)*, **126**, 940-950.

Ausubel, F.M. (1987) *Current protocols in molecular biology*. Greene Publishing Associates ;
J. Wiley order fulfillment, Brooklyn, N. Y.
Media, Pa.

Bacic, A., Kahane, I. and Zuckerman, B.M. (1990) *Panagrellus redivivus* and *Caenorhabditis elegans*: evidence for the absence of sialic acids. *Exp.Parasitol.*, **71**, 483-488.

Baird, S.E. and Emmons, S.W. (1990) Properties of a class of genes required for ray morphogenesis in *Caenorhabditis elegans*. *Genetics*, **126**, 335-344.

Banyai, L. and Patthy, L. (1998) Amoebapore homologs of *Caenorhabditis elegans*. *Biochim Biophys Acta*, **1429**, 259-264.

Barron, G.L. (1977) The nematode-destroying fungi. In *Canadian Biological Publications*, Guelph.

Berninsone, P. and Hirschberg, C.B. (1998) Nucleotide sugars, nucleotide sulfate, and ATP transporters of the endoplasmic reticulum and Golgi apparatus. *Ann.N.Y.Acad.Sci.*, **842**, 91-99.

Berninsone, P., Hwang, H.Y., Zemtseva, I., Horvitz, H.R. and Hirschberg, C.B. (2001) SQV-7, a protein involved in *Caenorhabditis elegans* epithelial invagination and early embryogenesis, transports UDP-glucuronic acid, UDP-N- acetylgalactosamine, and UDP-galactose. *Proc.Natl.Acad.Sci.U.S.A*, **98**, 3738-3743.

Birnboim, H.C. and Doly, J. (1979) A rapid alkaline extraction procedure for screening recombinant plasmid DNA. *Nucleic Acids Res*, **7**, 1513-1523.

Blaxter, M., Page, A.P., Rudin, W. and Maizels, R.M. (1992) Nematode Surface coats: Actively evading immunity. *Parasitology Today*, **8**, 243-247.

Blaxter, M. and Robertson, W.M. (1998) The Cuticle. In Perry, R.N. and Wright, D.J. (eds.), *The physiology and biochemistry of free-living and plant-parasitic nematodes*. C.A.B. International, New York, pp. 25-48.

Blaxter, M.L. (1993) Cuticle surface proteins of wild type and mutant *Caenorhabditis elegans*. *J.Biol.Chem.*, **268**, 6600-6609.

Blaxter, M.L., De Ley, P., Garey, J.R., Liu, L.X., Scheldeman, P., Vierstraete, A., Vanfleteren, J.R., Mackey, L.Y., Dorris, M., Frisse, L.M., Vida, J.T. and Thomas, W.K. (1998) A molecular evolutionary framework for the phylum Nematoda. *Nature*, **392**, 71-75.

Blumenthal, T. and Steward, K. (1997) RNA processing and gene structure. In Riddle, D.L. (ed.), *C. elegans II*. Cold Spring Harbor Laboratory Press, Plainview, N.Y., pp. 117-146.

Borgonie, G., Van Driessche, R., Leyns, F., Arnaut, G., De Waele, D. and Coomans, A. (1995) Germination of *Bacillus thuringiensis* spores in bacteriophagous nematodes (Nematoda: Rhabditida). *J Invertebr Pathol*, **65**, 61-67.

Boyer, H.W. and Roulland-Dussoix, D. (1969) A complementation analysis of the restriction and modification of DNA in *Escherichia coli*. *J Mol Biol*, **41**, 459-472.

Brandli, A.W., Hansson, G.C., Rodriguez-Boulan, E. and Simons, K. (1988) A polarized epithelial cell mutant deficient in translocation of UDP-galactose into the Golgi complex. *J.Biol.Chem.*, **263**, 16283-16290.

Brenner, S. (1973) The genetics of behaviour. *Br Med Bull*, **29**, 269-271.

Brenner, S. (1974) The genetics of *Caenorhabditis elegans*. *Genetics*, **77**, 71-94.

Buechner, M., Hall, D.H., Bhatt, H. and Hedgecock, E.M. (1999) Cystic canal mutants in *Caenorhabditis elegans* are defective in the apical membrane domain of the renal (excretory) cell. *Dev Biol*, **214**, 227-241.

Chalfie, M., Tu, Y., Euskirchen, G., Ward, W.W. and Prasher, D.C. (1994) Green fluorescent protein as a marker for gene expression. *Science*, **263**, 802-805.

Chen, S., Spence, A.M. and Schachter, H. (2003) Isolation of null alleles of the *Caenorhabditis elegans gly-12, gly-13* and *gly-14* genes, all of which encode UDP-GlcNAc: alpha-3-D-mannoside beta1,2-N-acetylglucosaminyltransferase I activity. *Biochimie*, **85**, 391-401.

Chitwood, B.G. and Chitwood, M.B.H. (1950) *An introduction to nematology*. Monumental Printing Company, Baltimore.

Choy, R.K. and Thomas, J.H. (1999) Fluoxetine-resistant mutants in *C. elegans* define a novel family of transmembrane proteins. *Mol Cell*, **4**, 143-152.

Clark, D.V., Rogalski, T.M., Donati, L.M. and Baillie, D.L. (1988) The *unc-22*(IV) region of *Caenorhabditis elegans*: genetic analysis of lethal mutations. *Genetics*, **119**, 345-353.

Crosby, A. (1989) *America's Forgotten Pandemic*. Cambridge University Press, Cambridge.

Darby, C., Cosma, C.L., Thomas, J.H. and Manoil, C. (1999) Lethal paralysis of *Caenorhabditis elegans* by *Pseudomonas aeruginosa*. *Proc.Natl.Acad.Sci.U.S.A*, **96**, 15202-15207.

Darby, C., Hsu, J.W., Ghori, N. and Falkow, S. (2002) *Caenorhabditis elegans*: plague bacteria biofilm blocks food intake. *Nature*, **417**, 243-244.

Davey, M.E. and O'Toole, G.A. (2000) Microbial biofilms: from ecology to molecular genetics. *Microbiol Mol Biol Rev*, **64**, 847-867.

Davis, R.E. (1996) Spliced leader RNA trans-splicing in metazoa. *Parasitology Today*, **12**, 33-40.

De Gregorio, E., Spellman, P.T., Rubin, G.M. and Lemaitre, B. (2001) Genome-wide analysis of the *Drosophila* immune response by using oligonucleotide microarrays. *Proc.Natl.Acad.Sci.U.S.A*, **98**, 12590-12595.

Descoteaux, A., Luo, Y., Turco, S.J. and Beverley, S.M. (1995) A specialized pathway affecting virulence glycoconjugates of *Leishmania*. *Science*, **269**, 1869-1872.

Descoteaux, A. and Turco, S.J. (1999) Glycoconjugates in *Leishmania* infectivity. *Biochim Biophys Acta*, **1455**, 341-352.

Dong, C., Davis, R.J. and Flavell, R.A. (2002) MAP kinases in the immune response. *Annu.Rev.Immunol.*, **20**, 55-72.

Dubois, A. (1995) Spiral bacteria in the human stomach: the gastric helicobacters. *Emerg Infect Dis*, **1**, 79-85.
Edwards, M.K. and Wood, W.B. (1983) Location of specific messenger RNAs in *Caenorhabditis elegans* by cytological hybridization. *Dev.Biol.*, **97**, 375-390.
Felgner, P.L., Gadek, T.R., Holm, M., Roman, R., Chan, H.W., Wenz, M., Northrop, J.P., Ringold, G.M. and Danielsen, M. (1987) Lipofection: a highly efficient, lipid-mediated DNA-transfection procedure. *Proc Natl Acad Sci U S A*, **84**, 7413-7417.
Finlay, B.B. and Falkow, S. (1997) Common themes in microbial pathogenicity revisited. *Microbiol Mol Biol Rev*, **61**, 136-169.
Fire, A., Harrison, S.W. and Dixon, D. (1990) A modular set of lacZ fusion vectors for studying gene expression in *Caenorhabditis elegans*. *Gene*, **93**, 189-198.
Fire, A., Xu, S., Montgomery, M.K., Kostas, S.A., Driver, S.E. and Mello, C.C. (1998) Potent and specific genetic interference by double-stranded RNA in *Caenorhabditis elegans*. *Nature*, **391**, 806-811.
Fleming, A. (1929) On the Antibacterial Action of Cultures of a Penicillium, with Special Reference to Their Use in the Isolation of *B. influenzae*. *British Journal of Experimental Pathology*, **X**, 226.
Fujita, T. (2002) Evolution of the lectin-complement pathway and its role in innate immunity. *Nat.Rev.Immunol.*, **2**, 346-353.
Gamble, H.R. (1985) *Trichinella spiralis*: immunization of mice using monoclonal antibody affinity-isolated antigens. *Exp Parasitol*, **59**, 398-404.
Garsin, D.A., Sifri, C.D., Mylonakis, E., Qin, X., Singh, K.V., Murray, B.E., Calderwood, S.B. and Ausubel, F.M. (2001) A simple model host for identifying Gram-positive virulence factors. *Proc Natl Acad Sci U S A*, **98**, 10892-10897.
Gerardy-Schahn, R. and Eckhardt, M. (2000) Oligosaccharides in Chemistry and Biology. In Ernst, B., Hart, G.W. and Sinaèy, P. (eds.), *Carbohydrates in chemistry and biology*. Wiley-VCH, Weinheim ; New York, Vol. II, pp. 19-36.
Gerardy-Schahn, R., Oelmann, S. and Bakker, H. (2001) Nucleotide sugar transporters: biological and functional aspects. *Biochimie*, **83**, 775-782.
Gietz, R.D. and Woods, R.A. (2002) Transformation of yeast by lithium acetate/single-stranded carrier DNA/polyethylene glycol method. *Methods Enzymol*, **350**, 87-96.
Gottfried, R.S. (1983) *The black death : natural and human disaster in medieval Europe*. Free Press ;
Collier Macmillan, New York
London.
Gottlieb, S. and Ruvkun, G. (1994) *daf-2*, *daf-16* and *daf-23*: genetically interacting genes controlling Dauer formation in *Caenorhabditis elegans*. *Genetics*, **137**, 107-120.
Gravato-Nobre, M., Nicholas, H., O'Rourke, D., Whittington, D. and Hodgkin, J. (2001) Multiple genetic loci determine sensitivity of *C. elegans* to the deformation-causing pathogen *M. nematophilum*. *International Worm Meeting abstract*, Los Angeles.
Griffitts, J.S., Whitacre, J.L., Stevens, D.E. and Aroian, R.V. (2001) Bt toxin resistance from loss of a putative carbohydrate-modifying enzyme. *Science*, **293**, 860-864.
Guillen, E., Abeijon, C. and Hirschberg, C.B. (1998) Mammalian Golgi apparatus UDP-N-acetylglucosamine transporter: molecular cloning by phenotypic correction of a yeast mutant. *Proc.Natl.Acad.Sci.U.S.A*, **95**, 7888-7892.
Hacker, J. (2002) Offensive pathogenicity factors. In Hacker, J. and Heesemann, J. (eds.), *Molecular infection biology : interactions between microorganisms and cells*. Wiley-Liss ;
Spektrum, Hoboken, NJ
Heidelberg, Germany, pp. 57-76.

Hauck, C.R. (2002) Cell adhesion receptors - signaling capacity and exploitation by bacterial pathogens. *Med Microbiol Immunol (Berl)*, **191**, 55-62.
Hemmer, R.M., Donkin, S.G., Chin, K.J., Grenache, D.G., Bhatt, H. and Politz, S.M. (1991) Altered expression of an L1-specific, O-linked cuticle surface glycoprotein in mutants of the nematode *Caenorhabditis elegans*. *J.Cell Biol.*, **115**, 1237-1247.
Himmelhoch, S. and Zuckerman, B.M. (1983) *Caenorhabditis elegans*: characters of negatively charged groups on the cuticle and intestine. *Exp Parasitol*, **55**, 299-305.
Hinnebusch, B.J., Perry, R.D. and Schwan, T.G. (1996) Role of the *Yersinia pestis* hemin storage (*hms*) locus in the transmission of plague by fleas. *Science*, **273**, 367-370.
Hiramatsu, K., Aritaka, N., Hanaki, H., Kawasaki, S., Hosoda, Y., Hori, S., Fukuchi, Y. and Kobayashi, I. (1997) Dissemination in Japanese hospitals of strains of *Staphylococcus aureus* heterogeneously resistant to vancomycin. *Lancet*, **350**, 1670-1673.
Hirschberg, C.B., Robbins, P.W. and Abeijon, C. (1998) Transporters of nucleotide sugars, ATP, and nucleotide sulfate in the endoplasmic reticulum and Golgi apparatus. *Annu.Rev.Biochem.*, **67**, 49-69.
Hodgkin, J., Horvitz, H.R. and Brenner, S. (1979) Nondisjunction mutants of the nematode *Caenorhabditis elegans*. *Genetics*, **91**, 67-94.
Hodgkin, J., Kuwabara, P.E. and Corneliussen, B. (2000) A novel bacterial pathogen, *Microbacterium nematophilum*, induces morphological change in the nematode *C. elegans*. *Curr.Biol.*, **10**, 1615-1618.
Hoffmann, J.A., Kafatos, F.C., Janeway, C.A. and Ezekowitz, R.A. (1999) Phylogenetic perspectives in innate immunity. *Science*, **284**, 1313-1318.
Hwang, H.Y. and Horvitz, H.R. (2002) The SQV-1 UDP-glucuronic acid decarboxylase and the SQV-7 nucleotide-sugar transporter may act in the Golgi apparatus to affect *Caenorhabditis elegans* vulval morphogenesis and embryonic development. *Proc.Natl.Acad.Sci.U.S.A*, **99**, 14218-14223.
Ishida, N., Miura, N., Yoshioka, S. and Kawakita, M. (1996) Molecular cloning and characterization of a novel isoform of the human UDP-galactose transporter, and of related complementary DNAs belonging to the nucleotide-sugar transporter gene family. *J Biochem (Tokyo)*, **120**, 1074-1078.
Jansson, H.B. (1994) Adhesion of conidia of *Drechmeria coniospora* to *Caenorhabditis elegans* wild type and mutants. *Journal of Nematology*, **26**, 430-435.
Jansson, H.B., Jeyaprakash, A., Marban-Mendoza, N. and Zuckerman, B.M. (1986) *Caenorhabditis elegans*: comparisons of chemotactic behavior from monoxenic and axenic culture. *Exp Parasitol*, **61**, 369-372.
Joshua, G.W., Karlyshev, A.V., Smith, M.P., Isherwood, K.E., Titball, R.W. and Wren, B.W. (2003) A *Caenorhabditis elegans* model of *Yersinia* infection: biofilm formation on a biotic surface. *Microbiology*, **149**, 3221-3229.
Karlsson, K.A. (1998) Meaning and therapeutic potential of microbial recognition of host glycoconjugates. *Mol Microbiol*, **29**, 1-11.
Kato, Y., Aizawa, T., Hoshino, H., Kawano, K., Nitta, K. and Zhang, H. (2002) *abf-1* and *abf-2*, ASABF-type antimicrobial peptide genes in *Caenorhabditis elegans*. *Biochem J*, **361**, 221-230.
Ketting, R.F., Haverkamp, T.H., van Luenen, H.G. and Plasterk, R.H. (1999) *Mut-7* of *C. elegans*, required for transposon silencing and RNA interference, is a homolog of Werner syndrome helicase and RNaseD. *Cell*, **99**, 133-141.
Khoo, K.H., Maizels, R.M., Page, A.P., Taylor, G.W., Rendell, N.B. and Dell, A. (1991) Characterization of nematode glycoproteins: the major O-glycans of *Toxocara* excretory-secretory antigens are O-methylated trisaccharides. *Glycobiology*, **1**, 163-171.

Kim, D.H., Feinbaum, R., Alloing, G., Emerson, F.E., Garsin, D.A., Inoue, H., Tanaka-Hino, M., Hisamoto, N., Matsumoto, K., Tan, M.W. and Ausubel, F.M. (2002) A conserved p38 MAP kinase pathway in *Caenorhabditis elegans* innate immunity. *Science*, **297**, 623-626.

Ko, F.C. and Chow, K.L. (2000) Mutations with sensory ray defect unmask cuticular glycoprotein antigens in *Caenorhabditis elegans* male tail. *Dev Growth Differ*, **42**, 69-77.

Kumamoto, K., Goto, Y., Sekikawa, K., Takenoshita, S., Ishida, N., Kawakita, M. and Kannagi, R. (2001) Increased expression of UDP-galactose transporter messenger RNA in human colon cancer tissues and its implication in synthesis of Thomsen-Friedenreich antigen and sialyl Lewis A/X determinants. *Cancer Res*, **61**, 4620-4627.

Kurz, C.L. and Ewbank, J.J. (2000) *Caenorhabditis elegans* for the study of host-pathogen interactions. *Trends Microbiol.*, **8**, 142-144.

Labrousse, A., Chauvet, S., Couillault, C., Kurz, C.L. and Ewbank, J.J. (2000) *Caenorhabditis elegans* is a model host for *Salmonella typhimurium*. *Curr.Biol.*, **10**, 1543-1545.

Lemaitre, B., Nicolas, E., Michaut, L., Reichhart, J.M. and Hoffmann, J.A. (1996) The dorsoventral regulatory gene cassette spatzle/Toll/cactus controls the potent antifungal response in *Drosophila* adults. *Cell*, **86**, 973-983.

Libby, B.J. (1998) Molecular Genetic Analysis of *srf-6*, a Gene involved in Surface Antigen Switching in *Caenorhabditis elegans*. *Department of Biology & Biotechnology*. Worcester Polytechnic Institute, Worcester.

Link, C.D., Silverman, M.A., Breen, M., Watt, K.E. and Dames, S.A. (1992) Characterization of *Caenorhabditis elegans* lectin-binding mutants. *Genetics*, **131**, 867-881.

Lübke, T., Marquardt, T., Etzioni, A., Hartmann, E., von Figura, K. and Korner, C. (2001) Complementation cloning identifies CDG-IIc, a new type of congenital disorders of glycosylation, as a GDP-fucose transporter deficiency. *Nat Genet*, **28**, 73-76.

Lübke, T., Marquardt, T., von Figura, K. and Korner, C. (1999) A new type of carbohydrate-deficient glycoprotein syndrome due to a decreased import of GDP-fucose into the golgi. *J Biol Chem*, **274**, 25986-25989.

Lühn, K., Wild, M.K., Eckhardt, M., Gerardy-Schahn, R. and Vestweber, D. (2001) The gene defective in leukocyte adhesion deficiency II encodes a putative GDP-fucose transporter. *Nat.Genet.*, **28**, 69-72.

Maduro, M. and Pilgrim, D. (1995) Identification and cloning of *unc-119*, a gene expressed in the *Caenorhabditis elegans* nervous system. *Genetics*, **141**, 977-988.

Mahajan-Miklos, S., Tan, M.W., Rahme, L.G. and Ausubel, F.M. (1999) Molecular mechanisms of bacterial virulence elucidated using a *Pseudomonas aeruginosa*-*Caenorhabditis elegans* pathogenesis model. *Cell*, **96**, 47-56.

Maizels, R.M. and Selkirk, M.E. (1988) The Biology of parasitism : a molecular and immunological approach. In Englund, P.T., Sher, A. and Mass.), M.B.L.W.H. (eds.), *MBL lectures in biology ; v. 9*. Liss, New York, pp. 285-308.

Mallo, G.V., Kurz, C.L., Couillault, C., Pujol, N., Granjeaud, S., Kohara, Y. and Ewbank, J.J. (2002) Inducible antibacterial defense system in *C. elegans*. *Curr.Biol.*, **12**, 1209-1214.

Marroquin, L.D., Elyassnia, D., Griffitts, J.S., Feitelson, J.S. and Aroian, R.V. (2000) *Bacillus thuringiensis* (Bt) toxin susceptibility and isolation of resistance mutants in the nematode *Caenorhabditis elegans*. *Genetics*, **155**, 1693-1699.

Martinez-Duncker, I., Mollicone, R., Codogno, P. and Oriol, R. (2003) The nucleotide-sugar transporter family: a phylogenetic approach. *Biochimie*, **85**, 245-260.

Meiss, H.K., Green, R.F. and Rodriguez-Boulan, E.J. (1982) Lectin-resistant mutants of polarized epithelial cells. *Mol.Cell Biol.*, **2**, 1287-1294.

Mello, C.C., Kramer, J.M., Stinchcomb, D. and Ambros, V. (1991) Efficient gene transfer in *C.elegans*: extrachromosomal maintenance and integration of transforming sequences. *Embo J*, **10**, 3959-3970.

Mendoza de Gives, P., Davies, K.G., Morgan, M. and Behnke, J.M. (1999) Attachment tests of *Pasteuria penetrans* to the cuticle of plant and animal parasitic nematodes, free living nematodes and srf mutants of *Caenorhabditis elegans*. *J Helminthol*, **73**, 67-71.

Mendoza De Gives, P.M., Davies, K.G., Clark, S.J. and Behnke, J.M. (1999) Predatory behaviour of trapping fungi against *srf* mutants of *Caenorhabditis elegans* and different plant and animal parasitic nematodes. *Parasitology*, **119 (Pt 1)**, 95-104.

Menozzi, F.D., Pethe, K., Bifani, P., Soncin, F., Brennan, M.J. and Locht, C. (2002) Enhanced bacterial virulence through exploitation of host glycosaminoglycans. *Mol.Microbiol.*, **43**, 1379-1386.

Miura, N., Ishida, N., Hoshino, M., Yamauchi, M., Hara, T., Ayusawa, D. and Kawakita, M. (1996) Human UDP-galactose translocator: molecular cloning of a complementary DNA that complements the genetic defect of a mutant cell line deficient in UDP-galactose translocator. *J Biochem (Tokyo)*, **120**, 236-241.

Mohler, W.A., Simske, J.S., Williams-Masson, E.M., Hardin, J.D. and White, J.G. (1998) Dynamics and ultrastructure of developmental cell fusions in the *Caenorhabditis elegans* hypodermis. *Curr Biol*, **8**, 1087-1090.

Mounsey, A., Molin, L. and Hope, I.A. (1999) Gene expression patterns. In Hope, I.A. (ed.), *C. elegans : a practical approach*. Oxford University Press, Oxford ; New York, pp. 181-199.

Mumberg, D., Muller, R. and Funk, M. (1995) Yeast vectors for the controlled expression of heterologous proteins in different genetic backgrounds. *Gene*, **156**, 119-122.

Oelmann, S., Stanley, P. and Gerardy-Schahn, R. (2001) Point mutations identified in Lec8 Chinese hamster ovary glycosylation mutants that inactivate both the UDP-galactose and CMP-sialic acid transporters. *J Biol Chem*, **276**, 26291-26300.

Ofek, I., Hasty, D.L. and Sharon, N. (2003) Anti-adhesion therapy of bacterial diseases: prospects and problems. *FEMS Immunol Med Microbiol*, **38**, 181-191.

O'Quinn, A.L., Wiegand, E.M. and Jeddeloh, J.A. (2001) *Burkholderia pseudomallei* kills the nematode *Caenorhabditis elegans* using an endotoxin-mediated paralysis. *Cell Microbiol*, **3**, 381-393.

Page, A.P., Hamilton, A.J. and Maizels, R.M. (1992) *Toxocara canis*: monoclonal antibodies to carbohydrate epitopes of secreted (TES) antigens localize to different secretion-related structures in infective larvae. *Exp.Parasitol.*, **75**, 56-71.

Perez, M. and Hirschberg, C.B. (1987) Transport of sugar nucleotides into the lumen of vesicles derived from rat liver rough endoplasmic reticulum and Golgi apparatus. *Methods Enzymol.*, **138**, 709-715.

Philipp, M., Parkhouse, R.M. and Ogilvie, B.M. (1980) Changing proteins on the surface of a parasitic nematode. *Nature*, **287**, 538-540.

Philipp, M. and Rumjanek, F.D. (1984) Antigenic and dynamic properties of helminth surface structures. *Molelcular and Biochemical Parasitology*, **10**, 245-268.

Politz, S.M., Chin, K.J. and Herman, D.L. (1987) Genetic analysis of adult-specific surface antigenic differences between varieties of the nematode *Caenorhabditis elegans*. *Genetics*, **117**, 467-476.

Politz, S.M., Philipp, M., Estevez, M., O'Brien, P.J. and Chin, K.J. (1990) Genes that can be mutated to unmask hidden antigenic determinants in the cuticle of the nematode *Caenorhabditis elegans*. *Proc.Natl.Acad.Sci.U.S.A*, **87**, 2901-2905.

Prasher, D.C., Eckenrode, V.K., Ward, W.W., Prendergast, F.G. and Cormier, M.J. (1992) Primary structure of the *Aequorea victoria* green-fluorescent protein. *Gene*, **111**, 229-233.

Pujol, N., Link, E.M., Liu, L.X., Kurz, C.L., Alloing, G., Tan, M.W., Ray, K.P., Solari, R., Johnson, C.D. and Ewbank, J.J. (2001) A reverse genetic analysis of components of the Toll signaling pathway in *Caenorhabditis elegans*. *Curr.Biol.*, **11**, 809-821.
Riddle, D.L. (1988) The Dauer Larva. In Wood, W.B. (ed.), *The Nematode Caenorhabditis elegans*. Cold Spring Harbor Laboratory, Cold Spring Harbor, N.Y., pp. xiii, 667.
Riddle, D.L., Swanson, M.M. and Albert, P.S. (1981) Interacting genes in nematode dauer larva formation. *Nature*, **290**, 668-671.
Röhrig, S. (2000) Modulation of UNC-86 acitivity during *Caenorhabditis elegans* neurogenesis. *Department of Biochemistry, Gene Center*. Ludwigs-Maximilian University, Munich, p. 164.
Rudin, W. (1990) Comparison of the cuticular structure of parasitic nematodes recognized by immunocytochemical and lectin binding studies. *Acta Trop*, **47**, 255-268.
Sambrook, J., Fritsch, E.F. and Maniatis, T. (1989) Molecular Cloning: A laboratory manual. Cold Sping Harbor Laboratory Press, Cold Spring Harbor, NY.
Sandvig, K. and Van Deurs, B. (2002) Membrane traffic exploited by protein toxins. *Annu.Rev.Cell Dev.Biol.*, **18**, 1-24.
Schinkmann, K. and Li, C. (1992) Localization of FMRFamide-like peptides in *Caenorhabditis elegans*. *J. Comp. Neurol.*, **316**, 251-260.
Segawa, H., Kawakita, M. and Ishida, N. (2002) Human and *Drosophila* UDP-galactose transporters transport UDP-N-acetylgalactosamine in addition to UDP-galactose. *Eur J Biochem*, **269**, 128-138.
Sherman, F. (1991) Getting started with yeast. *Methods Enzymol*, **194**, 3-21.
Shirtliff, M.E., Mader, J.T. and Camper, A.K. (2002) Molecular interactions in biofilms. *Chem.Biol.*, **9**, 859-871.
Silhavy, T.J. and Beckwith, J.R. (1985) Uses of lac fusions for the study of biological problems. *Microbiol Rev*, **49**, 398-418.
Simmer, F., Tijsterman, M., Parrish, S., Koushika, S.P., Nonet, M.L., Fire, A., Ahringer, J. and Plasterk, R.H. (2002) Loss of the putative RNA-directed RNA polymerase RRF-3 makes *C. elegans* hypersensitive to RNAi. *Curr Biol*, **12**, 1317-1319.
Singh, R.N. and Sulston, J.E. (1978) Some observations on molting in *C. elegans*. *Nematologica*, **24**, 63-71.
Skurnik, M. (2003) Molecular genetics, biochemistry and biological role of *Yersinia* lipopolysaccharide. *Adv Exp Med Biol*, **529**, 187-197.
Smith, W.L., Nakajima, T. and Ballou, C.E. (1975) Biosynthesis of yeast mannan. Isolation of *Kluyveromyces lactis* mannan mutants and a study of the incorporation of N-acetyl-D-glucosamine into the polysaccharide side chains. *J.Biol.Chem.*, **250**, 3426-3435.
Stanley, P. (1985) Membrane mutants of animal cells: rapid identification of those with a primary defect in glycosylation. *Mol Cell Biol*, **5**, 923-929.
Stein, L.D., Bao, Z., Blasiar, D., Blumenthal, T., Brent, M.R., Chen, N., Chinwalla, A., Clarke, L., Clee, C., Coghlan, A., Coulson, A., D'Eustachio, P., Fitch, D.H., Fulton, L.A., Fulton, R.E., Griffiths-Jones, S., Harris, T.W., Hillier, L.W., Kamath, R., Kuwabara, P.E., Mardis, E.R., Marra, M.A., Miner, T.L., Minx, P., Mullikin, J.C., Plumb, R.W., Rogers, J., Schein, J.E., Sohrmann, M., Spieth, J., Stajich, J.E., Wei, C., Willey, D., Wilson, R.K., Durbin, R. and Waterston, R.H. (2003) The Genome Sequence of *Caenorhabditis briggsae*: A Platform for Comparative Genomics. *PLoS Biol*, **1**, E45.
Stiernagel, T. (1999) Maintenance of *C. elegans*. In Hope, I.A. (ed.), *C. elegans : a practical approach*. Oxford University Press, Oxford ; New York, pp. xxi, 281.
Takiff, H.E., Chen, S.M. and Court, D.L. (1989) Genetic analysis of the *rnc* operon of *Escherichia coli*. *J Bacteriol*, **171**, 2581-2590.

Tan, M.W. and Ausubel, F.M. (2000) Caenorhabditis elegans: a model genetic host to study Pseudomonas aeruginosa pathogenesis. *Curr Opin Microbiol*, **3**, 29-34.
Tan, M.W., Mahajan-Miklos, S. and Ausubel, F.M. (1999) Killing of *Caenorhabditis elegans* by *Pseudomonas aeruginosa* used to model mammalian bacterial pathogenesis. *Proc Natl Acad Sci U S A*, **96**, 715-720.
Thein, M.C., McCormack, G., Winter, A.D., Johnstone, I.L., Shoemaker, C.B. and Page, A.P. (2003) *Caenorhabditis elegans* exoskeleton collagen COL-19: an adult-specific marker for collagen modification and assembly, and the analysis of organismal morphology. *Dev Dyn*, **226**, 523-539.
Walsh, C. (2000) Molecular mechanisms that confer antibacterial drug resistance. *Nature*, **406**, 775-781.
Warren, C.E., Krizus, A. and Dennis, J.W. (2001) Complementary expression patterns of six nonessential *Caenorhabditis elegans* core 2/I N-acetylglucosaminyltransferase homologues. *Glycobiology*, **11**, 979-988.
Warren, C.E., Krizus, A., Roy, P.J., Culotti, J.G. and Dennis, J.W. (2002) The *Caenorhabditis elegans* gene, *gly-2*, can rescue the N-acetylglucosaminyltransferase V mutation of Lec4 cells. *J Biol Chem*, **277**, 22829-22838.
Wood, W.B. (1988) *The Nematode Caenorhabditis elegans*. Cold Spring Harbor Laboratory, Cold Spring Harbor, N.Y.
Woodcock, D.M., Crowther, P.J., Doherty, J., Jefferson, S., DeCruz, E., Noyer-Weidner, M., Smith, S.S., Michael, M.Z. and Graham, M.W. (1989) Quantitative evaluation of *Escherichia coli* host strains for tolerance to cytosine methylation in plasmid and phage recombinants. *Nucleic Acids Res*, **17**, 3469-3478.
Ziebuhr, W. (2002) Development of Antibiotic Resistance in Bacteria. In Hacker, J. and Heesemann, J. (eds.), *Molecular infection biology : interactions between microorganisms and cells*. Wiley-Liss ;
Spektrum, Hoboken, NJ
Heidelberg, Germany, pp. xvii, 339.
Zuckerman, B.M., Kahane, I. and Himmelhoch, S. (1979) *Caenorhabditis briggsae* and *C. elegans*: Partial characterization of cuticle surface carbohydrates. *Exp Parasitol*, **47**, 419-424.

Appendix

Used and constructed *C. elegans* strains

Table 5: **used *C. elegans* strains**

Strain	Genotype	Reference
AT6	*srf-2(yj262)* I	(Politz et al., 1990)
AT10	*srf-3(yj10)* IV	(Politz et al., 1990)
BC1217	sDf22/nT1 IV; +/nT1 V	(Clark et al., 1988)
BR2374	*unc-31 (e169) srf-3 (yj10) lev-1 (e211)* IV	this study
BR2391	*unc-31 (e169) srf-3 (yj10)* IV	this study
CB2238	*lon-2(e678) unc-84(e1410)* X	CGC (provided by B. Horvitz)
CB5430	*srf-3(e2680)* ÎV	this study
BR2905	*gly-14(id48)* III; *gly-12(is47)* X	(Chen et al., 2003)
CB5439	*srf-3(e2689)* IV	this study
CB5608	*srf-3(e2789)* IV	this study
CB5670	*srf-3(e2797)* IV; *him-5(e1490)*V	this study
CL183	*him-5(e1490) srf-4(ct109)*V	(Link et al., 1992)
CL208	*srf-9(dv4) him-5(e1490)*V	(Link et al., 1992)
CL261	*him-5(e1490)*V*; srf-5(ct115)*X	(Link et al., 1992)
CL264	*srf-8(dv38)*V	(Link et al., 1992)
DP?	*unc-119(ed4)*III	(Maduro and Pilgrim, 1995)
DA491	*dpy-20 (e1282) unc-30 (e191)* IV	CGC (provided by L. Avery)
DC1047	*srf-3(br6)* IV	this study
DR210	*dpy-5(e61) daf-16(m26) unc-75(e950)*I	CGC (provided by M. MacMorris)
DR66	*daf-13(m66)*X	(Riddle et al., 1981)
DR466	*him-5(e1490)* V	(Hodgkin et al., 1979)
EM68	*col-34(bx25)* IV*; him-5(e1490)*V	(Baird and Emmons, 1990)
EM81	*him-5 (e1490)* V *ram-5((bx30)* X	(Baird and Emmons, 1990)
EM113	*dpy-10(e128) ram-3(bx32)* II *him-5(e1490)* V	(Baird and Emmons, 1990)
EM131	*ram-2(bx39)* II *him-5(e1490)* V	(Baird and Emmons, 1990)
EM139	*ram-1(bx34)* I *him-5(e1490)* V	(Baird and Emmons, 1990)
HY483	*bre-3(ye26)* III	(Marroquin et al., 2000)
HY485	*bre-4(ye27)* IV	(Marroquin et al., 2000)
HY494	*bre-2(ye31)* III	(Marroquin et al., 2000)
HY496	*bre-1(ye4)* IV	(Marroquin et al., 2000)
HY498	*bre-5(ye17)* I	(Marroquin et al., 2000)
NJ51	*exc-1(rh26)* X	(Buechner et al., 1999)
NJ242	*exc-2(rh90)*X	(Buechner et al., 1999)
NJ555	*exc-3(rh207)* X	(Buechner et al., 1999)
NJ683	*exc-7(rh252)* II	(Buechner et al., 1999)
NJ731	*exc-5(rh232)*IV	(Buechner et al., 1999)
NJ833	*exc-6(rh103)* III	(Buechner et al., 1999)
NL2099	*rrf-3(pk1426)* II	(Simmer et al., 2002)
NW1287	*gly-1 (ev686)* II	(Warren et al., 2001)

Strain	Genotype	Reference
MT6169	*exc-4(n2400)* I	(Buechner et al., 1999)
MT6984	*exc-9(n2669)* IV	(Buechner et al., 1999)
XA762	*gly-2(qa703)* I	(Warren et al., 2002)
XA763	*gly-16(qa701)* I	(Warren et al., 2001)
XA749	*gly-1(qa702)* II	(Warren et al., 2001)
SU93	*jcIs* [pJS191, pRF4, unc-29(+)] IV	(Mohler et al., 1998)

Table 6: **constructed *C. elegans* strains**

Strain	Genotype
BR2408	*srf-3(e2789) unc-30(e191)* IV
BR2416	*srf-3(e2680) unc-30(e191)* IV
BR2438	*srf-3 (e2680) unc-30 (e191)*IV *byEx238* [M02B1, BSSKII, pBY218]
BR2439	*srf-3(e2789) unc-30(191)*IV *byEx239* [M02B1, BSSKII, pBY218]
BR2440	*srf-3(e2680) unc-30(e191)*IV *byEx239* [M02B1, BSSKII, pBY218]
BR2443	*srf-3(e2789) unc-30(e191)*IV*; byEx241* [ZK896, BSSKII, pBY1153]
BR2444	*srf-3(e2789) unc-30(e191)*IV*; byEx242*[ZK896, BSSKII, pBY1153]
BR2461	*srf-3(e2689) unc-30(e191)* IV
BR2515	*srf-3(e2789) unc-30(e191)*IV*; byEx262* [pBY1453, BSSKII, pBY1153]
BR2516	*srf-3(e2789) unc-30(e191)*IV*; byEx263* [pBY1453, BSSKII, pBY1153]
BR2517	*srf-3(e2789 unc-30(e191)* IV*; byEx264* [pBY1453, BSSKII, pBY1153]
BR2520	*srf-3(e2789) unc-30(e191)*IV*; byEx266* [pBY1454,BSSKII, pBY1153]
BR2521	*srf-3(e2789) unc-30(e191)* IV*; byEx265* [pBY1454, BSSKII, pBY1153]
BR2563	*srf-3(e2789) unc-30(e191)* IV*; byEx276* [pBY1509, BSSKII, pBY1153]
BR2564	*srf-3(e2789) unc-30(e191)* IV*; byEx277* [pBY1509, BSSKII, pBY1153]
BR2569	*srf-3(e2789) unc-30(e191)* IV*; byEx280* [pBY1508, BSSKII, pBY1153]
BR2572	*srf-3(e2789) unc-30(e191)* IV*; byEx281* [pBY1508, BSSKII, pBY1153]
BR2597	*unc-31(e928) srf-3(yj10)* IV; *him-5 (e1490)* V
BR2625	*unc-30(e191)* IV; *him-5(e1490)* V
BR2655	*srf-3(yj10) unc-30(e191)* IV
BR2675	*srf-3(e2680)* IV*; him-5(e1490)*V
BR2676	*srf-3(e2689)* IV*; him-5(e1490)*V
BR2691	*srf-3(yj10)* IV; *him-5(1490)* V
BR2692	*daf-2(e1370)* III*; srf-3(e2680)* IV
BR2700	*daf-2(e1370)* III; *srf-3(e2789)* IV
BR2705	*daf-2(e1370)* III; *srf-3(e2689)* IV
BR2732	*srf-3(e2797)* IV
BR2733	*srf-3(e2797)* IV; *him-5(e1490)* V
BR2748	*srf-3(e2797)* IV*; unc-30(e191)* IV
BR2806	N2*; byEx321* [pBY1565, N2 genomic DNA, pRF4]
BR2807	N2*; byEx322* [pBY1565, N2 genomic DNA, pRF4]
BR2808	N2*; byEx323* [pBY1565, N2 genomic DNA, pRF4]
BR2809	N2*; byEx324* [pBY1570, BSSKII, pRF4]
BR2810	*unc-119(ed4); byEx325* [pBY1603, BSSKII, pBY232]
BR2811	*unc-119(ed4); byEx326* [pBY1603, BSSKII, pBY232]
BR2829	*srf-3(e2789) jcls1* IV
BR2830	*srf-3(e2789) jcls1* IV; *him-5(e1490)* V
BR2831	*srf-3(yj10) jcls1* IV
BR2832	*srf-3(yj10) jcls1* IV; *him-5(e1490)* V

Strain	Genotype
BR2841	*daf-2(e1370)* III; *srf-3(e2797)* IV
BR2847	*unc-119(ed4)*III*; byEx331* [pBY1605, BSSKII, pBY232]
BR2848	*unc-119(ed4)*III*; byEx332* [pBY1605, BSSKII, pBY232]
BR2849	*unc-119(ed4)*III*; byEx333* [pBY1605, BSSKII, pBY232]
BR2871	*daf-2(e1370)* III; *srf-3(yj10)* IV
BR2940	*gly-2(qa703)* I*; him-5 (e1490)*V
BR2941	*gly-2(qa703)* I*; srf-3(e2789)*IV*; him-5(e1490)* V
BR2942	*gly-2(qa703)*I*; srf-3(e2789)*IV
BR2995	*srf-2(yj262)* I*; him-5(e1490)* V; *srf-5(ct115)* X
BR2996	*srf-2(yj262)* I*; srf-3(e2789)* IV; *him-5(e1490)* V
BR2997	*gly-16(qa701)* I; *him-5(e1490)* V
BR2999	*gly-16(qa701)* I*; srf-3(e2789)* IV; *him-5(e1490)* V
BR3000	*gly-14(id48)* III*; srf-3(2789)* IV; *him-5(e1490)* V; *gly-12(is47)* X
BR3001	*gly-18(qa704)* I*; srf-3(e2789)* IV; *him-5(e1490)* V
BR3016	*srf-3(2789)/ dpy-20(e1282) unc-30(e191)* IV; *srf-4(ct109)* V
BR3031	*by158* [Deletion mutant of ZK896.9]
BR3028	*srf-3(e2789)* IV*; him-5 (e1490)* V*; srf-5(ct115)* X
BR3080	*srf-3(e2789) unc-30(e191)*IV*; byEx385* [pBY1810, BSSKII, pBY218]
BR3081	*srf-3(e2789) unc-30(e191)*IV*; byEx386* [pBY1810, BSSKII, pBY218]
BR3082	*srf-3(e2789) unc-30(e191)*IV*; byEx387* [pBY1810, BSSKII, pBY218]

Used yeast strains

Table 7: used yeast strains

Strain	Genotype	Reference
S. cerevisiae **PRY225**	*ura3-52*, *lys2-801am*, *ade2-1020c*, *his3*, *leu2*, *trp1Δ1*	
K. lactis **KL3**	Mat a, uraA, mnn2-2, $arg^{-}K^{+}$, pKD1+	(Guillen et al., 1998)

Used E. coli strains

Table 8: used E. coli strains

Strain	Genotype	Reference
OP50	*ura*$^{-}$	(Brenner, 1974)
HB101	*mcr*B *mrr hsd*S20 ($r_B^{-}m_B^{-}$) *leu*B6 *sup*E44 *ara*14 *gal*K2 *lac*Y1 *pro*A2 *rps*L20(Sm^r) *xyl*-5 *mtl*-1 *rec*A14	(Boyer and Roulland-Dussoix, 1969)
HT115	W3110, *rnc*14::ΔTn*10*	(Takiff et al., 1989)
DH5α	*rec*AI, *end*A1, *gyr*A96, *thi*, *hsd*R17(r_K^{-},m_K^{+}),*rel*A1, *sup*E44, ϕ80d*lac*ZΔM15, Δ(*lac*ZYA-*arg*F)U169	(Woodcock et al., 1989)

Constructed and used Plasmids

Table 9: Plasmids

Plasmidname	Description/ Reference
Bluescript	Cloning vector (Stratagene)
SKII-	
F07C6	Cosmid
Litmus 28	Cloning vector (New England Biolabs)
M02B1	Cosmid
pBY1451	*Pst*I derived subclone of M02B1
pBY1452	*Bgl*II derived subclone of M02B1
pBY1453	*Pac*I derived subclone of M02B1
pBY1454	*Aat*II derived subclone of M02B1
pBY1455	*Pst*I derived subclone of M02B1
pBY1481	*Pst*I derived subclone of M02B1
pBY1508	pBY1454 carrying a *EcoN*I deletion
pBY1509	pBY1454 carrying a *Sap*I deletion
pBY1520	ZK896.9 cDNA in Bluescript
pBY1523	ZK896.9 cDNA in pPD129.36
pBY1554	*M02B1.1::GFP*
pBY1555	*M02B1.1::GFP*
pBY1564	*ZK896.9::GFP*
pBY1565	*ZK896.9::GFP*
pBY1570	*pZK896.9::GFP*
pBY1571	*pZK896.9::GFP*
pBY1601	vector containing multiple cloning site and unc-54 3' UTR
pBY1603	*srf-3* promoter in pPD118.15
pBY1604	partial *srf-3* cDNA clone including 5'UTR
pBY1605	*GFP::M02B1.1*
pBY1606	*GFP::M02B1.1*
pBY1614	ZK896.9 cDNA including 5'UTR
pBY1618	partial *srf-3* cDNA in pPD129.36
pBY1817	*srf-3* full length cDNA in Bluescript
pBY1818	Bluescript containing *srf-3* 5' and 3' regulatory elements
pBY1819	*srf-3* cDNA fused to a VSV tag coding sequence at the 3' end (SRF-3VSV)
pBY1820	*srf-3* cDNA fused to a VSV tag coding sequence at the 5' end (VSVSRF-3)
pBY1821	SRF-3VSV in pCDNA3.1-
pBY1822	VSVSRF-3 in pG426
pBY1824	SRF-3VSV in pG426
pBY1825	VSVSRF-3 in pCDNA3.1-
pBY1865	*srf-3* cDNA in pBY1818
pBY1866	SRF-3VSV in pE4
pBY1867	VSVSRF-3 in pE4
pBY1869	VSVSRF-3 in pBY1818
pBY1870	SRF-3VSV in pBY1818
pBY1907	*srf-3::NLS::lacZ*
pCDNA3.1$^-$	vector for expression in mammalian cells (Invitrogene)
pDP#MM016B	*unc-119* rescue injection marker (Maduro and Pilgrim, 1995)

Plasmidname	Description/ Reference
pPD95.57	promoterless *NLS::lac-Z* vector (ftp://www.ciwemb.edu/pub/FireLabInfo/FireLabVectors/)
pPD95.75	promoterless *GFP* vector (ftp://www.ciwemb.edu/pub/FireLabInfo/FireLabVectors/)
pPD118.15	vector to tag the protein of interest with GFP at the N-terminus of the protein (ftp://www.ciwemb.edu/pub/FireLabInfo/FireLabVectors/)
pPD129.36	vector for the generation of dsRNA in vitro and in vivo (ftp://www.ciwemb.edu/pub/FireLabInfo/FireLabVectors/)
pE4	*K. lactis* expression vector (Guillen et al., 1998)
pG426	*S. cerevisiae* expression vector (Mumberg et al., 1995)
pGEM-T	vector for A-overhang cloning (Promega)
pRF4	dominant behavioural injection marker [*rol-6(su1006)*] (Mello et al., 1991)
ZK896	Cosmid

Solutions, reagents and buffers

If not stated otherwise or amount of substance is given, all details given below are for one liter. If plates for growing bacteria or yeast were needed the corresponding media were supplemented with 2 % Agar.

M9
3 g/l KH_2PO_4
6 g/l Na_2HPO_4
5 g/l NaCl
0.1 M $MgSO_4$

TBS
137 mM NaCl
25 mM Tris
2.6 mM KCl

Nystatin solution
4 g Nystatin
200 ml EtOH
200 ml 7.5 M NH_4Ac
sterilize by filtrating

NGM plates
3 g/l NaCl
2.5 g/l Bacto-Peptone
17 g/l Agar
add 967 ml H_2O
autoclave
+ 1 ml 0.1 M $CaCl_2$
+ 1 ml 0.1 M $MgSO_4$
25 ml 1 M KH_2PO_4
5 ml Nystatin solution
1 ml Cholesterol (5 mg/ml in EtOH)

Freezing Buffer
5.8 g/l NaCl
6.8 g/l KH_2PO_4
30% Glycerol
5.6 ml 1M NaOH
add H_2O to a final volume of 1 l
autoclave
after cooling add 1 ml of 1 M $MgSO_4$

Hypochlorite solution
6 ml NaOCl (4%)
2.5 ml 5 M KOH
add H_2O to a final volume of 50 ml

Worm lysis buffer
50 mM KCl
10 mM Tris pH 8.2
2.5 mM $MgCl_2$
0.45% NP-40
0.45% Tween 20
0.01% Gelatine
pior to use Proteinase K is added to a final concentration of 0.5 mg/ml

S-Medium for liquid medium
5.8 g NaCl
ad 900 ml dH_2O
autoclave
+ 50 ml KH_2PO_4 (1M, pH 6.0)
+ 3 ml 1 M $MgSO_4$
+ 3 ml 1 M $CaCl_2$
+10 ml 1 M NaCitrat
+ 10 ml trace metal solution
+ 1 ml Cholesterol
+ 5 ml Nystatin solution
+ 1 ml Streptomycin/PSN-Antibiotic Mixture

Trace metals solution
0.93 g Na_2EDTA
0.35 g $FeSO_4$*7 H_2O
0.1 g $MnCl_2$*4 H_2O
0.15 g $ZnSO_4$*7 H_2O
0.008 g $CuSO_4$
add 500 ml dH_2O
sterilize

β-galactosidase staining solution (1ml)

614.5 µl	H_2O
250 µl	0.8 M sodium phosphate buffer pH 7.4
20 µl	50 mM $MgCl_2$
4 µl	1% SDS
100 µl	100 mM Redoxpuffer
1.5 µl	50 mg/ml Kanamycin
2 µl	1 mg/ml DAPI
8 µl	5% X-Gal in Dimethylformamide

Redoxbuffer
100 mM K_4 [$Fe(CN)_6$]
100 mM K_3 [$Fe(CN)_6$]

LB medium
1 % tryptone
0.5 % yeast extract
1 % NaCl
sterilized by autoclaving

YPD Medium
1% Bacto Yeast extract
2% Bacto Peptone
2% D-(+)-Glucose

SD-Medium
0.67% Yeast Nitrogen Base
2% D-(+)-Glucose
30µg/ml Lysin
30µg/ml Leucine
30µg/ml Histidine
30µg/ml Tryptophane
30µg/ml Uracil

Membrane buffer
10 mM triethanolamine pH 7.2
0.8 M sorbitol
1 mM EDTA

Transport buffer
30 mM triethanolamine pH 7.2
0.3 M sucrose
5 mM $MgCl_2$
5 mM $MnCl_2$

2 x Spheroblast buffer
2.8 M sorbitol
0.1 M potassiumphosphate pH 7.5
10 mM NaN_3

Stop solution
0.5 M sucrose
1 mM EDTA

TE buffer (x1)
10 mM Tris
1 mM EDTA pH 8.0
autoclave

TBE buffer (x1)
90 mM Tris
90 mM boric acid
2.5 mM EDTA

DNA sample buffer (10x)
0.5 % SDS
0.25 % Orange G
25 % glycerol
25 mM EDTA

Protein sample buffer (x2)
4 % SDS
100 mM DTT
150 mM Tris/HCl, pH 6.8
0.5 % Bromphenolblau
8 M Urea

Transferbuffer
250 mM Tris
1.92 M glycine
0.1 % SDS
20% methanol

Electrophorese buffer
60 mM Tris
0.55 % glycine
0.1 % SDS

Phosphate buffered saline pH 7.5 (PBS)
100 mM NaCl
20 mM NaH_2PO_4
80 mM Na_2HPO_4

SSC (x20)
3M NaCl
0.3 M NaCitrate
pH 7.0

Oligonucleotides

Name of oligonucleotide	sequence 5' → 3'	Description
RB639	ACG TGG ATC CGG TTT AAT TAC CCA AGT TTG AG	SL1 specific primer
RB640	ACGTGGATCCGGTTTTAACCCAGTTACTCAAG	SL2 specific primer
RB744	TGT TCG AAG CCA CGT TAC AAT GGC	Tc1 specific primer (L1)
RB745	TCAAGTCAAATGGATGCTGAG	Tc1 specific primer (L2)
RB1367	TTGCTCGATTGGCCAAGTCAG	Tc1 specific primer (R1)
RB1368	ATTCACAAGCTGATCGACTCG	Tc1 specific primer (R2)
RB1476	TTT CCG AAA ATC CGG CAG ACC TGT TTC	for amplification of M02B1.1 genomic region. Inner forward primer for nested PCR
RB1477	GCCCGAGAGTTCGGTTAAAATACCTGTG	for amplification of M02B1.1 genomic region. Outer forward primer for nested PCR
RB1478	AAATGACGACGCATTTCATCCACTGC	for amplification of M02B1.1 genomic region. Outmost forward primer for nested PCR
RB1479	CTCAGGTCAAATCGGGTTTCCAACAGGA	for amplification of M02B1.1 genomic region. Inner reverse primer for nested PCR
RB1480	GCG ACT TCT CCA CGA GGA GTA CAA AAG TTG	for amplification of M02B1.1 genomic region. Outer reverse primer for nested PCR
RB1481	GTGTTAGAGCTTTCCCGCTCATTCTT	for amplification of M02B1.1 genomic region. Outmost reverse primer for nested PCR
RB1483	TCTGTGTGTCCACGTTGCAGAGTGCAAT	for deletion of ZK896.9 genomic region. Outer forward primer for nested PCR
RB1484	AAA CCA GCA GTG TGT GCT TGA GAG ACG	for deletion of ZK896.9 genomic region. Inner forward primer for nested PCR
RB1516	GAC TAA GCT TAT GGG GCT CAC AAA AGC AG	for amplification of ZK896.9 cDNA; used for cloning pBY1520
RB1517	GAC TAC GCG TTT ATG ATT TGC TGC TCT CGA C	for amplification of ZK896.9 cDNA; used for cloning pBY1520

Name of oligonucleotide	sequence 5' → 3'	Description
RB1518	GACTAAGCTTATGAAGACGGCAATTTTGAT	for amplification of M02B1.1 cDNA; used for cloning pBY1817
RB1551	CAA AAG GAA ATA TGA AGA CGG	forward nested primer for amplification of M02B1.1 cDNA
RB1552	CGAATTTTCTAGAATTTCAAACTATAAAAC	reverse nested primer for amplification of M02B1.1 cDNA
RB1553	ATT TCC AGG CCA CAA TGG GGC TC	forward nested primer for amplification of ZK896.9 cDNA
RB1554	ATTTCTAAGAGATGAAATTTATGATTTGCTGC	reverse nested primer for amplification of ZK896.9 cDNA
RB1555	CAG CAA ATC CGG ATA GAA CGC AAG CGA TGA	reverse outmost primer for deletion of ZK896.9
RB1556	CTAATGAACTCACCGAGCACCGAATTTTCTG	outer reverse primer for deletion of ZK896.9
RB1557	TTA GAC GAT GCC AGT GAC GCT GTT GTG	inner reverse primer for deletion of ZK896.9
RB1598	GGT CTG CGC CTT TAA AGA G	forward primer for sequencing of M02B1.1 genomic region
RB1599	CTT TTC TAC GTG GCA GCT TC	forward primer for sequencing of M02B1.1 genomic region
RB1600	TGTAGTCGATGTACGGAGTC	forward primer for sequencing of M02B1.1 genomic region
RB1601	AATGACTACTGTAGCGCTGG	reverse primer for sequencing of M02B1.1 genomic region
RB1602	ACCATGAAAGTTGCGGCGTC	reverse primer for sequencing of M02B1.1 genomic region
RB1603	CGCAAAACTATGAAAAGTAGATAC	reverse primer for sequencing of M02B1.1 genomic region
RB1619	AGTTGAACGAGAGAGACTCC	reverse primer for sequencing of the M02B1.1 genomic region and cDNA
RB1620	TAG AGC GTG GAT GAA TCT GG	reverse primer for sequencing of the M02B1.1 genomic region and cDNA
RB1621	GTCAAACGTCGATGAAGTAC	forward primer for sequencing of the ZK896.9 cDNA
RB1622	TCAGCTGAAAATTCTGACGA	forward primer for sequencing of the ZK896.9 cDNA
RB1623	GTCTGGGTTACTGTAGCCAT	forward primer for sequencing of the ZK896.9 cDNA
RB1624	ACTGCAACAACGAGTCCTCC	reverse primer for sequencing of the ZK896.9 cDNA
RB1679	CAG TAA CCA TTT AGC GCG TC	forward primer for sequencing of M02B1.1 genomic region
RB1699	GAT CTC TAG ACG AAC TAT AAA ACT TTT TAA TCT C	reverse primer for cloning M02B1.1 genomic region in Fire expression vector;used for cloning pBY1554 and pBY1555
RB1700	GAT CGT CGA CGC TTT CCC CAA ACA TTT TTA G	forward primer for cloning M02B1.1 genomic region in Fire expression vector; used for cloning pBY1554, pBY1555, pBY1603 and 1907

Name of oligonucleotide	sequence 5' → 3'	Description
RB1702	GAT CAC TAG TTA CTT CCT GTT GGA AAC CCG	forward primer for cloning ZK896.9 genomic region in Fire expression vector; used for cloning pBY1564 and pBY1565
RB1743	CGG CAA TTT TGA TAT GGT TAA	forward sequencing primer for M02B1.1 genomic region and cDNA
RB1744	GAT TTC AGC TAA ATT TAG CCC	forward sequencing primer for M02B1.1 genomic region
RB1745	GAC GAA TGG AGA TTC ACC AG	reverse sequencing primer for M02B1.1 genomic region and cDNA
RB1746	TCAAACTATAAAACTTTTTAATCTC	reverse sequencing primer for M02B1.1 genomic region
RB1762	GAT CTG GCC AGT GAT TTG CTG CTC TCG ACC A	reverse primer for cloning ZK896.9 genomic region in Fire expression vector; used for cloning pBY1564 and pBY1565
RB1829	GAT CCT GCA GAT GTT TGC AGA TCC GTC G	anneals to a different ATG site 1.5 kb upstream of the predicted M02B1.1 ATG; used to determine START codon
RB1830	GAT CGT CGA CAA GAA TTG GGA CAA CTC C	reverse GFP primer anneals within the first exon of GFP from the fire vectors; used for cloning pBY1604
RB1831	GAT CCT GCA GAT GTT TGT TAG TAC TGT AGC TG	anneals to a different ATG site 150 bp downstream of the predicted M02B1.1 ATG; used to determine START codon
RB1832	GAT CCT GCA GAT GGG TAG AAA TGA CGA CG	anneals to a different ATG site 1.1 kb upstream of the predicted M02B1.1 ATG; used to determine START codon
RB1849	GAT CGC TAG CGT CAT TGT GGC CTG GAA ATT	reverse primer for amplification of the ZK896.9 promoter; used for cloning pBY1570 and pBY1571
RB1873	GAT CGA TAT CCA TAT TTC CTT TTG ATT GTG AAG AT	reverse primer for amplification of M02B1.1 promoter; used for cloning pBY1603
RB1920	GAT CGC TAG CAT GAA GAC GGC AAT TTT GAT ATG	for amplification of M02B1.1 to generate a N-terminal GFP fusion; used for cloning pBY1605
RB1921	GAT CGA CGT CGC CTG GAA ATT GGA GGA ATT	for amplification of M02B1.1 to generate a N-terminal GFP fusion; used for cloning pBY1605
RB2046	GAT CTC TAG AAT TTC CTT TTG ATT GTG AAG ATT C	for amplification of *srf-3* promoter; used for cloning pBY1818
RB2047	GAT TGT TGT ATG GTT TTG AC	forward primer for sequencing of the M02B1.1 genomic region and cDNA

Name of oligonucleotide	sequence 5’ → 3’	Description
RB2048	TAC AAG TGA GTA ATT CGG GT	forward primer for sequencing of the ZK896.9 genomic region and cDNA
RB2059	GAT CCT CGA GTG TGG CCT GGA AAT TGG AGG	reverse primer for amplification of *srf-3* 3'UTR; used for cloning pBY1818
RB2062	TGC GTC TCT CCA CAT ATA CTG CTC	forward primer for detection of *gly-2* deletion in *qa703*.
RB2063	CCACTTGGTGAACTTCTTCAATG	forward primer for detection of *gly-2* deletion in *qa703*.
RB2064	TGG ACC ATT TTC TCA ACG GAA TC	forward primer annealing within the deletion of *qa703*.
RB2099	TTC TTC TCG GGA TGA TGG AAT CCG	reverse primer for detection of *gly-1(qa703)*
RB2100	TCT AGT TTA CAC CCT GTT CGT CAG	forward primer for detection of *gly-1(qa703)*
RB2101	TTTC CTG GGCTCATTGAGCTTCCA	forward primer for detection of *gly-16(qa701)*
RB2102	TTC CTA ATC TTG CTC GAG GAG CTC	reverse primer for detection of *gly-16(qa701)*
RB2103	CCCGTTGTTGTGAGTGGAAGCATA	forward primer for detection of *gly-18(qa704)*
RB2104	CAG TGG AGA CTG AGT CTC CTG AAA	reverse primer for detection of *gly-18(qa704)*
RB2106	AAATTATAAAAGCAGCAGA	reverse primer for reverse transcription to clone 3’ end of M02B1.1
RB2107	TGA TAA TAA ATC ACA GAT TC	reverse primer for reverse transcription to clone 3’ end of M02B1.1
RB2108	GCATTTTTTAAGCGTCACTA	reverse primer for reverse transcription to clone 3’ end of M02B1.1
RB2109	GAT CAA GCT TTT ACA GAC AAA ACG CCT CTT	reverse primer for amplification of *srf-3* cDNA. Anneals to the putative Exon 6 downstream of the predicted stop; used for cloning pBY1817
RB2110	GAG ATG ACA AAG GCG TGC GAA AAT	forward primer for detection of *by158*
RB2111	AGAGAACACAGTCCACAATCAGGC	reverse (inner) primer for detection of *by158*
RB2112	CTC CTC GCG GAG AAA ATT TTG CAG	reverse (outer) primer for detection of *by158*
RB2113	GTCAAGATGGCAATAAGACCGCCG	forward primer for detection of *gly-12* deletion.(F1)
RB2114	GAA CAA CTA CCC AGC CAT CTC GGC	forward primer for detection of *gly-12* deletion.(F2)
RB2115	CAATCACCCGTATCGTCACAGG	reverse primer for detection of *gly-12* deletion.(R3)
RB2116	GAG ACA TGA CGT GGC GGT CGC	reverse primer for detection of *gly-12* deletion.(R4)
RB2117	GCGCCTTTAAAAATCGAGTACGG	forward primer for detection of *gly-14* deletion.(F1)

Name of oligonucleotide	sequence 5' → 3'	Description
RB2118	CGT GCT CAT CTA CTT TTC ATG G	forward primer for detection of *gly-12* deletion.(F2)
RB2119	CACCAAGAAGAATCATAACCAGG	reverse primer for detection of *gly-14* deletion(R3)
RB2120	GGT ATA CGG TAG GGT ACT GTA GGG	reverse primer for detection of *gly-14* deletion(R4)
RB2124	GATCTCGAGATTCTCGTCTGTATATTATAGTGACGCT	forward primer for amplification of *srf-3* 3'UTR; used for cloning pBY1818
RB2136	GAT CGA GCT CGC TTT CCC CAA ACA TTT TTA G	for amplification of *srf-3* promoter; used for cloning pBY1818
RB2138	GAT CTC TAG ATT ACA GAC AAA ACG CCT CTT	reverse primer for amplification of *srf-3* cDNA; used for cloning pBY1820
RB2141	GATCTCTAGAATGAAGACGGCAATTTTGAT	forward primer for amplification of *srf-3* cDNA; used for cloning pBY1819
RB2142	GATCTCGAGATTCTCGTCTGTATATTATAGTGACGCT	reverse primer for cloning M02B1.1 genomic region in Fire expression vector; used for cloning pBY1907
RB2145	GAT CTC TAG AAT GTA CAC TGA TAT CGA AAT GAA CCG CCT GGG TAA G A T G AA GAC GGC AAT TTT GAT	forward primer for amplification of srf-3 cDNA; used for cloning pBY1820
RB2146	GATCTCTAGATTACTTACCCAGGCGGTTCATTTCGATATCAGT GTACAGACAAAACGCCTCTTTTG	reverse primer for amplification of *srf-3* cDNA; used for cloning pBY1819
RB2180	GATCGTCGACATGAAGACGGCAATTTTGATATG	forward primer for amplification of *srf-3* cDNA tagged with a VSV-G tag at the c-terminus; used for cloning pBY1870
RB2181	GAT CGT CGA CTT ACT TAC CCA GGC GGT T	primer for amplification of *srf-3* cDNA tagged with a VSV-G tag at the c-terminus; used for cloning pBY1870
RB2182	GATCGTCGACTTACAGACAAAACGCCTC	forward primer for amplification of *srf-3* cDNA tagged with an VSV-G tag at the n-terminus; used for cloning pBY1869
RB2183	GAT CGT CGA CAT GTA CAC TGA TAT CGA AAT G	reverse primer for amplification of *srf-3* cDNA tagged with an VSV-G tag at the n-terminus; used for cloning 1969
RB2218	CTCTTTGGATGAGAAATGTTC	forward sequencing primer for M02B1.1 genomic region
RB2219	GAA AGA GAT TCA AAG CTT GTG	reverse sequencing primer for M02B1.1 genomic region
RB2220	GGT CTC TCT GTT GCT GTT TG	forward sequencing primer for M02B1.1 genomic region and cDNA

Name of oligonucleotide	sequence 5’ → 3’	Description
RB2226	GAAGATCGCGGCCGCATGAAGACGGCAATTTTGATATG	for amplification of *srf-3* cDNA together with RB2227; used for cloning pBY1873
RB2227	GAA GAT CGC GGC CGC TTA CAG ACA AAA CGC CTC TTT TG	for amplification of *srf-3* cDNA together with RB2226; pBY1873
RB2235	CTAAAATCCCCCGGCCGAAA	forward sequencing primer for M02B1.1 genomic region

Curriculum vitae

Name	Jörg Höflich
Geboren am	02. Mai 1972
Geburtsort	Wilhelmshaven
Familienstand	ledig

Schulausbildung

1978 – 1982	Grundschule am Dannhalm, Jever
1982 – 1984	Orientierungsstufe Jever
1984 – 1988	Realschule Jever
1988 – 1991	Mariengymnasium Jever

Berufsausbildung und Wehrdienst

1991 – 1993	Ausbildung zum Industriekaufmann bei der BAWI Bekleidungswerke GmbH in Wilhelmshaven Abschluss: Kaufmannsgehilfenbrief
1993 – 1994	Wehrdienst in Oldenburg

Studium

1994 – 1996	Grundstudium der Biochemie an der Universität Bayreuth Abschluss: Vordiplom
1996 – 1999	Hauptstudium der Biochemie an der Universität Bayreuth
1999 – 1999	Diplomarbeit am Lehrstuhl für Genetik Dr. Christian Lehner Thema: „Evaluation von Methoden zur Charakterisierung der Komplexbildung des *Drosophila pimples* proteins“
11/1999	Abschluss: Diplom-Biochemiker
ab 05/2000	Lehrstuhl für Stoffwechselbiochemie/Molekulare Neurogenetik der Ludwig-Maximilians-Universität München; Prof. Dr. Ralf Baumeister. Thema: „Genetic and functional characterization of *Caenorhabditis elegans srf-3*, a gene involved in regulating surface antigenicity.”

Abbreviations

aa	amino acid
Bah	biofilm absent on the head phenotype
Bre	bacillus-toxin resistant phenotype
bp	base pair
C. briggsae	*Caenorhabditis briggsae*
C. elegans	*Caenorhabditis elegans*
cDNA	complementary (to mRNA) cDNA
CMP	cytosine-5'-monophosphate
CMP-Sia	CMP-sialic acid
col	collagen mutant
Da	Dalton
Daf	dauer larva formation abnormal phenotype
Dar	deformed anal region phenotype
DNA	desoxyribonucleic acid
Dpy	dumpy phenotype
dsRNA	double stranded RNA
E. coli	*Escherichia coli*
ER	endoplasmatic reticulum
Esp	enhanced susceptibility to pathogens phenotype
Exc	excretory canal abnormal
FITC	fluorescein-isothiocyanate
GDP	guanosine-5'-diphosphate
GDP-Fuc	GDP-fucose
gly	glycosylation related mutant
GFP	green fluorescent protein
GSII	*Griffonia simplicifolia* II
K. lactis	*Kluyveromyces lactis*
Lev	levamisole resistance abnormal phenotype
LPG	lipophosphoglycan
LPS	lipopolysaccharide
MDCK	Madin-Darby canine kidney
M. nematophilum	*Microbacterium nematophilum*
mRNA	messenger RNA
NLS	nuclear localization signal
NST	nucleotide sugar transporter
nt	nucleotide
ORF	open reading frame
PCR	polymerase chain reaction
P. aeruginosa	*Pseudomonas aeruginosa*
Ram	ray morphology abnormal phenotype
RNA	ribonucleic acid
RNAi	RNA mediated interference
RT-PCR	reverse transcription PCR
S. cerevisiae	*Saccharomyces cerevisiae*
SDS	sodium dodecyl sulphate
SL	splice leader
Srf	surface antigenicity abnormal phenotype
Sqv	squashed vulva phenotype

T. spiralis	*Trichnella spiralis*
ts	temperature sensitive
UDP	uridine-5'-diphosphate
UDP-Gal	UDP-galactose
UDP-GlcA	ÛDP-glucuronic acid
UDP-GlcNAc	UDP-N-acetylglucosamine
UDP-Glu	UDP-glucose
UDP-GalNAc	UDP-N-acetylgalactosamine
Unc	uncoordinated movement phenotype
UTR	untranslated region
VSV-G	Vesicular Stomatitis Virus Glycoprotein
WGA	wheat germ agglutinin
Y. pestis	*Yersinia pestis*
Y. pseudotuberculosis	*Yersinia pseudotuberculosis*